第九届全国脑电与脑成像学术年会

2022 年 11 月 10 日-13 日 中国 · 东莞

论 文 摘 要

主办单位

中国心理学会脑电相关技术专委会

广东省认知科学学会

承办单位

深圳市神经科学研究院

广东医科大学人文与管理学院

协办单位

深圳大学心理学院

暨南大学管理学院

中国认知科学学会社会认知分会

目录

Ⅰ 基本认知和情绪

Ⅱ 语言脑科学

Ⅲ 社会认知神经科学

Ⅳ 认知和情绪障碍与脑疾病

Ⅴ 其它类：运动、干预和 EEG 技术等

Facilitated processing of emotional eye regions under limited attentional resources

Lan Yang[a,b], Shuaixia Li[a,b], Weiqi He[a,b], Wenbo Luo[a,b,*]

[a] Research Center of Brain and Cognitive Neuroscience, Liaoning Normal University, Dalian, China, 116029
[b] Key Laboratory of Brain and Cognitive Neuroscience, Liaoning Province, Dalian, China, 116029
[*] Corresponding author, Email: luowb@lnnu.edu.cn

Objective

The eye region in a face plays a fundamental role in social interaction, which can convey rich gaze direction and emotional signals. However, little is known about how and when people perceive and respond to emotional cues depicted in the eye region. To this end, the present study used event-related potentials (ERPs) to investigate the temporal dynamics underlying the influence of perceptual load and emotional valence on the processing of isolated eye regions under limited attentional resources.

Methods

24 right-handed students were recruited as paid volunteers. The dual-target RSVP task was applied in our study. Six upright eye regions varying in valence (2 happy, 2 neutral, and 2 fearful) were presented as the second target (T2) stimuli to elicit emotional responses. And twelve neutral eye regions were inverted and presented as distractors. The remaining 2 upright neutral eye regions were overlaid by five arrows arranged side by side to generate four T1 stimuli with low (<<<<< and >>>>>) or high (<<><< and >><>>) perceptual load level. Each item in the stream was presented for 116 ms. The time interval between T1 and T2 was 232ms to ensure the appearance of an attention blink.

Results & Discussion

The response accuracies for fearful and happy eye regions were higher than those for neutral eye regions while the difference between the former two conditions was not significant, reflecting the enhanced processing of emotional eye regions. At the electrophysiological level, fearful eye regions evoked a larger P1 amplitude than happy eye regions, which is in line with the notion of an automatic negativity bias at the early face processing stage. For the N170, the amplitudes in response to fearful and happy eye regions were larger than those for neutral eye regions, with no differences between the former two conditions, suggesting the preferential processing of emotional information. In the third stage, the increased responses of P3 elicited by emotional eye regions relative to neutral eye regions reflect more elaborative

processing and sustained attention to emotionally salient information.

Conclusions

In summary, we found that emotional eye regions, especially fearful eye regions could be processed preferentially regardless of the available attentional resources, which reflected the higher visual saliency. Furthermore, these findings provide novel contributions to our understanding of the neural correlates underlying the processing of emotional eye regions under limited attentional resources.

冲突观察诱发冲突适应及其神经机制

陈永强 1，陈安涛 2*
1. 西南大学心理学部，认知与人格教育部重点实验室，重庆，400715；
2. 上海体育学院心理学院，上海，200438
（chenantao@sus.edu.cn）

目的

研究表明，在观察学习过程中同样需要认知控制的参与。近期一项研究发现观察动作冲突可以诱发冲突适应，但其所诱发的冲突适应是反转的冲突适应这可能与其使用的任务情境不同有关。因此，冲突观察能否诱发经典的冲突适应及其神经机制还存在争议，有待进一步澄清。本研究采用同一任务情境（Stroop 任务）来考察这一问题。具体来说，本研究预测在相同情境中，冲突观察能够诱发经典的冲突适应。这对于深入理解观察学习和认知控制的相互作用有着重要启示。

方法

本研究采用观察范式的词-色 Stroop 任务。实验 1~3 从行为上考察在冲突观察诱发经典的冲突适应，实验 4 采用 ERP 技术探究其背后的神经机制。刺激材料由红、绿、黄、蓝四种颜色印刷的“红”、“绿”、“黄”、“蓝”四个汉字组成。刺激伪随机排列以排除特征整合与及偶发学习的影响。伪随机插入观察和反应试次，以防止“观察-反应”的反应定势。实验 1（N=40）采用 2 (观察条件一致性：一致、不一致) × 2 (反应条件一致性：一致、不一致)的被试内设计，其中观察刺激呈现 1500ms。实验 2（N=45）设置三种观察时间。实验 3（N=34）加入探测试次，要求被试按键反应，以保证被试认真观察。实验 4（N=32）中观察时间为 400ms，考察冲突观察诱发冲突适应的神经动态机制。

结果与讨论

实验 1 结果发现，在观察 1500ms 时未能观测到显著的冲突适应，这可能是由于观察时间较长，降低了被试的唤醒水平和警觉性，导致被试无法将观察阶段的冲突信号充分用于反应阶段的控制调整。实验 2 操纵观察时间，结果发现冲突适应随观察时间延长而减小，在观察 400ms 时发现显著的冲突适应效应。实验 3 在观察 400ms 时观测到冲突适应，重复了实验 2 的结果。实验 4 结果发现，在观察试次中，在 N450 成分（Fz；400~500ms）上发现了显著的 Stroop 效应，说明观察到了冲突;在“观察-反应”试次中,N450 成分和 SP 成分(Pz, POz;850~1000ms）均表现出冲突适应。本研究扩展了观察学习的意动理论（ideomotor theories），为认知控制参与观察学习提供了行为和神经证据。

结论

（1）在相同任务情境中，冲突观察能够稳定地诱发“纯净”的冲突适应；（2）冲突观察诱发冲突适应的神经机制主要表现在反映冲突监测加工的 N450 和反映冲突解决过程的 SP 成分上。

Decoding the specificity of post-error adjustments using EEG-based multivariate pattern analysis

Qing Li[1], Jing Wang[1], Zhifang Li[1], Antao Chen[2]*

[1]Key Laboratory of Cognition and Personality of Ministry of Education, Faculty of Psychology, Southwest University, Chongqing China, 400715

[2]School of Psychology, Shanghai University of Sport, Shanghai China, 200438

(chenantao@sus.edu.cn)

Objective

Error commission usually induces the necessary adjustments to avoid repeating errors, which are termed "post-error adjustments". An essential but unsolved issue is that whether post-error adjustments are domain-general or domain-specific, which was investigated in the present study through eliciting different types of errors. For this study, we examined the aforementioned issue by combining event-related potential and multivariate pattern analysis.

Methods

32 right-handed volunteers participated in the present study with a compensation of ¥70. Behavioral and electrophysiological data were recorded when they performed the Eriksen flanker task. The congruent trial included flankers facing the same direction as the middle arrow (e.g., < < < < < or > > > > >), whereas the incongruent trial included flankers facing the opposite direction as the middle arrow (e.g., < < > < < or > > < > >). Subjects had to respond to the direction of the middle arrow and ignore the flankers on each side. Post-error adjustments between different types of errors were examined using this task — namely, the errors on congruent trials (congruent errors) and those on incongruent trials (incongruent errors).

Results & Discussion

Post-error slowing, error-related negativity, and error positivity were comparable between congruent and incongruent errors, indicating that errors triggered domain-general interference mechanisms. Whereas post-error accuracy and late positive potential elicited by incongruent errors were larger than those elicited by congruent errors, exhibiting domain-specific control adjustment mechanisms. Importantly, no successful decoding soon after errors was found between congruent and incongruent errors, but above-chance decoding was observed between these two types of errors with increasing time, which further support that domain-general

adjustments occurred in the early stage, whereas domain-specific adjustments appeared in the late stage.

Conclusions

This study revealed that early domain-general interference adjustments induced by errors are reflected in error detection and error awareness, which are independent of error types; on the contrary, late domain-specific control adjustments are reflected in attentional adjustments, which are modulated by error types. These provides the first piece of neurophysiological evidence that post-error adjustments involved domain-general and domain-specific adjustments at various stages.

Acknowledgement: This work was supported by both National Natural Science Foundation of China (32171040) and Chongqing Research and Innovation Funds for Postgraduates (CYB22096).

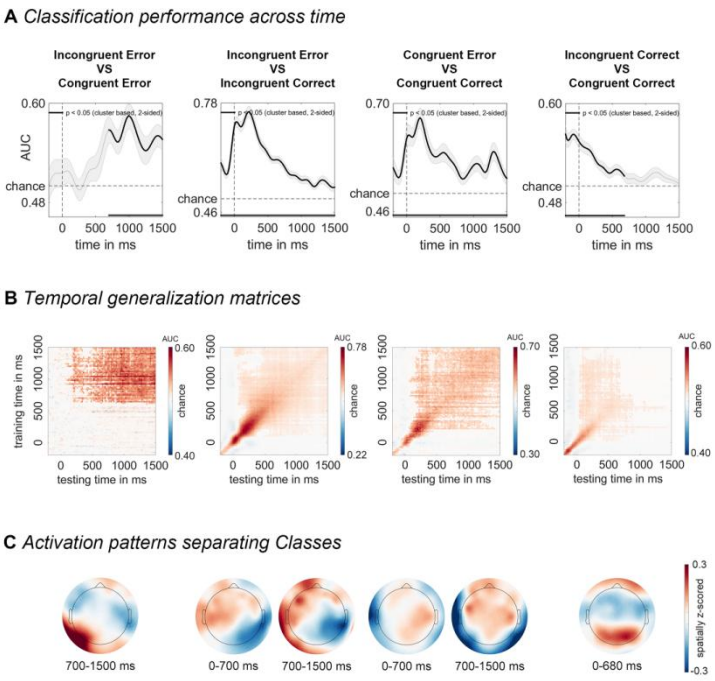

Figure 1. MVPA results in the flanker task. (A) Classification accuracy for the four datasets. The thicker lines represent the time windows of significant classification performance ($p < 0.05$, cluster-corrected). (B) Time generalization matrix of classifier performance. Significant samples are indicated by saturated colors. (C) Maps of forward transformation weights averaged over the time windows of significant classification performance.

Feedback-related Negativity Reflects Performance Prediction Error but not Consumptive Prediction Error

Shuyuan Xu[1,*], Meilin Wu[1], Yuanyuan Di[1], Jing Han[1], Yingfang Tian[3], Wei Ren[1, 2,*]

[1]MOE Key Laboratory of Modern Teaching Technology, Shaanxi Normal University, Xi'an, 710062, China

[2]Faculty of Education, Shaanxi Normal University, Xi'an, 710062, China

[3]College of Life Science, Shaanxi Normal University, Xi'an, 710062, China

(xushuyuan@snnu.edu.cn OR renwei@snnu.edu.cn)

Objective

The reward prediction error (RPE) is an important signal in outcome evaluation, and an event-related potential (ERP) component, the feedback-related negativity (FRN), has been proposed as an electrophysiological index of RPEs. However, whether the FRN reflects quantitative RPEs is still on debate. The FRN responses to the RPEs may differ in the light of whether they are relevant to action value updating (performance PE) or pure reward consumption (consumptive PE). In the present study, we strived to reveal in the electroencephalogram (EEG) the cortical activities, especially the FRN responses, induced by the performance and consumptive PEs.

Methods

Thirty-eight healthy undergraduates from Shaanxi Normal University participated in this study. In a two-choice probabilistic learning task, the performance (correct/wrong) and consumption (monetary outcomes) information were presented successively in two feedback phases of each trial. For the performance feedback phase, the likelihood of being correct for the left and right stimuli were set as 40%-60%, 50%-50%, or 60%-40% for each block. The performance feedback determined the context of the consumptive outcome. If the former was a 'correct', the latter would be a gain; if it was a 'wrong', a loss followed. However, independent of participants' performance, infrequent small or large monetary outcomes were displayed in addition to the frequent medium outcome in the gain/loss context to elicit the consumptive PEs. A frequent gain (FG) was a 50-cent gain ('+50', 0.5 RMB) with an occurring likelihood of 60%. An infrequent large gain (ILG) was a gain randomly drawn from [80, 100] appearing in 20% of the gain trials, and an infrequent small gain (ISG) was from [0, 20] with the same likelihood. Likewise, infrequent small loss (ISL, [-20, 0], 20%), frequent loss (FL, '-50', 60%) and infrequent large loss (ILL, [-100, -80], 20%) in the loss context were set. We used single-trial PEs derived from model

estimates to regress single-trial EEG voltages and determined cluster activities revealed by beta values for regression coefficients of interest.

Results & Discussion

The cluster activity associated with the FRN was sensitive to the performance PEs, but not to the consumptive PEs, and manifested as a bivalent PE encoder (though less sensitivity in negative feedback). The P3a and P3b were larger in 'wrong' than in 'correct' trials. Whereas in the consumption phase, the early posterior negativity (EPN) and late positive potential (LPP) which are associated with attentive and emotional processing were induced by the salience of the consumptive PEs.

Conclusions

We demonstrated that the brain processes the PEs related to action selection and reward consumption in a different way. The system underlying the FRN is specialized for a rapid processing of performance information based on the demand of environment, but indifferent to the consumptive utility of rewards which mainly involves attention and motivation processes. This configuration can provide a speed advantage in behavior adaptation, especially when the outcome is complicated and contains diverse dimensions of information.

The development of brain network dynamics during childhood and adolescence: a resting-state co-activation pattern analysis

Yuqi Zhang, Jianfeng Zhang*, Yuejia Luo*

School of Psychology, Shenzhen University, Shenzhen China, 816050

(luoyj@szu.edu.cn)

Objective

Recent studies demonstrated that brain activity can be characterized by several typical co-activation patterns (CAPs), and their dynamics are associated with cognitive functions and altered in brain disorders. How the dynamics of CAPs develop with age growth, and thus support brain maturity remains unknown. For this purpose, we applied a data-driven analytic technique to identify recurring states of CAPs in a resting state functional MRI dataset (i.e., Healthy Brain Network (HBN) program) in both childhood and adolescence.

Methods

After preprocessing, quality control, and matching demographic information, 585 subjects were included. The co-activation pattern analysis was then performed. Six CAPs were identified, and the overall dwell time was calculated as the percentage for each CAP's occurring time over the whole scan. The correlations between 6 states' dwell time with age were also calculated to identify the development-related CAPs. The dwell time differences between the six states were detected in childhood and adolescence separately to reveal the fact that the six brain states come into effect differently with brain maturity varying.

Results & Discussion

Six CAPs were identified, corresponding to Primary Visual Network (pVIS) state, Frontoparietal Network (FPN) state, Default Mode Network (DMN) state, Sensorimotor Network (SMN) state, High Visual Network (hVIS) state, and Salience Network (SN) state. After controlling sex and site, the dwell time of pVIS, FPN, DMN, and SMN (especially DMN and SMN) were positively correlated with age, while the dwell time of SN and hVIS were negatively correlated with age. In other words, brain development from childhood to adolescence can be characterized as increased DMN and SMN CAPs, together with decreased SN and hVIS. During childhood, pVIS, FPN, and SN dwell time was relatively higher than DMN, SMN,

and hVIS. During adolescence, the dwell time of pVIS, FPN, DMN, and SMN was relatively higher than SN and hVIS. The result indicates that the weights of six states in dwell time vary with age growth.

Conclusions

During childhood and adolescence, with the increase of age, the dwell time of DMN and SMN increased and the dwell time of SN and hVIS decreased. And the weightiness of six brain states varied at different developing stages. This study shed light on the developmental patterns of brain dynamics during childhood and adolescence, providing evidence of the neural basis for dramatic changes in cognition and emotion during the developmental stage before adulthood.

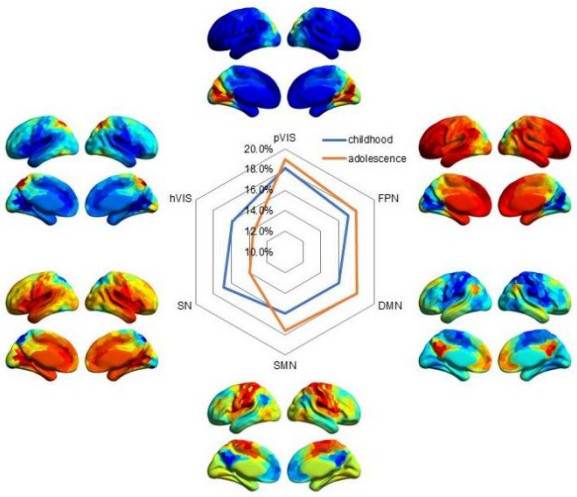

Figure 1. 6 brain states identified by co-activation pattern analysis and their dwell time.

Inhibition mechanisms of passive state representations in visual working memory

Wenjin Guo, Ziyuan Li, Qiang Liu*

Institute of Brain and Psychological Sciences, Sichuan Normal University, Chengdu China, 610066 (lq780614@163.com)

Objective

Working memory representations can be retained in the active and passive state, which performed different functions for online processing and robustly silent maintenance, respectively. That opened up a question whether active suppression was imposed on the passive representations for a silent maintenance by preventing them entering to the active state, due to the exposure to the intrinsic and extrinsic noise. In the current study, we adopted a sequential presentation task and recorded EEG signals of lateralization to investigate suppression of passive maintenance.

Methods

We adopted a sequential presentation task and recorded EEG signals of lateralization during the memory task. The items in the first array putatively were transferred into the passive state during the active processing of the second array. Thus the memory items in the first array were presented laterally and the second array was along the midline. That allowed us to isolate the brain activity elicited by the passive representations. A total of 90 participants completed three experiments. In Experiment 1, the passive memory load ranged from one to two. Experiment 2 examined the possibility that positional alignment between passive and active items resulted in the observed inhibitory effect. Experiment 3 designed the passive memory load ranged from two and three to detect whether active suppression of passive maintenance is modulated by passive memory load.

Results & Discussion

In Experiment 1, we observed significant CDA component following the first array, indicating the effective encoding for the initially presented items that were transferred into the passive state later. Importantly, two passive representations presented laterally were neurally suppressed during the delay of active items processing, which was supported by the presence of CDAp component; while no suppression was observed when one representation was retained in the passive state. Experiment 2 ruled out the possibility that the observed suppression on the passive representation resulted from the similar spatial configuration. Furthermore,

Experiment 3 modulated the passive memory load which ranged from two to three. The results suggested that the suppression effect was independent of the passive memory load.

Conclusions

Together, the current study demonstrated that the passive maintenance recruited suppression mechanism to inhibit the passive representations for a silent maintenance during an online processing of other items. Notably, the suppression effect on the passive representations was unrelated to the passive memory load, while one passive representation insufficiently triggered the suppression functioning, leading to the absence of suppression effect.

Acknowledgement: This work was supported by the NSFC (31970989).

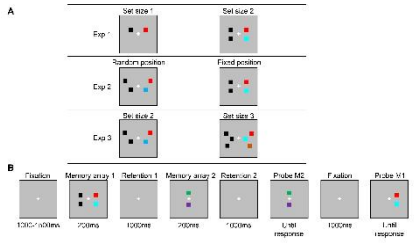

Figure 1. Schematic diagram of the experiments.

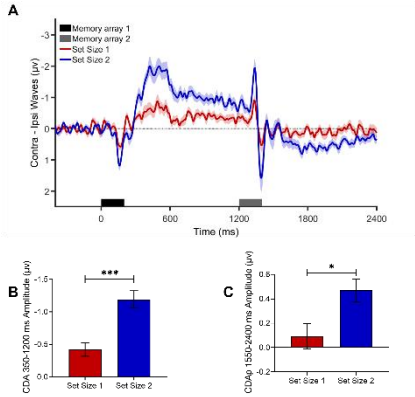

Figure 2. (A) Grand average ERP waveforms of CDA across different loads. Shaded error bars represent one SEM. (B) Retention 1 (350-1200 ms) average CDA amplitude in different loading conditions. Error bars indicate the SEM. (C) Retention 2 (1550-2400 ms) average CDAp amplitude in different loading conditions. Error bars indicate the SEM.

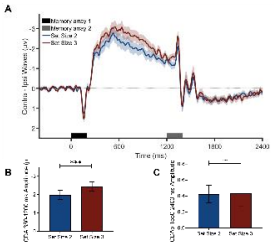

Figure 3. (A) Grand average ERP waveforms of CDA across different positions. Shaded error bars represent one SEM. (B) Retention 1 (350-1200 ms) average CDA amplitude in different position conditions. Error bars indicate the SEM. (C) Retention 2 (1550-2400 ms) average CDAp amplitude in different position conditions. Error bars indicate the SEM.

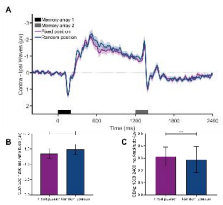

Figure 4. (A) Grand average ERP waveforms of CDA across different loads. Shaded error bars represent one SEM. (B) Retention 1 (350-1200 ms) average CDA amplitude in different loading conditions. Error bars indicate the SEM. (C) Retention 2 (1550-2400 ms) average CDAp amplitude in different loading conditions. Error bars

The Neural Basis of Curiosity in Social Conflict Situation

Yanghua Ye, Qi Huang, Luoyao Pang, Yue-Jia Luo*, Haiyan Wu*

Institute of Affective and Social Neuroscience, College of Psychology and Sociology, Shenzhen University, Shenzhen China, 816050

(luoyj@szu.edu.cn)

Objective

Humans show a strong curiosity about their environments, exhibit information seeking for both the natural and social items.Social curiosity promotes our social life, orients our social interactions. However, the curiosity-related research mainly focus on the realms of perceptual experience and knowledge acquisition instead of the social aspects. It remains unknown whether social curiosity share the similar mechanisms with other types of curiosity that have been investigated. Furthermore, what is the effect of social incongruity on social curiosity and information seeking from others and what are the corresponding neural basis? Here, we first develop an experimental task to study curiosity and information-seeking behavior in a social context with fMRI.

Methods

36 right-handed students were recruited as paid volunteers from Shenzhen university. We designed a social context involving the participant and another two off-site peers where a human-face picture will be presented and a judgement whether the corresponding person is pretending will be given by one of the peers as follows. The participants would be told that the peers have possessed more information about the person in that picture, and the entire experiment included two tasks. In task1, they only needed to rate their curiosity level for the reason why the off-site peers judge like that after passively viewing the faces and the following peer's opinion. But in task2, they were asked to give their own judgement after viewing the faces thus a contrast of opinions emerged, here we want to see the effect of conflict on participants' social curiosity level and information seeking behavior. Psychopy 3.0 is applied to present all of these stimuli and MRI data were acquired on a Siemens TrioTim 3.0 T MRI machine at Shenzhen University.

Results & Discussion

We performed first- and second-level analysis of task- fMRI data with SPM, focusing on the underlying mechanisms when participants curious about other's opinion during task1 and capture the brain activity when conflict emerged and its

effect on social curiosity in task2. The results showed that activation in striatal regions including putamen and nucleus was stronger when high-curiosity state contrast with low-curiosity state in both tasks. Furthermore, in task2, the activity in right temporal parietal junction(rTPJ) was positively correlated with individual rated curiosity level.

Conclusions

Consistent with classical epistemic curiosity study, in our work, the reward system were strongly activated when participants were highly curious about other's opinion. Notably, participants became more curious about the peer's thought when it contrasted with their own opinion, and the rTPJ's activation when participants viewing peer's opinion can predict their self-rated curiosity later.

Acknowledgement: This study is supported by the FDCT of Macau(0127/2020/A3), National Natural Science Foundation of China(U1736125).

The outcome evaluation in sequential decision making: An ERP study

Jiayu Fan, Ruolei Gu, Yongling Lin, Yue-jia Luo*

Shenzhen Key Laboratory of Affective and Social Neuroscience, Center for Brain Disorder and Cognitive Science, Shenzhen University, Shenzhen, China, 518061

(luoyj@szu.edu.cn)

Objective

"Outcome evaluation" refers to the experience and evaluation of human decision outcome, which can effectively navigate human subsequent choices. The psychological mechanism of outcome evaluation in a sequential decision scenario may be more complex than a one-shot decision. However, the representations in a sequence have not been well-known yet. Here, using the ERP technique, we investigated the neural correlates of outcome evaluation in sequential decisions.

Methods

Thirty-five healthy, right-handed participants were recruited. A sequential decision task was performed: an array of eight boxes were displayed, where seven boxes were empty and one contained a randomly distributed loss (devil) or a reward (gold). Participants could open the boxes from left to right, and they can keep making a series of choices and get the final outcome; they can also stop their choices early at any time and are informed the potential final outcome.

Results & Discussion

When people were exposed to final outcomes, the ERP results were consistent with one-shot decisions. However, when people did not get the final outcomes, humans process separately the valence of the potential outcome factor (reward vs. loss) and the distance factor which reflected in the FRN amplitude. Subsequently the brain centrally encoded the distance factor——the low distance elicited an enhanced P3 amplitude; finally, the potential outcome and distance factors are processed interactively which reflected in the LPP amplitude.

Conclusions

Using the ERP technique with high time resolution, the study showed a straightforward processing mode when people got the potential outcome and a hierarchical processing pattern when people did get the potential outcome.

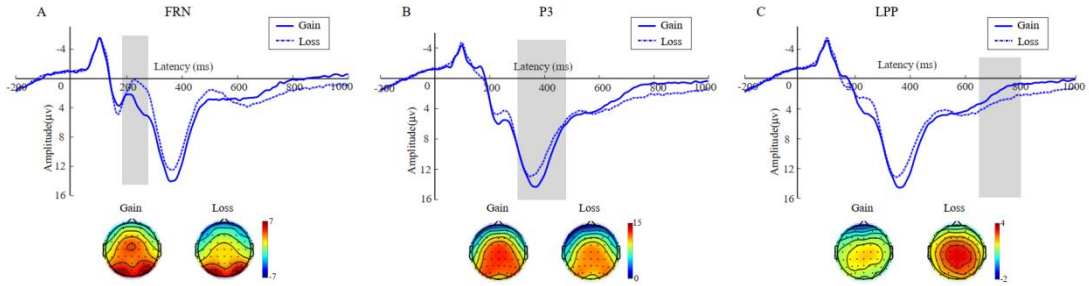

Figure 1. Grand average waveforms of the ERPs under the exposed condition. The corresponding scalp topographies for every condition are provided below. (A) The time window of the FRN is highlighted. These waveforms represent the mean values of the data at the electrode sites F1, Fz, F2, FC1, FCz, and FC2. (B) The time window of the P3 is highlighted. These waveforms represent the mean values of the data at the electrode sites P1, Pz, P2, PO3, POz, and PO4. (C) The time window of the LPP is highlighted. These waveforms represent the mean values of the data at the electrode sites CP1, CPz, CP2, P1, PZ and P2.

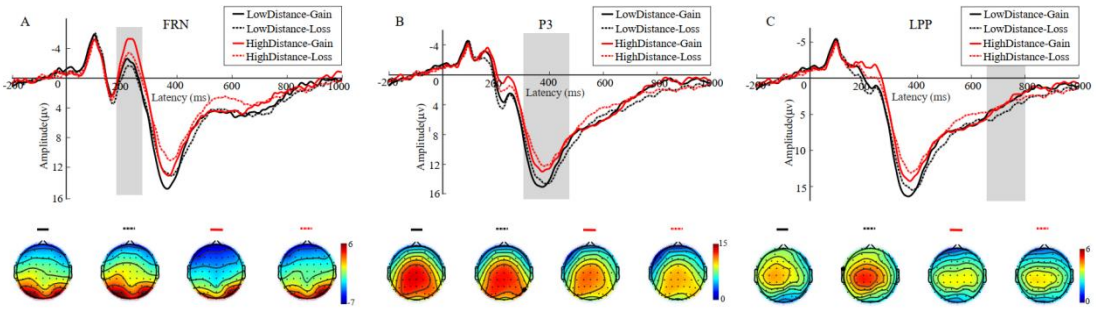

Figure 2. Grand average waveforms of the ERPs under the unexposed condition. The corresponding scalp topographies for every condition are consistent with the exposed condition.

Facial Attractiveness in the Eye of the High Arousal Men

Jie Gao; Shangfeng Han; Wenjuan Xing; Xinyi Zhou;Yuejia Luo*

Institute of Affective and Social Neuroscience, College of Psychology and Sociology, Shenzhen University, Shenzhen China, 816050

(luoyj@szu.edu.cn)

Objective

The judgement of facial attractiveness showed individual difference, while litter is known about the influence of arousal level on the facial attractiveness and its gender difference. Here, we used the resting-state alpha oscillation divided the high and low arousal group in men. The connectome-based predictive modeling was used to predict the judgement of facial attractiveness.

Methods

Fifty men and 27 women were recruited as paid volunteers from local universities. A face dataset of 80 photos of normal-attractive faces was used as materials of the experiment. After a resting-state EEG acquisition for 200 seconds , the participants began to perform experimental tasks. Each trial was start with a fixation cross followed by a 2000 ms face image of a female face with random. Next, participants were asked to judge the facial attractiveness of the face. There are a total of 80 trials in the formal experiment.

Results & Discussion

The facial attractiveness judgement of high arousal man was significantly higher than low arousal man and women, Indicating that high arousal men judged the female faces more attractive. Alpha power of high arousal men was smaller than low arousal men and women. Alpha power of low arousal men was also significantly smaller than women. Indicating that the groups were successfully divided according to the arousal.

For the men, the CPM results revealed that the combined network successfully predicted the judgement of facial attractive by using alpha functional connectivity. For the women, the combined network of delta band significantly predicted the judgement of facial attractiveness.

Conclusions

Individual general arousal plays an important role in the judgment of facial attractiveness, especially in men. Men with high arousal are more attracted to female faces. The result suggested that individual biological character (i.e. arousal)

contributes to the diversity of social functions.

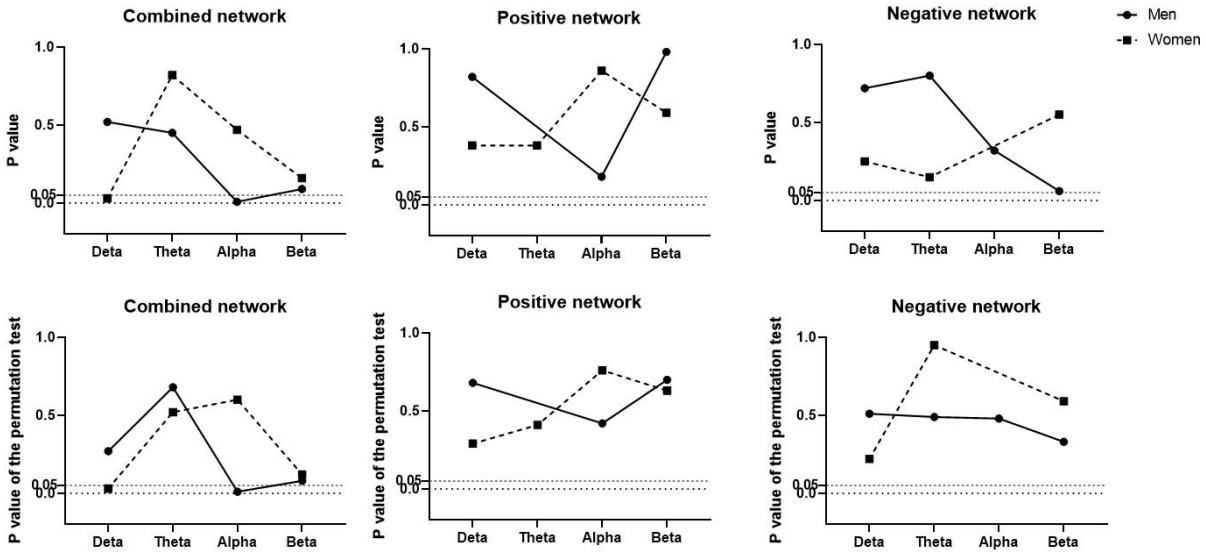

Figure 5 The p values without (the top line) and with (the bottom line) permutation test that were calculated by the connectome-based predictive modeling.

基于深度学习的面孔情绪图片库修订

周馨怡 韩尚锋 罗跃嘉*

深圳大学脑疾病与认知科学研究中心，深圳，518060

(luoyj@szu.edu.cn)

目的

以往面孔情绪图片库大多为静态图片，且其中不同的情绪面孔大多来自不同的身份，为解决这些问题，以进一步完善现有面孔情绪图片库，本研究拟基于深度学习生成标准化的高清彩色的亚洲面孔库。除了含有高清、真实等优点，本研究还将也增加面孔图片的年龄维度(即图片库中包含一个人不同年龄段的面孔图片)，以增加图片库的丰富性。同时，该图片库中的图片包含动态图，可适用于对面孔动态变化的认知研究，以丰富图片库的使用领域。

方法

基于StyleGAN2模型合成120个不同的人脸面孔,结合动作单位(action unit, AU）提取器得到每个人对应的愉快、愤怒、厌恶、恐惧、悲伤、惊讶和中性7种情绪面孔，对这些情绪面孔使用基于风格的年龄操纵方法（Style-based Age Manipulation, SAM）进行不同年龄面孔的合成，最终得到120个人不同情绪不同年龄段共6720的面孔图片。最后，征集120名大学生对其认同度、效价、唤醒度、优势度、年龄这五个维度进行评定。

结果与讨论

图片的唤醒度和优势度平均值分别为4.09、4.07。评分者对图片情绪的认同度较高，对情绪类别以及效价判断的正确率平均值为0.77、0.63。年龄评定的结果显示，本研究建立的图片库中包含5-85岁不同年龄段的图片，其中包括10-20岁（25.2%）、30-50岁（34.1%）和60-80岁（40.7%）的面孔图片。

结论

本研究中的图片具有高清、真实、动态、多维等优点，可用于未来的情绪及其跨文化研究，研究中所使用的基于深度学习的图片合成方法经验证有效，可用于将来情绪面孔库的完善与发展。

图表

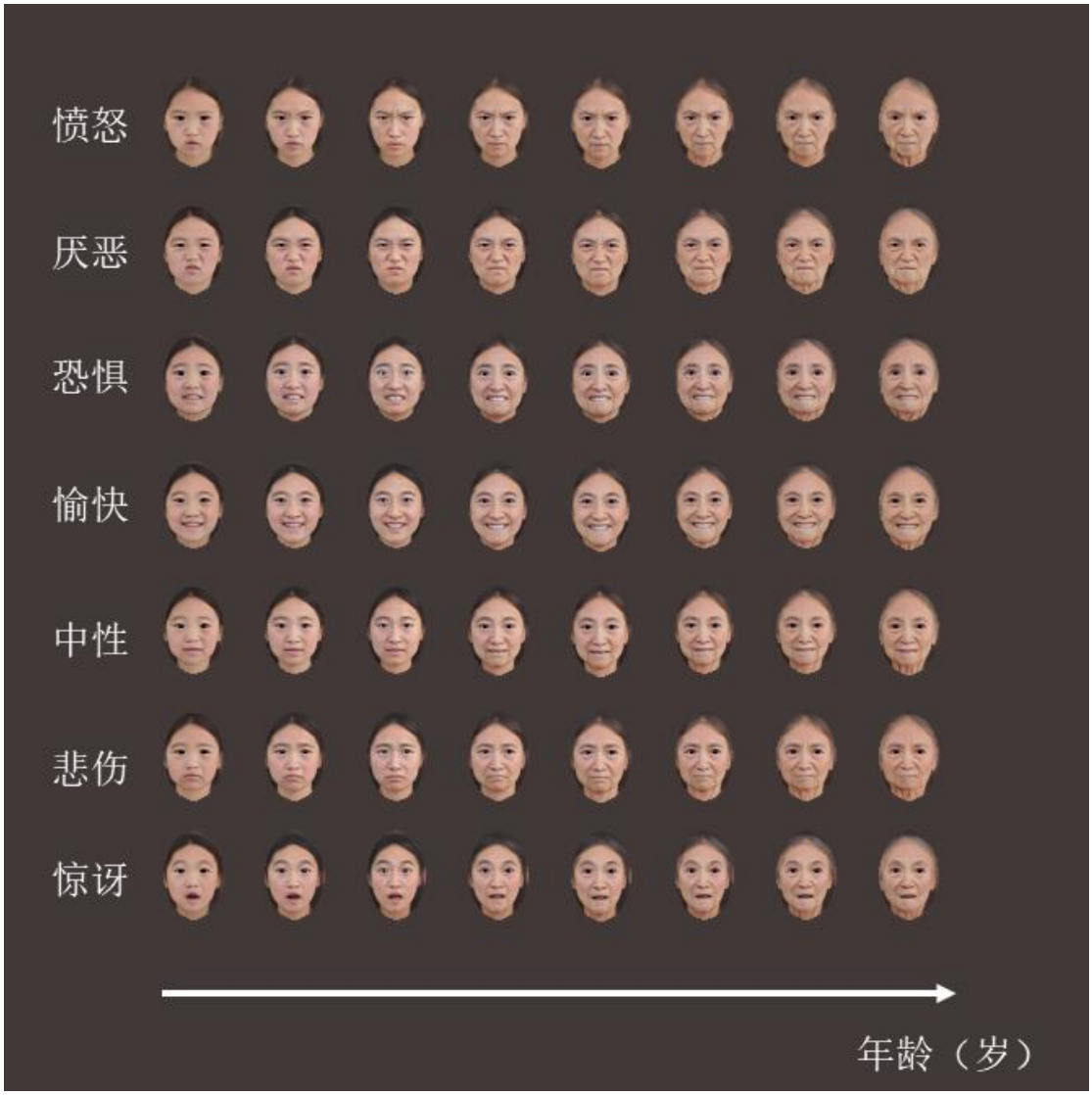

图 1 同一身份不同情绪不同年龄段的面孔图片示例

Different cerebral engagements for negative crowd faces

Dongfang Zhao, Shuaixia Li, Weiqi He*, Wenbo Luo*

Research Center of Brain and Cognitive Neuroscience, Liaoning Normal University, Dalian, China, 116029

Key Laboratory of Brain and Cognitive Neuroscience, Dalian, China, 116029

(weiqi79920686@sina.com) (wenbo9390@sina.com)

Objective

Crowd faces, compared with individual ones, often transmit more abundant and effective social information. Previous research focused on individual face, and researchers have found that recognition of fearful face is faster and more accurate than other types of face. However, it still remains unclear which negative expression (fear, anger and sadness) is of processing bias in multiple-face recognition and whether crowd faces of the three emotions show different activation patterns in the brain? Here, we used functional Magnetic Resonance Imaging (fMRI) to explore it.

Methods

27 volunteers (16 females) were recruited and paid for their participations. We created a set of 51 faces through face-morphing between two extremely emotional faces of the same person, taken from the Karolinska Directed Emotional Faces (KDEF). The emotional expressions ranged from happy to angry, happy to fearful and happy to sad. The mean emotion value of crowd faces was selected at -9, -3, 3,9 emotional unit. The crowd faces were presented 2000ms. Participants were asked to judge whether the test face emotions were happier than the crowd faces emotions or more angry, sad, or fearful.

Results & Discussion

When the fearful faces were presented, the accuracy was highest (87%), followed by the sad (82%) and angry faces (78%). In addition, the angry faces significantly activated the middle occipital gyrus. The crowd faces of fear had a higher level of neural responses in the middle frontal gyrus. The regions of activation by sadness were relatively more widespread, including medial frontal gyrus, superior frontal gyrus, precentral gyrus, postcentral gyrus, fusiform gyrus, and inferior temporal gyrus. The percent signal change of inferior parietal lobule involved in crowd recognition were found to be positively correlated with the accurate rate of all types of crowd faces.

Conclusions

In terms of crowd faces, sadness and fearful faces seem to be of processing bias,

which is consistent with findings of individual faces. Interestingly. the processing of sad faces is special, not only in behavior, but also in brain patterns. Our findings reveal the significant behavioral performance and distinguished the engaged brain regions in negative crowd faces, which may be helpful for the regulation of negative crowd emotions and disorder treatments.

群体面孔的整体编码与个体编码关系

刘人豪，叶倩君，何蔚祺*

辽宁师范大学脑与认知神经科学研究中心，辽宁省脑与认知神经科学研究重点实验室，大连 116029

(weiqi79920686@sina.com)

目的

群体面孔的加工因其在现实生活中的高生态性而逐渐得到研究者的关注，许多研究已证实人们能快速而准确地从一组不同效价强度的面孔表情中整体编码出平均情绪。然而，关于群体面孔的整体表征与群体中成员面孔的个体表征关系仍处于初步的探索阶段。时间依赖假说指出二者关系会受到加工时间的调节，但相关研究结果未达成普遍一致。因此，本研究运用脑电技术，操纵刺激的呈现时间探究面孔的群体与个体表征关系如何受加工时间的影响。

方法

共招募 23 名大学生被试参加实验。从 NimStim 面孔库选取 3 名女性和 2 名男性面孔各 3 张（高兴、愤怒以及中性表情）并且去除头发、耳朵以及其他外部信息。然后 FantaMorph 5 使用对同一身份的高兴与中性表情之间以及愤怒与中性表情之间进行变形，得到 51 张变形面孔，相邻变形面孔间隔 1 个情绪单元。在实验过程中，目标与干扰面孔集（通过不同颜色提示）在视野左右两侧呈现。面孔集由 1、2、3 或 4 张变形面孔组成，目标集的平均情绪单元随机选择，而干扰集的平均情绪单元固定为 26。面孔集呈现时间包括 100、700 毫秒两种条件。面孔集消失后会出现标尺并要求被试对目标面孔集的平均情绪进行主观判断。

结果与讨论

计算主观判断与实际平均情绪之间的误差值。在 100 毫秒条件下，被试对 1 张面孔的判断误差比多张面孔的更大；而在 700 毫秒条件下，对 1 张面孔的判断误差则小于多张面孔。另外，计算 P7、P8 电极的 N2pc（230-330 毫秒）成分平均波幅。在 100 毫秒条件下，不同面孔数量条件之间的 N2pc 没有差异；当呈现时间为 700 毫秒， 1 张面孔条件的 N2pc 显著小于多张面孔条件。这些结果表明群体情绪面孔的整体编码和及其成员的个体编码模式会受到加工时间长短的调节。

结论

当加工时间紧迫时，无法通过 N2pc 区分情绪面孔的群体和个体表征，而随着加工时间变得充足，N2pc 可以作为区分两种表征的神经指标。这意味着在同时加工多个情绪面孔信息时，时间因素是必要的。本研究支持时间依赖假说，短时间下虽然也可以表征信息，但相对模糊。若需要更精细的加工成员信息，则消耗更多时间。

情绪效价对自我优势效应形成的影响

周杏梅[1]，封春亮[2 3]，罗跃嘉[*1]

1北京师范大学心理学部，认知与学习国家重点实验室，北京

2华南师范大学心理学院，广州

3华南师范大学，广东省心理健康与认知科学重点实验室，广州

(luoyj@bnu.edu.cn)

目的

个体在判断属于自己的物品时总是能做出快速和准确的反应，称之为自我优势效应。以往的研究发现，自我优势效应从无到有需要个体在自我和物品之间形成心理连结，并且该过程是一个逐渐强化的过程。对这一过程进行探究有助于我们了解自我优势效应形成背后具体的心理机制。

在现实生活中，我们周围存在的物品会存在效价的区分。这两种效价带给我们的主观感受并不相同，由于具有积极效价的事物更能给人带来愉快的感受，个体也会更愿意接触积极事物。由此引发了本研究的问题：物品效价是否会影响自我-物品之间心理连结的过程？同时，这种影响是否会持续影响到自我优势效应形成后个体对自己所属的不同效价物品的态度。

方法

本研究进行了两个实验，采用愉快面孔和愤怒面孔。实验一首先探究情绪效价对自我优势效应形成过程的影响。被试在每个试次中去判断出现的面孔是属于自己的队友，好朋友的队友还是陌生人的队友。在学习结束后，被试随即便进行实验二：情绪效价对自我优势效应形成后在社会决策上的影响，对每一名队员进行金钱分配任务。本研究一共招募了 37 名大学生。

结果与讨论

实验一在行为结果上发现个体判断人脸属于自我队友的正确率在积极和消极条件下并不存在显著差异。同时，用于捕捉自我-物品心理连结形成速度的学习率参数也不存在显著差异。这说明情绪效价对自我优势效应的形成过程并不存在显著影响。学习策略分析发现，自己-积极队友对正反馈更加的敏感；而自己-消极队友则同时对正反馈和负反馈都更加的敏感，说明自我-消极队友心理连结的形成需要更多的加工策略。相应的脑成像结果也显示，自我-消极队友更多的激活了右侧背内侧前额叶(dmPFC)、左侧扣带回中后部等加工自我相关信息的脑区。由此我们推测尽管情绪效价在自我优势效应的形成过程中不存在显著的影响，但这个过程中个体可能使用了不同的策略来形成积极情绪效价和消极情绪效价

与自我之间的关系。实验二的结果揭示自己-积极队友会得到更加公平的对待，同时前侧脑岛也得到更加显著的激活，这说明积极队友可能引起了个体的道德反思从而促使个体对其做出更公平的决策。

结论

情绪效价并不影响自我优势效应的形成过程，但却可能会导致效应形成后个体对带有不同效价属性的物品持有不同的态度。

低频呼吸对负性情绪抑制控制的影响

武文艳，顾文强，杨苏勇*

上海体育学院心理学院，上海，200438，（ysy77@163.com）

目的

负性情绪会损害抑制控制等认知功能。低频呼吸训练是最常用的缓解负性情绪的方法之一，它是否能缓冲负性情绪对认知功能的影响还不清楚。因此，本研究情绪 Oddball 任务行为、脑电、心电等多水平，考察低频呼吸对负性情绪与抑制控制交互过程的影响。

方法

共招募 50 名无呼吸训练经验的大学生被试，随机分两组，其中实验组 25 人（年龄 21.66±2.54 岁，女性 12 人），控制组（年龄 22.12±2.12 岁，女性 13 人）。实验组进行 10 次/分钟的低频呼吸训练，对照组进行 17 次/分钟自主呼吸，干预时长均为 10 分钟。然后，所有被试进行双选择 OddBall 任务。该任务包括 3 个 block，每个 block 包含标准刺激（85 %）和偏差刺激（15 %）。标准刺激为一张钢笔图片，偏差刺激分为中性、积极或消极情绪图片。要求被试对标准和偏差刺激做出不同的按键反应。在每个 block 结束之后评估被试的愉悦程度，评分越高越积极。同步记录脑电。

结果与讨论

（1）实验组的呼吸频率显著慢于控制组，且与要求呼吸频率无显著差异，说明实验组的呼吸频率控制达到了实验要求；（2）实验组的心率变异性高频成分（HF-HRV）显著大于控制组，提示低频呼吸时个体心脏迷走神经活动增强；（3）实验组消极 block 的愉悦度评分显著高于控制组，提示面对消极情绪刺激实验组的情绪比控制组更积极；（4）情绪 Oddball 任务中的反应时差值（偏差刺激减去标准刺激）指标仅在消极情绪条件下，实验组的任务表现都显著好于控制组，提示低频呼吸可提高个体在消极情绪影响下的抑制控制能力；（5）脑电数据表明，消极情绪条件下实验组的 N2（265~275ms）差异波波幅显著小于控制组，提示实验组投入了较少的认知资源参与冲突监控。消极情绪条件下实验组 LPP（1000~1500ms）差异波（偏差刺激减去标准刺激）显著低于控制组，提示实验组对消极条件的评价加工减弱。

结论

低频呼吸不仅能改善个体的负性情绪，而且可以促进个体对负性情绪信息的抑制控制，潜在的机制可能是低频呼吸减少了个体对冲突监控的认知资源投入，抑制了对负性情绪的进一步加工。

下行反事实思维对情绪记忆的调节作用：来自fNIRS的证据

王子坤，叶娜*

武汉体育学院 运动医学院，湖北 武汉，430079

(345570920@qq.com)

观点

反事实思维（Counterfactual Thinking，CFT）是个体对不真实的条件或可能性进行替换的一种思维过程。基于其发生方向分为上行反事实思维（upward counterfactual thinking）和下行反事实思维（downward counterfactual thinking）。下行反事实思维（dCFT）最初是由负面情感引起的，人们参与到这个过程中来，是为了保护和增强其主观幸福感。生活中，厌恶的自传体记忆有时会使个体产生适应不良的情绪反应，并导致焦虑和抑郁等情感功能障碍。调节这种记忆影响的一种方法是形成一个 dCFT，即对事件产生一种可能更糟糕的心理模拟，再以积极的视角去看待当前发生的事件。目前研究表明 dCFT 在减少与记忆相关的负面情绪方面起着积极作用，但其作用背后的脑机制尚不清楚。

方法

本研究采用功能性近红外光学脑成像技术（fNIRS），考察个体使用 dCFT 时情绪体验的变化。以是否进行下行反事实思维为自变量，唤醒程度、后悔程度、氧合血红蛋白浓度变化量为因变量，预实验通过对个体过去遗憾的经历的主观体验进行评定，选取了 20 个最负面的自传体记忆作为正式实验材料。我们使用情绪调节问卷（ERQ; Gross and John, 2003）的重新评估和抑制分量表来解释实验训练前调节水平的个体差异。

结果和讨论

行为学结果发现，唤醒程度与重新评估和抑制得分之间不存在交互作用；重新评估不影响后悔程度，抑制使用会降低后悔程度；此外，实验组（采用下行反事实思维）的唤醒程度和后悔程度都低于对照组（未进行下行反事实思维）。fNIRS 结果发现，实验组和对照组不同程度的激活了海马、后中线结构、顶叶、颞叶、TPJ 和 mPFC 以及 PFC 相关脑区，实验组 mPFC 脑区的激活水平高于对照组，且个体进行反事实思维时激活了与遗憾、后悔有关的脑区（内测 OFC）。

结论

本研究进一步验证了下行反事实思维能够降低个体对过去后悔经历的情绪体验，同时为反事实思维对情绪记忆的影响在脑机制上提供了更多的证据。

The impact of emotional motivation dimension on time perception

Huazhan Yin

School of Education Science, Hunan Normal university, Chang Sha, 410081
(yhz19791979@sina.com)

Objective

Emotional effects on human time perception were generally attributed to valence and arousal speeding up or slowing down the internal clock. However, the results were inconsistent when exploring the emotional effect on time perception from the two dimensions. Therefore, it was not enough to fully explain the emotional effect on time perception from the perspective of valence and arousal. The aim of the present study was to investigate the emotional effect on time perception based on the emotional motivation dimension with the help of event-related potentials (ERPs).

Methods

31 right-handed students were recruited as paid volunteers from a university. The emotional pictures were taken from Bochum Emotional Stimulus Set (BESST). Target stimuli consisted of 30 approach-motivated negative pictures, 30 withdrawal-motivated negative pictures and 30 neutral pictures. The time reproduction task was selected including the two target intervals (700ms and 1700ms). The participants were told that they had to press the key when they thought that the second stimulus (gray square) had been presented for the same length of time as the first (emotional pictures).

Results & Discussion

Behavioral results revealed that compared with approach-motivated negative expression, withdrawal-motivated negative expression was estimated longer. Meanwhile, the ERP data revealed the similar results that approach-motivated negative expression showed stronger P1, P2, EPN and lower CNV amplitude than withdrawal-motivated negative expression, suggesting that the emotional effects on time perception based on the emotional motivation dimension considered the role of attention.

Conclusions

Compared with withdrawal-motivated negative expression, approach-motivated negative expression was likely to distract more attentional resources from timer. Our study provided initial evidence that attention processes indeed contribute to emotion-induced temporal distortions.

Differential unconscious representations of “toolness” and the global shape of tools revealed by backward masking and continuous flash suppression

Zhiqing Deng[1], Fuying Zhu[1], Zina Li[1], Jie Gao[1], Juan Chen[1,2]*

[1]Center for the Study of Applied Psychology, Guangdong Key Laboratory of Mental Health and Cognitive Science, and the School of Psychology, South China Normal University, Guangzhou, Guangdong Province, 510631, China

[2] Key Laboratory of Brain, Cognition and Education Sciences (South China Normal University), Ministry of Education

*Correspondence should be addressed to Juan Chen (juanchen@m.scnu.edu.cn)

Objective

Human beings are remarkably adept at linking tools' perceptual and functional properties to complicated actions. Unlike viewing objects such as animals and faces, viewing tools activate both the ventral visual stream mediating object recognition and the dorsal visual stream mediating object manipulation. Previous studies have shown that invisible tools are also represented in the dorsal visual pathway, which suggests that tool categorization can happen in the dorsal stream without conscious perception. Recent studies argued that it is the elongated shape, rather the “toolness” per se, that enabled the unconscious representation of tools. Resolving this debate is essential because it speaks to the scope and limits of unconscious perception along the visual ventral or dorsal stream.

Methods

Here, using electroencephalography (EEG), we resolve this debate by investigating the temporal evolution of the unconscious representation of global shape (elongated vs. stubby) and “toolness” (tools vs. non-tools) by backward masking (BM) or continuous flash suppression (CFS). In BM, the stimulus was presented for 33 ms immediately followed by a noise mask for 100 ms to make the stimuli invisible. In CFS, the stimulus was presented to the non-dominant eye of each participant for 200 ms, together with the high-contrast, random Mondrian mask to their dominant eye using a mirror stereoscope. In event-related potential (ERP) analysis, two-way repeated-measures ANOVAs were performed in each ERP component to reveal the main effects of global shape and toolness and the interactions between them. Next, computational modeling (deep convolutional neural network, DCNN) was utilized to dissociate the global shape representations from toolness. The layer-specific representational dissimilarity matrices (RDMs) were constructed by quantifying the

dissimilarity (1-Spearman's R) of response patterns observed along each DCNN layer. By correlating the RDM of each layer and the RDM of the EEG neural model, it would be possible to reveal whether the early-, middle- or high-level visual processing was reflected in the EEG activity in the BM and CFS conditions.

Results & Discussion

In BM, the ERP results revealed that the global shape effect emerged first over the occipital scalp and eventually moved over the parietal and central cortex. Consistent with the ERP results, DCNN results in BM revealed the EEG neural model was significantly correlated with layers 3-5 (middle-level convolution layers reflecting the global shape properties of objects) over almost the whole scalp. In contrast, ERP results in CFS showed that the main effects of toolness were observed in the central, parietal, and occipital scalp in the early phase, while the relatively late main effects of global shape were only observed in occipital electrodes. Furthermore, in CFS, EEG neural model was significantly correlated with layers 6, 7, and 8 (fully-connected layers reflecting both toolness and the global shape) of the DCNN in the frontal, central and parietal electrodes, and with layer 3 in the central and parietal electrodes in a relatively late phase. Both the ERP and DCNN results suggest the early and strong toolness representations and the relatively late and weak shape representation in CFS.

Conclusions

Overall, the results of ERP analysis and computational modeling demonstrated that the dynamic representations of global shape can be dissociated from that of "toolness" in unconsciousness with BM and CFS, which suggests that the unconscious representation of toolness, if any, cannot be solely attributed to the global elongated shape of tools. These findings provide insights into the scope and limits of unconsciousness perception and provide the first piece of evidence of DCNN applied in unconscious processing.

Acknowledgment: This research was supported by the National Natural Science Foundation of China (No. 31800908 and No. 31970981).

Attention capture by positive auditory information: Behavioral and ERP evidence

Yanmei Wang[1, 2*], Zhenwei Tang[1], Libing Yang[1]

1 Shanghai Key Laboratory of Mental Health and Psychological Crisis Intervention, The School of Psychology and Cognitive Science, East China Normal University, Shanghai, 200062, China, 2 Shanghai Changning Mental Health Center, Shanghai, China, 200335

(ymwang@psy.ecnu.edu.cn)

Objective

Emotion stimuli can be preferentially selected by emotional stimuli without conscious awareness. Previous studies always focused on attentional bias towards negative emotional stimuli. Recently, researchers have more recently expanded the investigation of attentional biases toward positive stimuli. Nevertheless, few studies examine attentional biases toward positive auditory information.

Methods

In three experiments, the present study employed an emotional spatial cueing task using positive and neutral natural sounds as cues, neutral auditory (Experiment 1) or visual stimuli as targets (Experiment 2 and 3) to explore whether auditory or visual spatial attention could be modulated by positive auditory cues, and to investigate the exact nature of these positive auditory biases. Experiment 3 also examined the temporal dynamics of cross-modal auditory bias towards positive sounds using event-related potentials (ERPs).

Results & Discussion

behavioral results of three experiments consistently demonstrated that response times to targets were faster after positive auditory cues relative to neutral auditory cues in valid condition, indicating facilitated attention engagement with positive sounds. The results of Experiment 3 showed that N1 amplitudes were more negative after positive sounds than neutral sounds, and P300 amplitudes were higher for positive sounds compared to neutral sounds in valid trials.

Conclusions

Both behavioral and electrophysiological data converge on the central finding that positive auditory stimuli capture auditory and visual attention, which occurs during early stages of attentional process in normal individuals.

Updating the dual-mechanism model for cross-sensory attentional spreading: the influence of space-based visual selective attention

赵松[1], 李洋[1], 王崇志[1], 冯成志[1], 冯文锋[1,2,*]

1 苏州大学教育学院心理学系, 江苏 215123

2 苏州大学心理与行为科学研究中心, 江苏 215123

* 通讯作者: 冯文锋 (fengwfly@gmail.com)

Objective

Selective attention to visual stimuli can spread cross-modally to task-irrelevant auditory stimuli through either the stimulus-driven binding mechanism or/and the representation-driven priming mechanism. The stimulus-driven attentional spreading occurs whenever a task-irrelevant sound is delivered simultaneously with an attended visual stimulus, whereas the representation-driven attentional spreading occurs only when the object representation of the sound is congruent with that of the to-be-attended visual object. Using event-related potentials (ERPs) to isolate the stimulus-driven and representation-driven attentional spreading effects, respectively, the current study aimed at examining the exact roles of space-based visual selective attention in the two types of cross-modal spread of attention, which remain controversial in the literature.

Methods

Subjects were instructed to attend selectively to the line drawings of target object category (dogs or cars) appearing at the designated visual field (left or right), while ignoring all drawings appearing at the other side and all centrally presented natural sounds (dogs' barks or cars' beeps). These sounds could occur synchronously (and congruently) with spatially attended or unattended peripheral drawings, occur alone, or be absent. Therefore, the present design manipulated 3 main within-subject factors consisting of stimulus type (audiovisual, auditory, visual), space-based visual attention (attended, unattended), and object-based visual attention (target object, nontarget object).

The representation-driven attentional spreading was isolated by contrasting the extracted auditory ERPs to audiovisual stimuli when their visual representations correspond to the target object (e.g. dogs with barks under target-dog blocks), versus the extracted auditory ERPs to the same audiovisual stimuli when their visual representations correspond to nontarget objects (e.g. dogs with barks under target-car

blocks). The stimulus-driven attentional spreading was isolated by comparing the extracted auditory ERPs to audiovisual stimuli when their visual representations correspond to nontarget objects (e.g. dogs with barks under target-car blocks), versus ERPs to auditory-only stimuli when their representations correspond to nontarget objects (e.g. barks alone under target-car blocks).

Results & Discussion

First, the representation-driven auditory Nd component (200–400 ms after sound onset) did not differ according to whether the peripheral visual representations of audiovisual target objects were spatially attended or not, but was less sustained when the auditory representations of target objects were presented alone. These findings demonstrate that the representation-driven attentional spreading, occurring as a by-product of top-down activation of target objects' visual representations, is independent of space-based visual selective attention but benefits in an all-or-nothing manner from object-based visual selection for actually presented visual representations of target objects.

Second, the stimulus-driven auditory Nd component (200–300 ms) was decreased but still prominent when the peripheral visual constituents of audiovisual nontarget objects were spatially unattended. These results suggest that although the stimulus-driven attentional spreading is modulated by space-based visual selective attention, attending to visual modality per se is more likely to be the endogenous determinant of the stimulus-driven attentional spreading.

Conclusion

By providing novel insights into the origins of the two types of cross-modal attentional spreading, the current study not only updates the existing dual-mechanism model for cross-modal attentional spreading in particular, but also extends our understandings regarding the subtle and complicated influences of various forms of top-down attentional deployment on multisensory processing in general.

This work has been published recently in Human Brian Mapping.

The P3b component is independent of task relevance in the no-report inattentional blindness paradigm

Aixin Liu[1], Minran Chen[1], Chengzhi Feng[1], Wenfeng Feng[1,2*]

1 Department of Psychology, School of Education, SooChow University, Suzhou, Jiangsu 215123, China.
2 Research Center for Psychology and Behavioral Sciences, Soochow University, Suzhou, Jiangsu 215123, China.
(fengwfly@gmail.com)

Objective

Neural correlates of consciousness (NCC) have been a long-standing debate in the field of neuroscience of consciousness. Recently, a series of studies using no-report inattentional blindness paradigm have shown that P3b (or late positivity, LP, >300 ms) is a neural correlate of task-relevant post-perceptual processing rather than visual awareness processing. However, the level of processing (LoP) hypothesis suggests that higher level processing is involved when performing stimulus discrimination (such as meaning or number magnitude), which has been found to be manifested in P3b. The present study recorded event-related potentials (ERPs) and used two meaningful pattern stimuli (car and bell) to investigate the function of P3b by manipulating conscious perception and task relevance.

Methods

Forty-one subjects in Experiment 1 and sixty-one subjects in Experiment 2 were recruited from Soochow university. The present study used a no-report inattentional blindness paradigm with three physically identical phases. In phase 1, subjects performed a bright dot detection distractor task while patterns of line drawings and matched control stimuli were presented at the center. Subjects were divided into awareness group (AW) and inattentional blindness group (IB) after phase 1 based on their awareness of unexpected patterns. In phase 2, the task was the same as in phase 1 and all subjects were aware of the pattern stimuli. In phase 3, subjects performed a background pattern discrimination task. Experiment 2 improved the visibility of the patterns and further explored the functional significance of the P3b component.

Results & Discussion

We found that in Experiment 1, awareness of patterns was accompanied by a visual awareness negativity (VAN, 260-340 ms, occipital region) in all phases in both groups, supporting that the early VAN component is a neural correlate of visual awareness. The P3b (400-600ms, parietal-occipital region) was present not only when the patterns were task relevant (phase 3), but also when the patterns were task irrelevant (AW group in phase 2), which contradicts with recent findings on P3b related to task-relevant post-perceptual processing. After the patterns were more visible in Experiment 2, awareness of the pattern was accompanied by VAN and P3b in both groups at all three phases, independent of the task relevance.

Conclusions

The present study showed that the P3b component was independent of task relevance in the no-report inattentional blindness paradigm, as demonstrated by the presence of the P3b component in both task-relevant and task-irrelevant conditions after subjects became aware of the patterns. Our study provides preliminary evidence that P3b component is task-independent and may reflect general post-perceptual processing or further processing of visual awareness rather than specific task-related post-perceptual processing.

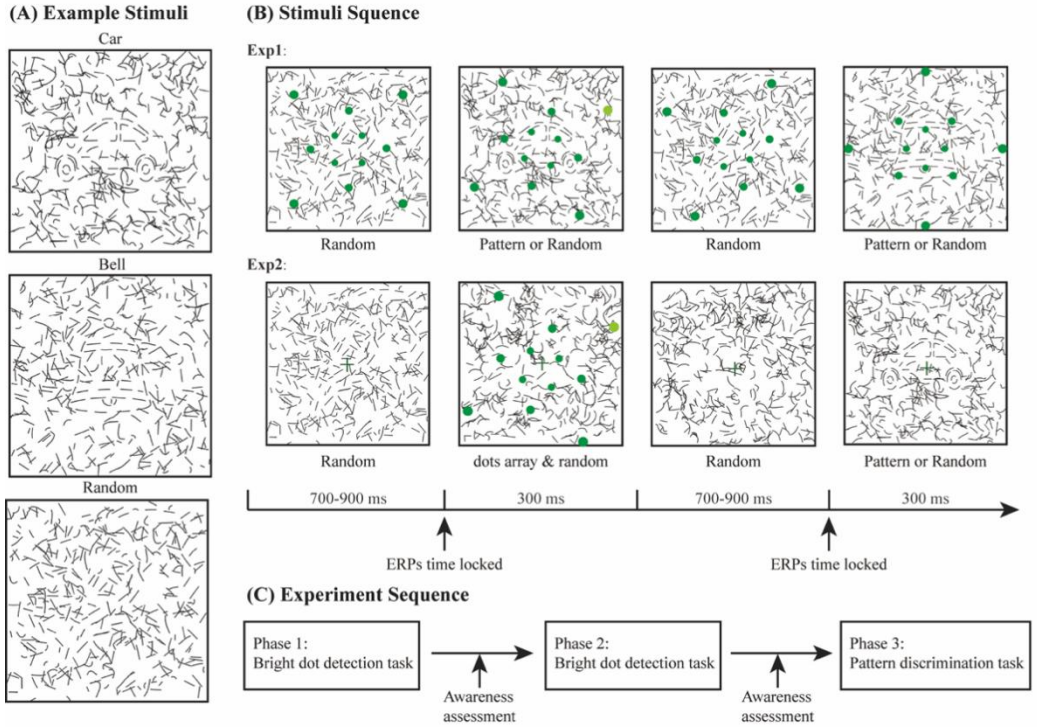

Figure 1. Stimuli and procedure.

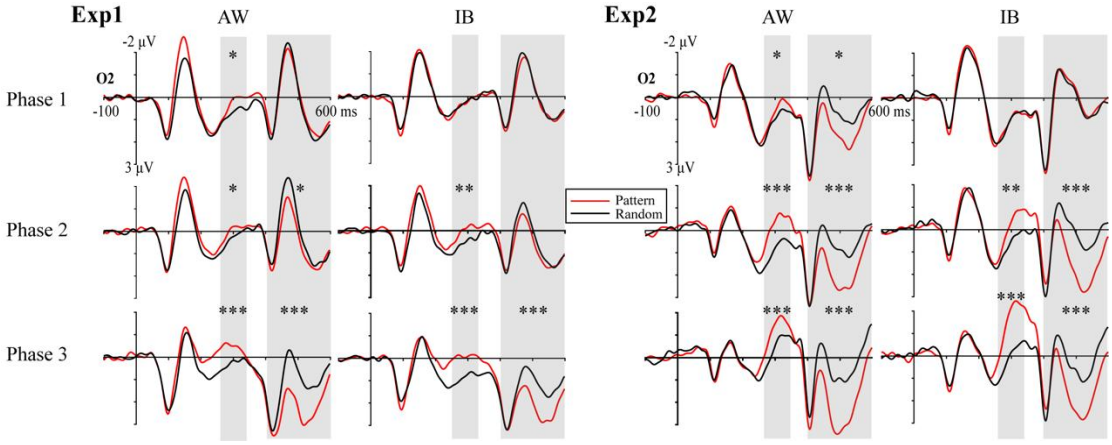

Figure 2. Grand-averaged ERPs elicited by patterns (red) and random (black) stimuli at O2 electrode for the awareness group (AW) and inattentional blindness group (IB) across the three experiment phases (top to bottom).

动作增强与目标促进在注意促进效应产生中的共同作用

郑思琦[1] 孟迎芳*[1] 董月晴[1] 肖芬妮[1] 叶泽童[1] 黄发杰[2]

(1福建师范大学心理学院，福州，350117)(2福建医科大学健康学院，福州，350117)

(通信作者：孟迎芳，E-mail：mengyf1978@126.com)

目的

注意促进效应（ABE）指的是，在同时进行记忆任务（如词汇）和与之无关的目标探测任务(如在呈现的绿色圆圈序列中对红色目标圆圈进行按键反应)时，对目标探测条件增加的注意不仅不会干扰，反而还会促进记忆任务的成绩，使其表现出比分心忽略条件下的记忆成绩更好的现象。作为一种并不常见的、反映了双任务之间“非零和博弈”关系的效应，对其产生机制的探讨有助于我们应用于日常生活中不得不面临的双任务情境。近期有研究通过设计 Go 目标探测任务（Go 目标 vs NoGo 分心）与 NoGo 目标探测任务（NoGo 目标 vs Go 分心）将动作反应与目标决策分离，即发现了动作效应的存在（Go 分心条件显著好于 NoGo 分心条件），也发现目标决策作用的存在（NoGo 目标显著好于 NoGo 分心），由此认为 ABE 的产生是目标决策的促进作用与动作反应的增强效应共同作用的结果。但在该研究中，Go 目标条件与 NoGo 目标条件在行为结果上，并未存在显著的记忆成绩差异。该结果可能是 Go 目标条件上目标促进与动作增强两个效应共同作用后发生冗余的结果，也有可能仅是其中一种效应起主导作用的结果。因此，我们使用事件相关电位（ERP）计数，以探讨 ABE 的产生究竟是否源于目标促进与动作增强共同作用的结果。

方法

共 25 名被试数据进入最后分析(其中 9 名男性)。实验采用编码-测验范式，编码阶段同时呈现探测任务刺激和记忆任务刺激（探测刺激呈现在记忆刺激下方，两者间隔 1cm）。探测任务刺激为视角大小为 1.03° × 2.15° 的五种颜色圆圈(红、黄、蓝、绿、紫；持续时间 100ms/个)，目标圆圈在一半被试中被指定为红色，在另一半被试中被指定为绿色，其余颜色为分心圆圈。记忆任务刺激则为趋于中性的中文双字词 480 个（持续时间 500ms/个），选自《现代汉语频率词典》和国家语委现代汉语语料库，呈现在屏幕中央，刺激间间隔（ISI）为 1600±200ms。测验阶段仅呈现双字词（直到按键后才消失），ISI 为 1800 ± 200ms。实验包含 NoGo 目标探测(1:1)条件和 Go 目标探测(1:1)条件，每个条件分别包含 60 个目标词（与目标圆圈一起呈现）和 60 个分心词（与分心圆圈一起呈现），及 120 个新词（仅在测验阶段呈现）。两个条件的差异主要体现在编码阶段：NoGo

目标探测任务要求被试在记忆词汇的同时，对除了目标圆圈之外的所有圆圈进行按键反应；Go 目标探测任务要求被试在记忆词汇的同时，只对目标圆圈进行按键反应。测验任务均为对词汇进行新旧再认判断。

结果和讨论

实验结果发现，无论是 NoGo 目标探测(1:1)条件和 Go 目标探测(1:1)条件，均发现了目标条件所诱发的 P300 平均波幅显著大于分心条件，并且该差异在 Go 目标探测条件下所涉及的脑区更多（如前额区和顶区，见图 1），体现了目标决策的促进作用；此外，跨条件对比发现，无论是目标条件还是分心条件，均发现了 Go 条件比 NoGo 条件诱发了更大的 P300，体现了动作反应的增强效应。综合两个对比结果可以说明，Go 目标与 NoGo 目标之所以在行为结果上未表现出记忆差异的原因在于，目标促进与动作增强共同作用后发生了冗余的结果。

结论

实验分别在目标条件与分心条件之间，以及动作条件和非动作条件之间，均发现了不同程度的 P300 平均波幅差异，表明 ABE 的产生是目标促进与动作增强共同作用的结果。

语篇情境和巩固时间对新词语义整合的影响

艾里菲热·艾力，买合甫来提·坎吉*

新疆师范大学心理学院，新疆乌鲁木齐，830017

(mkanji@163.com)

目的

在多种学习方式中，语境学习在词汇学习中占主要地位。阅读过程中，学习者通过语境提供的信息推理并学习新词的语义。学习者学习新词的语义之后，新词会被缓慢整合进语义网络并与其他概念节点建立联系。因此，前者被称为对新词的熟悉化，后者被称为新词的语义整合。以往研究发现，在多情境学习条件下学习新词，新词与该语境相关的语义关联词发生了语义启动效应，并据此提出新词的语义整合可以快速的发生。但研究者也发现，新词与语境不相关的语义关联词没有发生语义启动效应。另外一些研究则认为，新词的语义整合必须经历一段时间的巩固过程后才会发生。那么，语篇情境和巩固时间如何影响新词语义整合的过程呢？本研究采用事件相关电位(ERP)技术和新词学习范式来探讨语篇情境和巩固时间对新词语义整合的影响。

方法

18 名大学生被试参加本实验， 均为右利手，母语为汉语。实验采用 2（语篇情境：单情境、多情境）×2（巩固时间：0 小时、24 小时）×2（目标词类型：概念一致、语义关联词）多因素被试内设计。正式实验分两天进行，第一天被试学习 16 个分别在单和多语篇情境下的新词。时隔 24 小时以后，被试学习另外 16 个新词。两天的学习结束之后，对 32 个新词进行测试。测试阶段采用词汇判断任务，新词作为启动词，新词的对应概念、与学习语篇不相关的语义关联词和对应的 64 个假词作为目标词。被试需对目标词进行真假判断，考察被试对判断目标词的正确率、反应时和 N400 波幅。

结果和讨论

被试判断新词的语义关联词时，单情境条件下巩固 24 小时的新词比巩固 0 小时的新词正确率更高。多情境条件下，巩固 24 小时的新词比巩固 0 小时的新词诱发了更小的 N400。这表明，巩固对于新词语义整合起了重要的作用。

结论

习得的新词在经过 24 小时的巩固后实现了语义整合，与语义网络中的语义关联汇产生了联结；多语篇情境促进了新词的语义整合进语义网络，并形成稳定的语义表征。

句法和语义在汉英双语者大脑中的神经表征

侯泽琦，李何慧，徐敏*

深圳大学，心理学院，脑疾病与认知科学研究中心，深圳，518061（通讯作者邮箱：xumin@szu.edu.cn）

目的

句子理解离不开句法和语义加工等复杂的心理过程。基于西方印欧语言的研究表明，句法和语义由不同的神经基础支持。相对于印欧语言，汉语的句法具有独立性偏弱的特点。以往研究发现汉语句法和语义由相同的脑区加工，但在左额下回的精细结构水平上有不同的亚区负责句法和语义的加工。然而，目前尚不清楚汉英双语者大脑中，不同语言的句法和语义差异程度是否会不同。本研究采用功能磁共振成像（functional magnetic resonance imaging, fMRI）技术和启动范式来探究句法和语义在双语者大脑的神经表征。

方法

本研究招募了 44 名母语为汉语、二语为英语且水平较高的健康大学生，采集了被试在进行中英文句子理解任务下的 fMRI 数据。实验采用了启动范式，在呈现的句子中重复不同的语言成分来探测相应的启动效应（如重复呈现相同句法结构但语义不同的句子来探测句法启动效应，或者重复呈现语义相同而句法结构不同的句子来探测语义启动效应）。通过激活分析定位出神经活动随着句法和语义重复逐渐减弱的激活脑区（即表现出句法和语义的启动效应的脑区），并通过多元模式分析 (Multivariate Pattern Analysis, MVPA)分别对两种语言的句法和语义进行分类分析，考察汉英的句法和语义表征模式的差异。

结果和讨论

单变量分析结果表明，汉语和英语可以在双侧额颞叶观察到不同程度的句法和语义启动效应，进一步比较发现，汉语句法和语义启动效应的脑区无显著差异，而英语的句法启动效应比语义的在左额下回（三角部和岛盖部）、左颞中回、右顶上回，双侧中央前回、双侧扣带回等脑区激活更强。由此说明，在汉英双语者中也可以观察到与以往汉语或英语的研究相近的结果。MVPA 分析发现，汉语句子的句法和语义的分类准确率为 69.32%(p=0.0014)，英语句子的句法和语义分类准确率为 84.09%(p=0.0002)，说明句法和语义在两种语言中的神经表征模式是存在差异的。基于单变量分析和多变量分析都表明了英语句法和语义的差异比汉语的更大。

结论

这些结果表明句法和语义的神经表征模式是存在差异的，且英语的差异比汉语的更大，这为揭示双语的神经表征机制提供了新的证据。

儿童句法加工的脑功能偏侧化

严冬甦， 徐敏*

深圳大学，心理学院，脑疾病与认知科学研究中心，深圳，518061（通讯作者邮箱：xumin@szu.edu.cn）

目的

3-5 岁阶段是儿童句法发展的关键时期，儿童习得的句式类型越来越复杂。主谓宾简单句是儿童较早习得的句式，而涉及词序不规范性的复杂句则会较晚习得。在语言加工时，成人的脑神经模式呈现出左侧偏侧化的分布，但我们对于儿童语言发展过程中语言脑网络偏侧化模式却知之甚少。本研究结合近红外功能成像技术和图论的分析方法，考察儿童在加工不同句法复杂度句子时的大脑激活和偏侧化模式。

方法

本研究采集了 30 名 4-5 岁健康儿童（平均 65 个月）在进行语言理解任务下的近红外功能成像数据，以及认知行为数据。采用 32 个发射器和 32 个接收器，构成了左右对称的 24 * 24 个通道，覆盖了与语言加工相关的额叶和颞叶皮层。近红外实验中采用了句子/词汇--图片匹配任务。句子条件包含主动句、被动句和主语从句三种不同句法复杂度的句子类型。实验中被试听到一个句子或一个词汇后，从呈现的两张图片中选择一张符合音频内容的图片。数据分析中，我们主要分析（1）不同实验条件中的脑激活情况；（2）分别构建全通道和左右半球通道的脑功能连接矩阵，通过图论的方法计算不同实验条件下的 global efficiency、local efficiency 和 nodal efficiency，并基于这些指标计算大脑的偏指标 LI [LI=(L-R)/(L+R)]。

结果和讨论

脑激活结果表明，句子和词汇条件都激活了左侧和右侧的额下回，被动句相比简单句在左侧额叶、颞叶和右侧额叶有更强的激活，且右侧激活的通道比左侧通道更多。图论分析结果表明（1）被动句的全脑 global efficiency 显著高于简单句，其他条件无显著差异；（2）被动句的右侧大脑的 global efficiency 显著高于左侧；（3）基于 global efficiency 计算的偏侧化指标 LI 中，被动句显著小于词汇和主语从句，说明复杂的被动句式呈现更强的右侧化；（4）主语从句的偏侧化指标与主语从句理解任务的正确率呈显著正相关 (r=0.5271,p=0.0098)。结果表明，4-5 岁儿童的语言脑网络并没有呈现出显著

的左侧化模式，且在难度相对较大的被动句理解条件下，右侧大脑的网络的全局效率高于左侧大脑。

结论

从脑网络的层面，幼儿在语言加工中尚未体现出显著的左侧化分布模式，并且在加工难度较大的被动句式时，大脑的全局效率更强，右侧大脑的全局效率比左侧大脑更强。研究结果为儿童的语言脑网络发展提供了新的启示。

Functional mapping and cooperation between the cerebellum and cerebrum during word reading

Hehui Li [1], Junjie Wu[2], Rebecca A. Marks[3,4], Huiya Huang[1], Lina Li[1], Lin Dong[1], Yue-Jia Luo[1,5,6,*] , Wuhai Tao[1,*] , Guosheng Ding[5]

1 Center for Brain Disorders and Cognitive Sciences, Shenzhen University, Shenzhen 518060, P.R. China;

2 Key Research Base of Humanities and Social Sciences of the Ministry of Education, Academy of Psychology and Behavior, Tianjin Normal University, Tianjin,300387, P.R. China;

3 McGovern Institute for Brain Research and Department of Brain and Cognitive Sciences, Massachusetts Institute of Technology, Cambridge, MA 02139, USA;

4 Department of Communication Sciences and Disorders, MGH Institute of Health Professions, Boston, MA 02129, USA;

5 State Key Laboratory of Cognitive Neuroscience and Learning & IDG/McGovern Institute for Brain Research, Beijing Normal University, Beijing 100875, P.R. China;

6 College of Teacher Education, Qilu Normal University, Jinan 250200, P.R. China;

*Corresponding author: Center for Brain Disorders and Cognitive Sciences, Shenzhen University, Shenzhen 518060, P.R.

(luoyj@szu.edu.cn; taowh@szu.edu.cn)

Objective

Multiple areas in the cerebellum have been reported to be engaged in reading. However, how these regions cooperate with the reading-related areas in the cerebrum remains unclear.

Methods

Brain images of fifty-two adults were acquired via functional magnetic resonance imaging. The Chinese character recognition test and the character reading efficiency test were administrated to measure Chinese reading abilities. Three localization tasks and one reading task were performed. Localization tasks were used to localize areas specific to orthographic, phonological, and semantic processing. During each task, two Chinese characters were presented horizontally in the center of the screen, and participants made a similarity judgment by pressing left (“yes”) or right button (“no”). During the orthography task, participants were asked to judge whether the two characters looked similar, i.e. shared the same radical. During the phonology task, participants was required to determine whether the two characters were homophones. During the semantics task, participants needed to identify whether the meaning of two characters was related. The reading task was the silent word reading task, during which participants were required to silently read words presented

in the center of the screen and press a button if they saw a star appear.

Results & Discussion

By comparing the cerebellar activation across three localization tasks targeting orthographic, phonological, and semantic processing, we first identified three different reading-related areas in the cerebellum, biased toward orthography, phonology, and semantics, respectively (Figure 1). Functional connectivity (FC) analyses demonstrated that the mean FC between functionally corresponding areas across the cerebrum and cerebellum was greater than that between non-corresponding areas during silent word reading. FC patterns of functionally corresponding areas could significantly predict reading speed, with the FC driven from orthographic and semantic areas contributing the most (Figure 2). Effective FC analyses further showed that orthographic and semantic areas in the cerebellum had selective and direct connectivity to areas in the cerebrum with similar functional specificity (Figure 3).

Conclusions

These results suggest that reading-related areas vary in their functions to reading, and cooperation between areas with corresponding functions was greater than that between non-corresponding areas. These findings emphasize the importance of functional cooperation between the cerebrum and cerebellum during reading from a new perspective.

Acknowledgement:

This work was supported by grants from the National Natural Science Foundation of China (NSFC: 32100846, 31920103009, and 32000793), Shenzhen-Hong Kong Institute of Brain Science-Shenzhen Fundamental Research Institutions (2021SHIBS0003), the Major Project of National Social Science Foundation (20&ZD153), and Science and Technology Planning Project of Guangdong Province, China (2019A050510048). It was also supported by Project funded by China Postdoctoral Science Foundation (Grant No. 2020 M682846) and funded by Open Research Fund of the State Key Laboratory of Cognitive Neuroscience and Learning (Grant No. CNLYB2005).

“我没戴眼镜，听不清”辅助运动区在语音识别中的作用：一项近红外脑功能成像研究

周晨曦*

School of Psychology, Shaanxi Normal University, Xi'an China, 710062

(chenxizhou@snnu.edu.cn)

目的

为什么近视者不戴眼镜会听不清别人在说什么？准确地进行语音识别是人们进行日常交流的重要环节。辅助运动区（Supplementary motor area, SMA）不仅参与运动的计划、启动和执行，还参与语言的识别与处理。语音识别的运动理论认为，人们需要借助发音动作的识别来完成语音识别加工，SMA 在语音识别中的参与激活成为心理语言学研究的关注点。本研究使用近红外脑功能成像（fNIRS）技术，探究不同视听信息匹配度的语音识别的神经机制。

方法

21 名右利手大学生被试参加了本实验。本研究为单因素（视听材料类型：视听一致组、视听冲突组、对照组）被试内实验，采用 fNIRS （ETG- 7100）检测被试额颞区在进行实验任务时的激活情况。实验材料为典型 McGurk 效应的视听整合言语材料，通过预实验证明了材料的有效性，分别为 2 个视听一致材料（视觉信息-听觉信息：ba-ba、da-da），2 个视听冲突材料（视觉信息-听觉信息：ba-ga 、da-ga），1 个对照材料（视觉信息-听觉信息：ma-ma）。

结果与讨论

行为结果发现视听冲突组的正确率显著低于视听一致组和对照组。近红外功能成像的结果发现，：（1）语音感知任务激活了大脑左半球的中央前回(Ch17)、中央后回(Ch12)、额中回(Ch4、Ch9)、额下回(Ch13)、颞上回(Ch3)，右半球的额下回(Ch27)、颞上回(Ch24)显著激活。其中，额下回、额中回是可靠的语音整合区域，而辅助运动区位于中央前回，该区域被认为与计划或者预期有关(Teder-Salejarvii et al., 2002)，反映了被试对语音发音动作的一种期待。（2）语音材料一致性的主效应显著，视听冲突组比视听一致组更多激活了左半球的额中回(Ch4、Ch9)和额下回(Ch13)。表明当人们进行语音识别时，辅助运动区可能会根据感知到的发音动作信息作出预测，从而使语音识别更加快速和精确，而当视听觉信息发生冲突时，语音整合区域就会产生更强的激活。

结论

本研究发现语音识别任务激活了大脑双侧的额颞区，左侧辅助运动区的激活在语音识别中可能起到预测作用。研究结果丰富了语音识别的神经机制研究。

Electrophysiological Evidence of Lexical Processing Impacted by Foreign Language Reading Anxiety

Lina Li[a,b#], Qianqian Yu[c#], Yuru Wang[c], Zhihao Wang[c], Lin Dong[c], Xinyi Zhou[d], Huiya Huang[c], Hehui Li[c*], Yuejia Luo[c,d*]

aFaculty of Life science and Technology, Kunming University of Science and Technology, Kunming, P.R. China;

bEnglish department, Jilin Medical College, Jilin, P.R. China;

cCenter for brain disorders and cognitive sciences, Shenzhen University, Shenzhen, P.R. China;

dState Key Laboratory of Cognitive Neuroscience and Learning & IDG/McGovern Institute for Brain Research, Beijing Normal University, Beijing, P.R. China

#co-first author

*corresponding author

Yue-Jia Luo: luoyj@szu.edu.cn; Hehui Li: Hehuili@szu.edu.cn;

Objective

Extensive studies have investigated the impact of foreign language reading anxiety on reading from the perspective of pedagogy and behavior, but without considering electrophysiological evidence. The present study aimed to explore the influence of foreign language reading anxiety on reading and its associated neural mechanism by Event-related potential (ERP) components associated with reading in bilingual lexical decision tasks.

Methods

Sixty-eight Chinese-English bilinguals were recruited in the current study. Foreign Language Reading Anxiety Scales (FLRAS), English as a Foreign Language Reading Anxiety, and Reading Anxiety Source Questionnaire were administrated to assess the levels of foreign language (FL) reading anxiety. To control for the influence of reading anxiety in the native language (e.g., Chinese) on FL reading anxiety, the participants in the pool completed the Chinese Reading Anxiety Scale (CRAS) adapted from FLRAS. The Chinese version of the State-Trait Anxiety Inventory was also measured to distinguish general anxiety from FL reading anxiety. Besides, the participants were required to complete five reading-related tasks (3 for English and 2 for Chinese) to measure the word reading efficiency of both languages. The stimuli included 120 high-frequency Chinese disyllabic words based on a frequency list from the Chinese Lexical Database and 120 six-to-seven letters high-frequency English disyllabic words from Intelligent Web-base Corpus. For half number of the words for

each type of stimuli, we matched pronounceable pseudo-words by changing the configuration of those real words corresponding to Chinese or English orthographic rules. Participants were asked to perform a lexical decision task to judge whether the visual stimuli of Chinese or English were real or pseudo-word.

Results & Discussion

We found that foreign language reading anxiety was negatively correlated with the reading ability of foreign language regardless of native language. Adults with the low levels of foreign language reading anxiety (LFLRA) demonstrated significant differences in the early lexical component N170 amplitude between foreign and native language, however, this effect in adults with the high levels of foreign language reading anxiety (HFLRA) was absent. For native language, a significant difference between HFLRA and LFLRA was observed in N170 latency. Meanwhile, HFLRA was accompanied by longer latency for foreign language than that for native language. In terms of N400 latency, we observed that LFLRA demonstrated significant differences between foreign and native language processing, but not observed the significant effect in HFLRA.

Conclusions

These results indicated the inefficient activation of lexical information and the problem of semantic processing in individuals with high reading anxiety levels during word processing in a foreign language.

Acknowledgment:

This work was supported by a grant from the National Natural Science Foundation of China (NSFC, No. 32100846). It was also supported by Project funded by China Postdoctoral Science Foundation (Grant No. 2020M682846), Project funded by Guangdong Provincial Science and Technology Plan (Grant No.2019A050510048), Shenzhen-Hong Kong Institute of Brain Science – Shenzhen Fundamental Research Institutions (2022SHIBS0003).

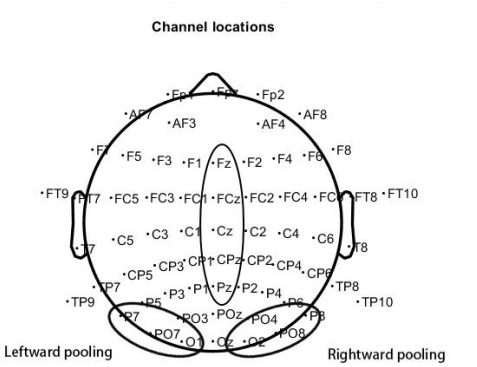

Figure 1. Channel locations. The posterior occipitotemporal and occipital electrodes were clustered on the left and right hemispheres together, while the centro-parietal electrodes were clustered in the central region. ERPs analysis was applied over these electrode sites.

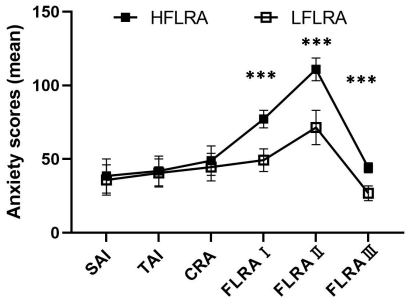

Figure 2. Results of the different anxiety scales. There were significant group differences in these three foreign language anxiety scales (FLRA I, FLRA II, FLRA III), while no group differences in SAI, TAI and CRA.*** depicts significance $p < 0.001$. Note: SAI, State Anxiety Inventory; TAI, Trait Anxiety Inventory; CRA, Chinese Reading Anxiety; FLRAI, Foreign Language Reading Anxiety developed by Satio (1999); FLRAII, English as a Foreign Language Reading Anxiety (EFLRA) by Zoghi (2012); FLRAIII, Reading Anxiety Source Questionnaire; HFLRA, high foreign language reading anxiety; LFLRA, low foreign language reading anxiety.

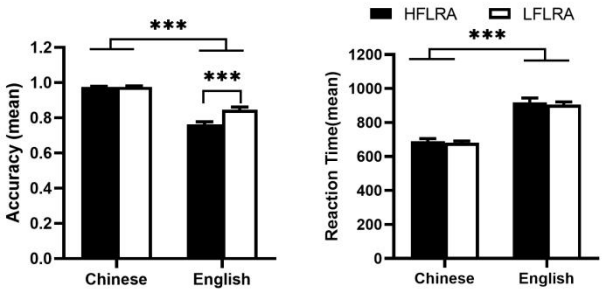

Figure 3. Behavioral performance (mean accuracy and response time) in different languages and

groups. The error bars represent the standard error of the mean.

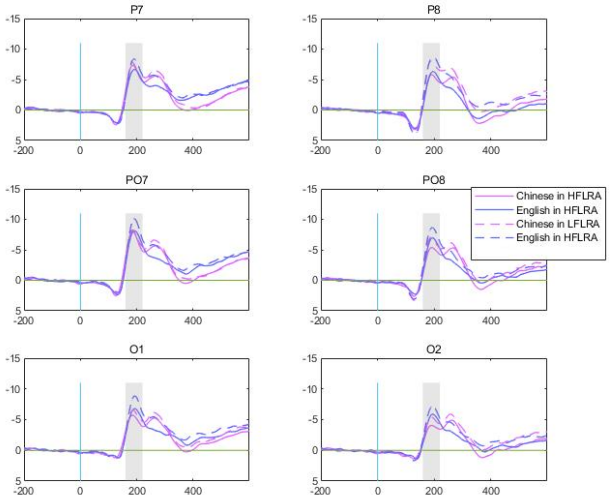

Figure 4. Leftward and rightward event-related potentials over occipitotemporal electrodes for Chinese characters and English words, averaged respectively in HFLRA and LFLRA groups. The y-axis is in μV with negative plotted up. The x-axis is in ms and the shaded areas marked the peak activity in 160-220 ms time window.

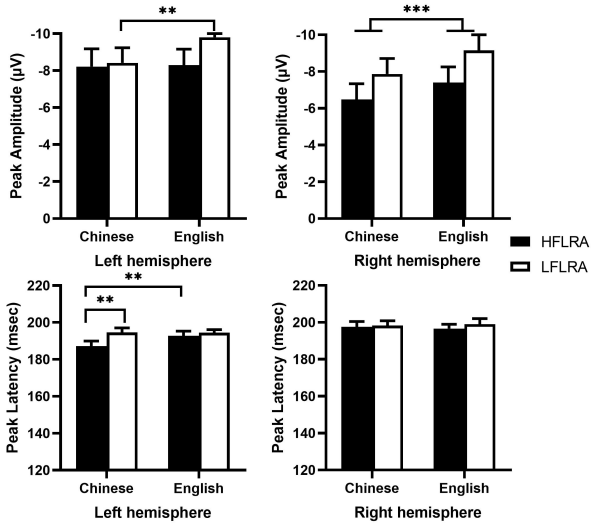

Figure 5. Illustrations of the peak amplitude and latency of the averaged ERPs over the occipitotemporal cortex. ** illustrates significance, $p < 0.01$; *** illustrates significance, $p < 0.001$.

The effect of light colour on moral judgement: event-related potential correlates

Lina Hu, Chengkai Wu, Hongyan Liu, Yan Zheng, Tian Gan*

Department of Psychology, Zhejiang Sci-Tech university, Hangzhou, China, 310018

(gantian@zstu.edu.cn)

Objective

Colour has been shown to have metaphorical meaning of morality. Previous studies found that individuals in white environment showed more moral behaviours than those in black environment. However, very limited study has focused on colour – moral metaphorical association in other coloured environment. This study used a Moral Stroop task and event-related potentials (ERPs) technique to explore the effects of light colours (white, green and red) on the judgement of words related to moral concepts.

Methods

We invited seventeen right-handed students from a university to participate in this experiment. The experiment was conducted in a windowless and sound-shielded room with four colour-adjustable bulbs set in the four corners of the ceiling. The light colours were red (255, 17, 0), green (49, 255, 0) and white (255, 255, 255), and we kept the brightness of the task location the same at 35 lx. The materials were 60 moral words (e.g., kind) and 60 immoral words (e.g., bully). Participants were instructed to judge whether the word was related to morality or immorality respectively in three light conditions.

Results & Discussion

Participants judged immoral words slower than they did moral words in red and white light conditions. This difference failed to reach significance in green light condition. Consistent with these findings, ERP results illustrated that the difference in the mean amplitude of late positive component (LPC) between immoral and moral words only reached significance in red and white lights but not in green light. No interactions were found in P200 or N300 component. The results confirmed the metaphorical associations between morality and white/red light in the late time window.

Conclusions

There are significant Stroop effects of response time and the mean amplitude of LPC in red and white light conditions, suggesting the automatic associations between white/red light and moral message which occurred in the late processing stage. Our work contributes to the literature on colour psychology as well as embodied cognition and conceptual metaphor theories with reliable neural evidence.

Acknowledgement: This work was supported by the NSFC (31400878), the Annual Project of Philosophy and Social Science in Zhejiang Province (22NDJC073YB), MOE Project of Humanities and Social Sciences (14YJC190005) and the Fundamental Research Funds of Zhejiang Sci-Tech University (2021Q055).

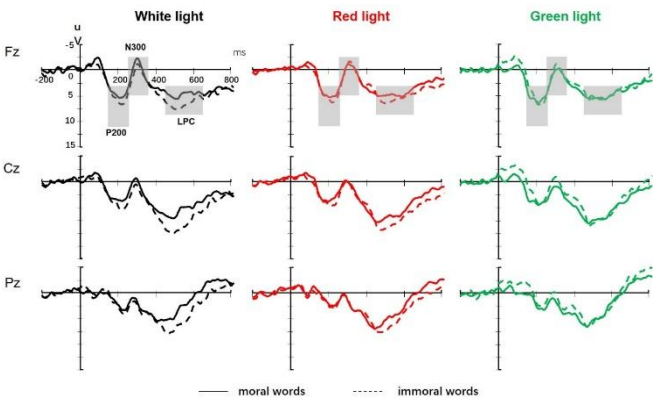

Figure 1. Overview of grand-averaged ERP waveforms in white, red and green lights (take Fz, Cz and Pz sites as examples)

How do moral dimensions and gender influence people's attitudes toward artificial intelligence as violating moral foundations

Yue He[1], Fang Cui[1], Ruolei Gu[2,3], Yuejia Luo[4]

1 School of Psychology, Shenzhen University, Shenzhen, 518060, China

2 CAS Key Laboratory of Behavioral Science, Institute of Psychology, Beijing, 100101, China

3 Department of Psychology, University of Chinese Academy of Sciences, Beijing, 100049, China

4 State Key Laboratory of Cognitive Neuroscience and Learning & IDG/McGovern Institute for Brain Research, Beijing Normal University, Beijing 100875, China

Objective

Previous studies hold that only humans can be the subject of immoral behavior. However, with the development of science and technology, Artificial intelligence (AI) is more and more widely involved in human social life, so it may also be perceived as the subject of violating moral behavior under certain circumstances. Do people use a different standard to evaluate others and AI? Recent studies have begun to focus on these issues, but tend to overlook the multidimensional construct of moral violation and seldom consider the role of gender differences.

Methods

Based on the moral foundation theory, we divide moral violations into six categories (harm, fairness, authority, loyalty, purity, and liberty) and set non-moral behavior (behavior unrelated to moral standards) as the baseline. 160 participants (half female) were asked to rate the morality of humans and AI in these seven conditions, respectively.

Results & Discussion

Results showed a significant gender effect, that is, the data on moral rating showed that men were more tolerant of "immoral AI" than "immoral human" in these six moral dimensions, in the same way as women on harm, fairness, purity and liberty dimension, but not the same way as women on authority and loyalty dimensions. These studies help us understand how people make moral judgments involving AI, and lay the foundation for further exploration of relevant brain mechanisms in the future.

Electrophysiological Signatures of moral intention and outcome learning in moral judgment

Gaojie Huang, Chen Qu*

Key Laboratory of Brain, Cognition and Education Sciences, Ministry of Education, China; School of Psychology, Center for Studies of Psychological Application, and Guangdong Key Laboratory of Mental Health and Cognitive Science, South China Normal University, Guangzhou, China, 510631

(fondest@163.com)

Objective

Moral judgment on individuals requires learning individuals' moral intention and outcome. The neural circuity involved in moral judgment has been well studied. Yet, it remains unclear how people learn individuals' moral intention and outcome in moral judgment. Here, we investigated the electrophysiological signatures of moral intention and outcome learning by using an "uncertainty harm decision task" in combination with event-related potentials (ERPs) and computational modeling.

Methods

38 right-handed students were recruited from a university. We developed the task to dissociate agent's intention and outcome by using probabilistic turntables caused uncomfortable noise. Participants were instructed to trail-by-trail predicted and observed the choices of turntable (intention) and noise result (outcome) of four agents identified by four faces taken from the Chicago Face Database. This allowed participants to separately perceive and learn agent's intention and outcome. The four agents differed in the probability of choosing dark turntable (good/bad) and the probability of noise (good/bad). A total of 200 choices in five blocks made by four agents, presented one at a time in random order. After observing a given choice and outcome, participants were asked to make moral judgment ('How much blame of the agent should be deserved for what happened') for the agent.

Results & Discussion

We found that participants learned and updated their expectations on agent's intention and outcome based on the trail-by-trail feedback, and these updates were well described by the prediction error based reinforcement learning algorithm. Learning of moral intention and outcome were evenly weighted for moral blame rating. Neurally, intention prediction error (iPE), especially for good intention agents, was encoded by the N170 component, which was measured at occipital-temporal

(PO7 and PO8) as the maximal negative peak in the time window 150-190ms. While the outcome prediction error (oPE) were reflected in the P300 component especially when learning good outcome agents measured at CPz in the time window 350-450ms. The dissociated result indicated that participants can quickly differentiate agents' intention when learning moral intention. Furthermore, the parietal activity (LPP) independently reflected iPE and oPE in the time window 600-700ms. The larger LPP effect was found when learning good intention or good outcome agents for moral outcome learning, but only when learning good intention agents for moral intention learning.

Conclusions

Our results suggested that the brain employed different processing mechanisms for moral intention and outcome learning. Our study provides initial evidence on electrophysiological signatures of moral intention and outcome learning in moral judgment.

Acknowledgement: This work was supported by the Program for National Natural Science Foundation of China (31970982; 32171019)

特质焦虑和框架效应对信任决策的交互影响-来自眼动实验的证据

王蓉，罗跃嘉*

心理学院，成都医学院，成都，610500(luoyj@szu.edu.cn)

目的

人际信任被定义为一个人 (即委托人) 的心理状态，包括对另一个人（受托人）互惠行为的积极期望以及信任另一个人带来的脆弱性。人际信任的复杂性和重要性促使研究人员多年来使用诸如信任博弈之类的标准化范式来获得大量实验数据。最近的研究表明，焦虑程度的减少会伴随着信任程度的增加，以及相比于获得框架，信任更有可能发生在损失框架中。然而，关于特质焦虑和框架效应对信任决策的影响仍然是不清楚的。因此，我们试图通过眼动技术来揭示特质焦虑和框架效应对信任决策的交互影响。

方法

通过特质焦虑问卷，从大学里筛选出 66 名被试。其中高特质焦虑 33 人，低特质焦虑 33 人。实验为 2*2 的两因素两水平设计，其中特质焦虑分为高，低两种水平，框架分为获得和损失两种水平，因变量为信任决策。被试需要完成 240 个实验试次。实验流程如下：首先，屏幕呈现第一个注视点，持续约 0.5 秒。然后呈现伙伴信息，持续 1 秒。在选择阶段中（最多 6 秒），被试将通过“左右”按键进行选择信任或者不信任。当被试选择不信任时，伙伴的选择无效，将直接按照被试的选择获得或损失相应积分；当被试选择信任时，将按照伙伴的选择获得或损失相应积分。接下来，在反馈阶段中（1.5 秒），被试将看到伙伴的真实选择。

结果与讨论

行为结果发现在男性个体上存在特质焦虑和框架的交互作用，其中，在高特质焦虑中，损失框架的信任率显著高于获得框架下的信任率。眼动结果：在划定的兴趣区中，被试更多关注自己的分数，较少关注伙伴的分数；在不同兴趣区之间的转换能够预测接下来的信任决策，其中，在自己得分中间的区域和得分最多的区域看得越多，被试越可能选择不信任；在自己得分最少和最多的区域看的越多,被试越可能选择信任。

结论

通过这个研究，我们揭示了高特质焦虑男性个体在做信任决策时，损失框架下信任程度更高。眼动数据说明了被试更关注自己的分数，并且通过比较自己获得或损失分数的大小来做出最终的决策。我们的研究对于揭示特质焦虑在信任决策中的加工过程提供了更直接的眼动证据，并且验证了框架效应对信任决策的影响。

The impact of social context on the neural signature of social hierarchy

Yaner Su [1, 2] Sander Martens [2] André Aleman [1, 2] Jiali Zhou [1]

Pengfei Xu* [3] Yue-jia Luo* [1]

(1) Shenzhen Key Laboratory of Affective and Social Neuroscience, Center for Brain Disorders and Cognitive Neuroscience, Shenzhen University, Shenzhen 518060, China

(2) Department of Biomedical Sciences of Cells & Systems, Section Cognitive Neuroscience, University Medical Center Groningen, University of Groningen, Groningen, The Netherlands

(3) Beijing Key Laboratory of Applied Experimental Psychology, National Demonstration Center for Experimental Psychology Education (BNU), Faculty of Psychology, Beijing Normal University, Beijing 100875, China

(Yue-jia Luo: luoyj@szu.edu.cn; Pengfei Xu: pxu@bnu.edu.cn)

Objective

Social hierarchy is a ubiquitous feature of social organization. The ability to quickly recognize social hierarchy information is crucial for social life. Although social contexts such as competition and cooperation have a different impact on the perception of social hierarchy, the findings about perception of social hierarchy are partly inconsistent. Here, we adopted fast periodic visual stimulation (FPVS) with electroencephalography (EEG) to assess the neural signature of social hierarchy in different social contexts.

Methods

Fifth-four participants were instructed to learn the social rank through either a competitive or cooperative context game. Subsequently, they were required to view oddball sequences of face pictures. In such sequences, a new face picture served as the base stimulus and was presented repeatedly at 6Hz (6 images appeared in one second). A face picture with the rank information they previously learned was inserted at every fifth picture, which served as the oddball stimulus and thus generated a periodic repeated change at 1.2Hz (6Hz/5 = 1.2Hz). Participants were asked to pay attention to the center of the screen and press the spacebar when the central fixation cross changed color.

Results & Discussion

Neural responses were observed at the specific frequency corresponding to the rank-specific face. Specifically, the superior and the inferior players induced greater

brain responses than the medium players, revealing neural markers in detecting social hierarchy information. The rank-specific response was more pronounced in the competitive context compared to the cooperative context, suggesting that participants were more sensitive to social hierarchy information in the competitive situation.

Conclusions

Our study provided neurophysiological evidence for the automatic processing of implicit social hierarchy information, supporting that the emergence of social hierarchy could be detected in a single glance. Importantly, individuals encode social hierarchical information in different ways under differently social contexts.

社会比较对合作决策的影响——来自ERP的证据

黄一璠，胡馨木，买晓琴*

中国人民大学心理学系，北京，100872，maixq@ruc.edu.cn

目的

以往研究表明，在各类社会困境任务中，互动对象的选择会对个体的合作决策产生影响，这说明可参照信息会通过社会比较，进而作用于社会决策的潜在心理加工过程。现有研究多在提供完整的他人决策信息下展开，而较少聚焦于不完整参照信息对合作选择的影响。本研究采用事件相关电位技术(event-related potential, ERP)考察不完整社会比较信息对合作行为的影响及其背后的神经机制。

方法

本研究共招募北京某高校大学生被试 32 名，使用 Biosemi 64 导联脑电设备记录其脑电活动。被试需完成改编后的多轮单次四人小组公共物品博弈任务(public goods game, PGG)，每一轮任务中，被试会先得知组内随机两名玩家的选择，之后需决定是将自己的当轮禀赋全部保留还是全部投出。其他两名玩家的选择共构成三类社会比较信息条件(两人均保留/一人投入一人保留/两人均投入)；此外，我们设置了其他组员为电脑玩家的实验条件，此时虚拟玩家的选择作为非社会性的参照信息，与来自人类玩家的社会性参照信息形成对照。

结果和讨论

行为结果表明：(1)合作率上，随着其他玩家投入的增加，个体的合作意愿增加，同时，在另两名玩家选择混合及均选择投入的情况下，个体均在与人类玩家的互动中表现出了更高的合作性；(2)反应时上，当已知两名玩家的选择混合时，个体的反应时显著长于他人均选择不投入时。ERP 结果显示：(1)当两名玩家均不投入和选择混合时，N1 波幅均在与电脑玩家进行任务时更负，但在均投入情况未发现此玩家身份的调节作用；(2)相较于均投入的情况，两名玩家均不投入和选择混合时显著诱发了更负的 FRN；(3)两名玩家均投入时的 P3 波幅显著高于二者选择混合和均不投入时,同时，与两名电脑玩家均不投入的情况相比，来自人类玩家的双双卸责会诱发更大的 P3；(4)LPP 对参照信息敏感，在其他玩家均投入时较混合选择时更正，而在两名玩家均不投入时，任务伙伴为人类玩家时所引发的 LPP 波幅更大。

结论

个体的合作程度随着其他玩家合作意愿的增加而增加，且这一可参照信息的影响更多地体现在与社会性伙伴的互动中；同时，相较于他人选择一致的情况，冲突性的社会比较信息会增加个体的决策时间，提示着更加复杂的决策过程。从神经加工进程上来看，可参照信息的社会性属性对个体关于他人合作选择的早期

加工存在较大影响，而该信息所包含的社会比较知识则对随后的中晚期加工过程有着持续的调节作用。本研究揭示了社会比较信息与个体合作决策间的联系，为进一步理解影响合作行为的相关情境因素具有一定的启示。

共情关怀对亲社会欺骗行为的影响及其神经机制

俞含露，张英良，买晓琴*

中国人民大学心理学系 北京 100872

(maixq@ruc.edu.cn)

目的

欺骗是一种有意诱导他人相信某种错误信念的行为。在我们的生活中，欺骗并不都只是为了自己获益或者避免损失，还存在一些具有亲社会行为性质的欺骗行为，比如个体为保护他人自尊心所说的“善意的谎言”（white lies）。亲社会欺骗是个体通过欺骗，自愿做出符合社会期望但并不直接使自己获益的行为。已有研究证实欺骗过程需要更多的认知资源。本研究采用事件相关电位（event-related potential, ERP）技术，考察在共情关怀作用下亲社会欺骗和亲自我欺骗在行为和神经活动方面的异同。

方法

31 名健康大学生完成了多轮改编版猜硬币任务（Coin-Guessing Task），被试需要为自己或者其他受益人猜测硬币结果。我们采用 Neuroscan 64 导联脑电系统进行数据采集。通过共情关怀启动，向被试提供不同受益人的背景信息，操控共情关怀水平，诱发被试的亲社会欺骗行为。我们在被试完成任务的同时记录了脑电数据，并分析了在欺骗决策阶段和欺骗反应阶段的脑电数据。

结果和讨论

行为结果显示，在欺骗的决策阶段，相比于无机会欺骗条件，被试在有机会欺骗条件下需要花更多时间完成欺骗行动。当欺骗的受益人为自己时，被试的欺骗频率最高。在欺骗频率上，我们还观察到了受益人和欺骗机会的交互作用，共情关怀启动诱发了被试的亲社会欺骗，当受益人为高共情他人时，相比无机会欺骗，在有机会欺骗条件下时，被试会有更高的欺骗频率。ERP 的结果发现，在欺骗决策阶段，有机会欺骗条件下存在 N2 波幅增大-P3 波幅减小的效应。并且在 N2 和 P3 均出现了欺骗频率和欺骗机会的交互作用，相较于欺骗频率低的被试，欺骗频率高的被试在有机会欺骗条件时，出现了 N2 增大-P3 减小的效应。在欺骗反应阶段，额中部负波（medial frontal negativity, MFN）和 P3 出现了受益人和欺骗机会的交互作用。进一步分析发现，当受益人为自己时，相较于无机会欺骗条件，有机会欺骗条件诱发了更负的 MFN 波幅和更大的 P3 波幅。但当受益人为高共情他人时，有机会欺骗和无机会欺骗条件并没有差异。

结论

本研究重复了前人在欺骗过程中发现的 N2-P3 效应，进一步发现了不同共情关怀启动水平下的亲社会欺骗与亲自我欺骗在行为和神经层面的差异。欺骗频

率不同的被试在冲突监控、冲突解决和结果评价等心理过程中出现了神经水平的差异。被试在进行亲自我欺骗时可能产生了最大的冲突和矛盾，而进行亲社会欺骗时可能经历的认知负荷最小。

共情关怀和结果公平性对第三方惩罚的影响

何怡娟，买晓琴*
中国人民大学心理学系 北京 100872
(maixq@ruc.edu.cn)

目的

第三方惩罚对于维护社会规范具有重要作用，了解其影响因素和机制至关重要。与以往探讨对受害者的共情对第三方惩罚的影响不同的是，本研究旨在采用事件相关电位技术(event-related potential, ERP)探讨对违规者的共情关怀是否会干扰第三方惩罚决策认知过程以及行为表现，同时关注特质共情的作用。一方面有助于我们从不同的角度理解共情对第三方决策的作用，另一方面可以提供科学证据应用于公众监管和教育中，避免媒体利用第三方的同情心操纵舆论干扰司法公正。

方法

24 名大学生完成了多轮单次第三方惩罚(the third-party punishment, TPP)任务。我们采用 Neuroscan 64 导联脑电设备记录其脑电活动。通过操纵提议者的身份来诱发被试的状态共情：有共情情境下提议者身份为留守学生，无共情情境中则为普通学生。接受者均为普通学生，分配方案包含公平分配、中度不公平分配和极度不公平分配三类，被试作为第三方可选择支出自己每一轮的收益来降低不公平提议者的收益，惩罚比率为 1：2。任务结束后测量个体的特质共情。

结果与讨论

行为结果发现相比于无共情情境, 个体对有共情情境下的不公平分配方案感知到的不公平程度更低, 相应地对独裁者的惩罚力度、道德义愤也更低；脑电结果显示：有共情情境下，P2 和 MFN 都未表现出公平性效应；无共情情境下，中度不公平诱发了更小的 P2 和更大的 MFN；LPC 仅表现出来公平性效应，不受共情关怀的调节。特质共情同样调节了公平效应，相比于公平条件，不公平条件下，个体的特质共情能够正向预测 TPP 力度和 MFN 波幅；中度不公平条件下，个体的特质共情水平能够正向预测个体的 P2 和 LPC 波幅。

结论

本研究通过对违规者身份的操纵将个体关注的重心转移到了违规者身上, 降低了个体对不公平结果的关注度, 削弱了不公平程度带来的效应, 同时通过调节公平感知度降低了第三方惩罚力度, 体现了共情关怀对第三方决策的干扰；在无共情情境中, 中度不公平引发了个体更大的认知和情绪冲突, 表明对违规者的共情关怀会削弱这种冲突。特质共情也会调节第三方惩罚力度以及相应的认知过程，可能是由于个体评估不公平程度和决策惩罚力度的角度的不同, 这提示我们在第三方决策中, 可以通过转移第三方的关注点来调节个体的感知和行为。

The neural pathway linking loss aversion to social conformity

Yiman Li[1], Nicholas T. Van Dam[2], Zhihao Wang[1], Jiali Zhou[1], Xinchun Wu[3*], Yuejia Luo[1,3], Pengfei Xu[3,4*]

1 Center for Brain Disorders and Cognitive Sciences, Magnetic Resonance Imaging Center, Shenzhen University, Shenzhen, China

2Melbourne School of Psychological Sciences, University of Melbourne,

Melbourne, Australia

3 Beijing Key Laboratory of Applied Experimental Psychology, National Demonstration Center for Experimental Psychology Education (BNU), Faculty of Psychology, Beijing Normal University, Bejing, China

4 Center for Neuroimaging, Shenzhen Institute of Neuroscience, Shenzhen, China

(pxu@bnu.edu.cn)

Objective

The influences of others' choices on individual decision-making are modulated by individual risk preferences. However, the role of loss aversion in social decision-making remains unclear. Here, we used a gambling task to examine the roles of individual preferences of risk and loss, as well as an examination of social conformity in decision-making under uncertainty.

Methods

Fifty-two healthy participants were recruited for the current study. we manipulated social pressure in a gambling task with functional magnetic resonance imaging (fMRI) to examine the neurocognitive mechanisms of loss aversion, risk aversion, and social pressure in decision making. To examine the roles of individual and social preferences in social decision-making, we employed a hierarchical Bayesian approach to estimate the parameters of loss aversion, risk aversion and other-conferred utility in two computational models. Next, to explore the mechanism of the interaction between loss aversion and social stress in the brain, we performed whole-brain activation analysis and psychophysiological interaction (PPI) analyses.

Results & Discussion

The results showed that loss aversion contributes the most to predicting decisions, and interacting with social information. Individuals with high loss aversion showed higher conformity when observing others' choices of safe options, which was associated with increased functional connectivity between the anterior insular cortex (AIC) and the temporoparietal junction (TPJ).

Conclusions

Our findings suggest the crucial roles of loss aversion and the AIC-TPJ neural pathway in social decision-making. This work provides important neural computational evidence for the way that individual preferences interact with social information in human behaviors.

Acknowledgement: This study was funded by the National Natural Science Foundation of China (31920103009 and 31871137), the Major Project of the National Social Science Foundation (20&ZD153), the Young Elite Scientists Sponsorship Program by the China Association for Science and Technology (YESS20180158), Guangdong International Scientific Collaboration Project (2019A050510048), Guangdong Key Basic Research Grant (2018B030332001), Shenzhen-Hong Kong Institute of Brain Science-Shenzhen Fundamental Research Institutions (2019SHIBS0003), and Shenzhen Science and Technology Research Funding Program (JCYJ20180507183500566).

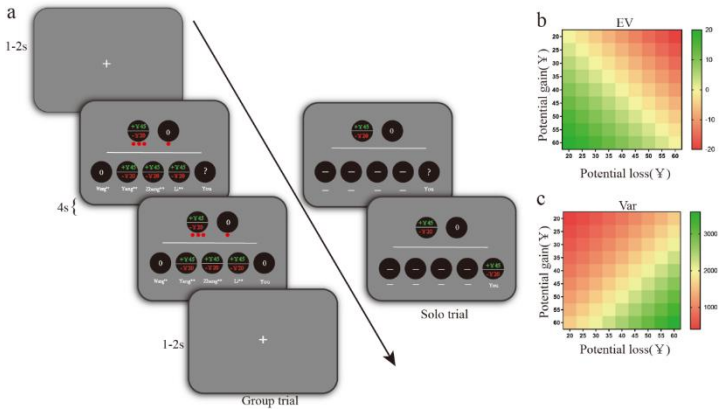

Figure 1. Task design. Participants were asked to choose between risky and safe options. (a)The task contained two types of trials: In Solo trials, participants made the choice alone; In Group trials, participants observed the choices of four other "players" before making their own choice. The safe option in all trials was fixed at "0", meaning no potential gain or loss; the risky option means there was a 50% chance of gaining the amount associated with the green number on the top and a 50% chance of losing the amount associated with the red number on the bottom. (b) The expected value and (c) variance of risky options in each trial.

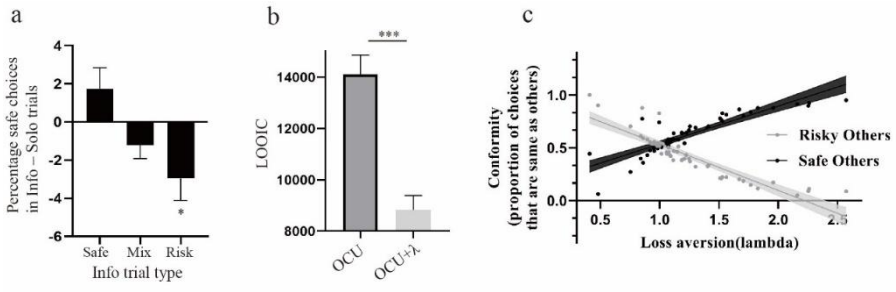

Figure 2. Behavior results. (a) Percentages of choosing the safe option in the safe influence condition, risky influence condition and mixed condition, compared to those in the Solo condition. (b) The LOOIC value in the models with and without the loss aversion. (c) Conformity in the safe and risky influence conditions. Participants with higher loss aversion were more inclined to follow the others' safe option and less inclined to follow the others' risky option.

Figure 3. Brain activity and connectivity of OCU-modified utility and its interaction with loss aversion. (a) Response of the utility difference (Uocu:safe- Uocu:risky) under the group condition was encoded in bilateral TPJ and bilateral vlPFC. (b) Relationships of loss aversion with activation of the anterior insula (AI), striatum and dorsal anterior cingulate cortex (dACC). Loss aversion was associated with responses in bilateral AI, left striatum and bilateral dACC. (c) Modulations of OCU-modified utility on

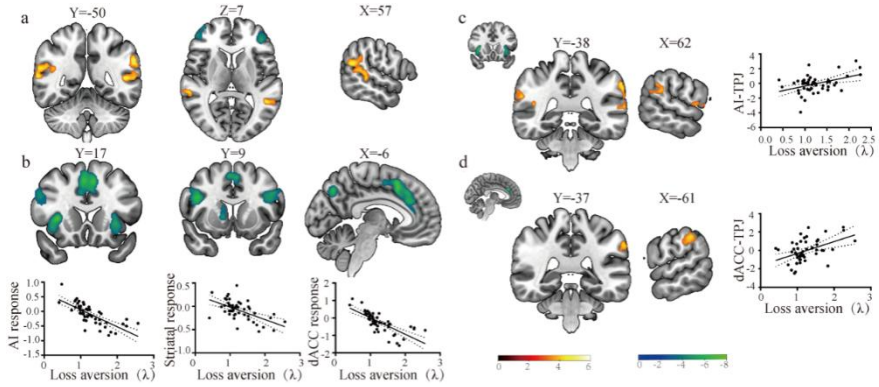

connectivity between bilateral AI and bilateral TPJ. (d) Connectivity between bilateral dACC and TPJ was positively related to loss aversion.

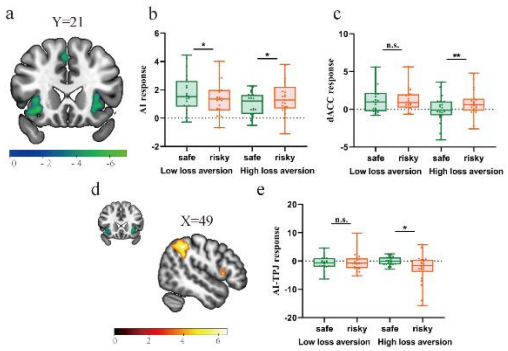

Figure 4. Brain activity and connectivity of the direction of social pressure and its interaction with loss aversion. (a) Responses of the AI and dACC to the interaction between the direction of social pressure and loss aversion in the conformity condition. (b) Activation of the AI in risky influence conditions and safe influence conditions in the high and low loss aversion groups. (c) Activation of the dACC in risky influence condition and safe influence condition in the high and low loss aversion groups. (d) Modulations of the direction of social pressure on connectivity between bilateral AI and TPJ were positively related to loss aversion. (e) Connectivity between the AI and rTPJ in the safe influence condition and risky influence condition in the high and low loss aversion groups.

损失框架对诚实和慷慨偏好的不同影响

石佩[1],周馨怡[1] 封春亮[2,3], 罗跃嘉[1*]

1北京师范大学心理学部，认知与学习国家重点实验室，北京; 2华南师范大学心理学院，广州; 3华南师范大学，广东省心理健康与认知科学重点实验室，广州<

(luoy j@bnu. edu. cn)

目的

亲社会行为泛指促进他人利益的行动，包含慷慨与诚实等多种形式，容易受到社会情境因素的调节。人类在决策时对损失往往比收益更加敏感，并且在收益与损失框架下表现出不同的决策行为。然而，损失/收益框架对亲社会行为的影响机制尚不清楚，以往研究发现损失框架相对于收益框架提高了亲社会行为，而其他研究则发现相反的结果。这些相互矛盾的证据可能是因为测量不同社会偏好的互动游戏对于损失情景的敏感性不同。本研究旨在分离慷慨和诚实这一亲社会行为的同时，评估情景对慷慨和诚实这两种亲社会行为的影响。

方法

本研究共招募 53 名在校学生作为有偿志愿者参与实验。采用的独裁者游戏和信息游戏来分离慷慨和诚实的偏好。慷慨被操作化为被试接受个人成本以惠及匿名陌生人的程度，诚实偏好被操作化为被试以发送者身份想接收者报告真实信息的程度。本研究特别采用 2（游戏类型：独裁制游戏 VS 信息游戏）×2（情景：损失 VS 收益）被试内设计来分离慷慨和诚实的亲社会偏好，独裁者游戏被用来探测慷慨偏好的基线，而信息游戏除了慷慨的关注，还包括诚实的关注，需要加以分离。

结果与讨论

我们使用 R 中的 lmerTest 工具包对被试的社会决策进行了广义混合线性模型分析。结果发现，游戏类型的主效应显著，与独裁者游戏相比，信息游戏中被试的利己率较低；游戏类型和情景的交互作用显著，在信息游戏中，在损失情境下的利己率显著高于收益领域，然而在独裁者游戏中没有明显的影响，也就是说损失情景减少了信息游戏中的利他行为(即诚实行为)的发生，但对独裁者游戏中利他行为没有影响。同样，诚实效应的分析发现与收益情景相比，损失情景的诚实转化率更低，即损失情境导致了更低层次的诚实关注。总的来说，根据信息游戏的结果，可以从一定程度上说明损失情景减少了对诚实行为，这一发现与损失厌恶理论相一致，即相比于喜欢平等，人们更讨厌忍受损失。

结论

我们的行为结果表明，在信息游戏中，损失情景降低了诚实的行为，支持了损失厌恶理论的观点。但是对于损失情景在独裁者游戏中的慷慨偏好和信息游戏中诚实偏好影响存在不一致的结果，对于此还需要进行进一步探讨。

Oxytocin modulates social brain network correlations in resting and task state

Qingyuan Wu, Qi Huang, Chao Liu*, Haiyan Wu*

Centre for Cognitive and Brain Sciences and Department of Psychology, University of Macau, Macau, China

State Key Laboratory of Cognitive Neuroscience and Learning & IDG/McGovern Institute for Brain Research,

Beijing Normal University, 100875, Beijing, China

E-mail: liuchao@bnu.edu.cn(C.L); haiyanwu@um.edu.mo(H.W)

Objective

The effects of oxytocin (OT) on the social brain can be tracked upon assessing the neural activity in resting and task states, and developing a system-level framework for characterizing the state-based functional relationships of its distinct effect. Here, we contribute to this framework by examining how OT modulates social brain network correlations during resting and task states, using fMRI.

Methods

First, we investigated network activation, followed by an analysis of the relationships between networks and individual differences. Subsequently, we evaluated the functional connectivity in both states. Finally, the relationship between networks across states was represented by the predictive power of networks in the resting state for task-evoked activities. Meanwhile, the differences in the predicted accuracy between the subjects were used to display individual variations in this relationship.

Results & Discussion

Our results showed that the activity of the dorsal default mode network (DDMN) in the resting state had the largest predictive power for task-evoked activation of the precuneus network (PN) only in the OT group. The results also demonstrated that OT reduced the individual variation of PN in the prediction process.

Conclusions

These findings suggest a distributed but modulatory effect of OT on the association between resting and task-dependent brain networks.

Acknowledgement: This work was supported by the NSFC (U1736125).

社会权力感和损益情境对不公平厌恶的影响

侯庆辉*　孟亮

上海外国语大学，国际工商管理学院，上海外国语大学脑与认知科学应用重点实验室，上海，201620(houqinghui1992@163.com)

目的

以往研究表明社会权力感会影响个体的不公平厌恶，但在不同损益情境下社会权力感如何影响不平等厌恶以及其中的大脑机制仍未知。本研究结合 ERP 技术探究社会权力感和损益不同情境对个体产生不公平厌恶的影响。

方法

48 名有效被试被随机分配到高低权力感组。本研究使用想象式写作任务的启动方法操纵个体的权力感，使用改进的最后通牒（UG）研究范式作为不公平厌恶范式。在 UG 范式中，共包含分配者和接受者，被试作为接受者参与其中。在获益情境下，被试被告知他和分配者共同获得 10 元收益；在损失情境下，被试被告知他和分配者共同承担 10 元的损失；在每轮中由分配者决定双方获益或损失的金额。面对不同公平程度的分配方案，被试可以选择接受或拒绝。如果被试选择接受该方案，那么该方案将被执行；如果拒绝，获益情境下双方都得到 0 元，损失情境下都会损失 10 元。

结果

行为结果发现，相比低权力感个体，高权力感个体对不公平分配方案的拒绝率更高，即不公平厌恶更高。脑电结果显示，高权力感组比低权力感组在面对不同公平性的分配方案时诱发了更显著的 d-FRN，这种差异仅存在于获益情境中。P300 成分的差异同样受权力感的影响，高权力感个体在损益两种情境下对不同公平程度的分配方案产生的 P300 振幅都有显著的差异，而低权力感个体则无差异。

结论

高权力个体对不公平厌恶更加敏感；FRN 可能仅对收益情境下对不公平反应更加敏感，而 P300 在收益和损失情境下对不公平反应都比较敏感。

Neural sensitivity to helping outcome predicts helping decision in real life

Tian Gan[1,*], Ying Zhang[1], Lisha Zhang[1], Ruolei Gu[2,3,*]

1 Department of Psychology, Zhejiang Sci-Tech University, Hangzhou, China, 310018 (gantian@zstu.edu.cn)

2 CAS Key Laboratory of Behavioral Science, Institute of Psychology, Chinese Academy of Sciences, Beijing, China, 100101 (gurl@psych.ac.cn)

3 Department of Psychology, University of Chinese Academy of Sciences, Beijing, China

Objective

Prosocial helping behavior is a highly valued social practice across societies, but the willingness to help others varies among persons. The current study aims to explain this variability from the perspective of helping outcome sensitivity.

Methods

Forty-one students were recruited as paid volunteers from Zhejiang Sci-Tech University in Hangzhou, China. Participants were asked to make helping decisions in a series of hypothetical scenarios, which provided outcome feedback (positive/negative) of those decisions. Event-related potential (ERP) response to helping outcome was recorded, such that the feedback-related negativity (FRN) and P300 were supposed to reflect the sensitivity to negative outcome and positive outcome, respectively. After the formal task, participants were asked if they would like to donate money to a charity.

Results & Discussion

Consistent with our hypothesis, we found that compared to those who were not willing to donate, the participants who donated money (22 of 41 individuals) showed a smaller FRN but a larger P300. Among these participants, the amount of donation was negatively correlated with FRN response to negative outcome, but positively correlated with P300 response to positive outcome.

Conclusions

The results showed that among those participants who were willing to donate, their donation amount decreased as a function of the FRN associated with negative outcome, but increased as a function of the P300 associated with positive outcome. These findings support the importance of helping outcome sensitivity to prosocial

behavior.

Acknowledgement: This work was supported by the Annual Project of Philosophy and Social Science in Zhejiang Province (22NDJC073YB), the Fundamental Research Funds of Zhejiang Sci-Tech University (2021Q055), and NSFC (32071083, 32020103008).

脑电大尺度网络构建及其在认知研究中的应用

易婵琳[1,2]，陈春丽[1,2]，邱源[1,2]，尧德中[1,2]，李发礼[1,2]，徐鹏[1,2,*]

1 电子科技大学 神经信息教育部重点实验室 成都脑科学研究院临床医院 中国成都 611731

2 电子科技大学 信息医学研究中心 生命科学与技术学院 中国成都 611731

(xupeng@uestc.edu.cn)

研究背景

脑电大尺度网络提供大脑交互毫秒级分辨率的复杂信息，对于理解大脑分布式处理，揭示大脑高效运作的本质具有重要意义。然而脑电大尺度网络分析受到信噪比、容积效应、空间信息模糊等影响，这为可靠的捕捉大脑内大尺度交互信息带来挑战。因此本文针对脑电大尺度网络分析面临的困境，提出系列从头表到皮层、静态到动态的大尺度网络构建方法，并将其应用到运动想象、P300、决策等大尺度网络分析当中。

方法过程

针对脑电信号的低信噪比问题，我们提出基于非参数格兰杰因果方法构建大尺度时变有向网络，以数据驱动的方式捕捉大脑内的定向因果信息。考虑到头表网络分析面临的容积效应和空间模糊等问题，提出在皮层空间基于先验模板和数据驱动两个方面的多种从静态到动态的脑电大尺度功能网络连接分析方法，实现了高时空分辨率的大尺度网络构建。

结果和讨论

研究结果表明，相较传统方法，非参数格兰杰因果方法对噪声具有更高的鲁棒性，更擅长捕获大尺度网络微小的时变信息，能够揭示运动想象各阶段的变化特征。系列皮层网络分析方法能够从不同视角可靠的描绘大脑内功能网络之间的交互，实现高时空分辨率场景下的大尺度网络分析，揭示了决策、P300 等认知过程特有的交互模式。

结论

我们的研究为脑电大尺度网络分析提供了系列不同视角的可靠构建方法，为深度挖掘大脑内大尺度瞬时交互模式提供了技术基础。

致谢：国家自然科学基金项目(#61961160705，#U19A2082， #62103085)；四川省科技厅项目(#2021YFSY0040， #2020ZYD013)；澳门特别行政区科技发展基金项目(文件编号: 0045/2019 / AFJ)。

EEG Complexity Analysis for Epilepsy Diagnosis and Seizure Detection in Normal, Acute and Chronic Stages

Shiming Zheng[1], Xi Gong[1], Panpan Song[2], Yue Hu[2] and Xiaoling Peng[1*]

[1] Guangdong Provincial Key Laboratory of Interdisciplinary Research and Application for Data Science, BNU-HKBU United International College, Zhuhai 519087, China

[2] Department of Neurology, Children's Hospital of Chongqing Medical University

Objective

Epilepsy is a brain dysfunction syndrome characterized by recurrent epilepsy caused by abnormal discharge of brain neurons. The automatic precision detection technology based on electroencephalography (EEG) has essential research value in epilepsy research. The purpose of this work is to study the normal, pre-acute, acute, and chronic phases during epileptogenesis via different complexity indicators.

Methods

After wavelet transform with haar level 5 wavelet, five common used complexity indicators including approximate entropy (ApEn), sample entropy (SampEn), permutation entropy (PE), fuzzy entropy (FuzzEn), and Kolmogorov Complexity (KC) are calculated on EEG in rat hippocampi at each epilepsy phases. Then an algorithm based on Kruskal-Wallis Test (K-W Test) is proposed to select the leads with statistical significance and the most considerable degree of change. To compare the performance of these complexity indicators in distinguishing normal, acute and chronic stages, three classifiers were employed, including support vector machine (SVM), artificial neural network (ANN), and K-nearest neighbor (KNN).

Results

As a result, the accuracy 95.63% for distinguishing the normal and acute phases is achieved by SVM employing PE. In classifying normal and chronic phases, an accuracy of 86.88% is achieved by KNN employing SampEn.

Conclusion

Our research practice based on real data shows that the characteristics of EEG complexity are indeed of great significance for the recognition of different states of epilepsy.

Keywords: EEG Complexity, Entropy, Channel Selection, Epilepsy Diagnosis, Machine Learning

Acknowledgement: This work is supported by UIC Research Grant R202108.

精神病风险综合征P300波幅的特异性及其与临床结局的关系：基于听觉Oddball范式复合声音刺激的分析

侯永青[1,2], 邱桂平[1,3,4], 夏海硕[1], 邓方渝[2], 刘小先[5], 陈安涛[6*]

1 西南大学心理学部, 重庆 400715; 2 广元市精神卫生中心，广元 628000; 3 澳大利亚弗林德斯大学教育心理和社会工作学院, 阿德莱德 3127; 4 宁夏大学教育学院，银川 750000; 5 河南师范大学教育学部，新乡 453000; 6 上海体育学院，上海 200438

(xscat@swu.edu.cn)

目的

精神病风险综合症（Psychosis risk syndrome，PRS）先于精神病出现。探讨 PRS 的神经生理特异性和预测其临床结局的神经生物学标志物对预防和诊疗重性精神病具有重要意义。本研究的目的是明确 PRS 个体由复合声音刺激诱发的 P300 波幅是否具有特异性，并与其之后的临床结局是否有关。

方法

从三所大学的 8763 名大学生中筛选了 226 名参与者，其中 PRS 个体 122 名，情绪障碍个体（ED）51 名，健康对照个体（HC）53 名。以不同频率的白噪音（20 HZ 和 40 HZ）组成的 click 声音为实验刺激，使用听觉 Oddball 范式对所有参与者的 P300 事件相关电位进行了测试，并在测试后对所有 PRS 个体随访追踪 12 个月。分析基线水平上各组参与者 P300 波幅的差异和不同刺激材料引发的 P300 波幅与 PRS 临床结局的关系。

结果与讨论

PRS 个体的 P300 波幅显著高于 ED 和 HC 个体，随访后分类中，PRS-conversion 和 PRS-symptomatic 个体的 P300 波幅显著大于 HC，且 PRS-conversion 个体的 P300 波幅显著大于 PRS-complete remission；不同刺激类型中，在 40 HZ 刺激引发的 P300 平均波幅上，PRS-conversion 和 PRS-symptomatic 个体显著大于 PRS-complete remission 也显著大于 HC；多元 logistic 回归分析显示，在以 PRS-complete remission 为参照对象时，40 HZ 刺激引发的 P300 波幅对 PRS-conversion 和 PRS-symptomatic 有显著影响。结果说明，PRS 个体具有明显的听觉注意神经功能异常，相较于 ED 个体，PRS 个体的听觉注意 P300 反应具有特异性；听觉刺激的加工难度和突显性对听觉注意加工具有重要影响，40 HZ click 声音刺激引发的听觉 P300 波幅可以更有效地预测 PRS 的临床结果。

结论

由复合声音刺激诱发的 P300 波幅是 PRS 个体的一个特异性的电生理指标，

并与其临床结局相关。特别是 40 Hz 刺激诱发的 P300 波幅可能对预测 PRS 的临床结局更敏感，包括转化为精神病和从 PRS 状态缓解。这些听觉 P300 波幅有望成为预测 PRS 临床结局的有效生物标志物。

致谢：本研究得到国家自然科学基金(32171040)和四川省卫健委科技计划项目(20PJ281)的支持。

图 1. PRS、ED 和 HC 在不同刺激条件下的 P300 波幅

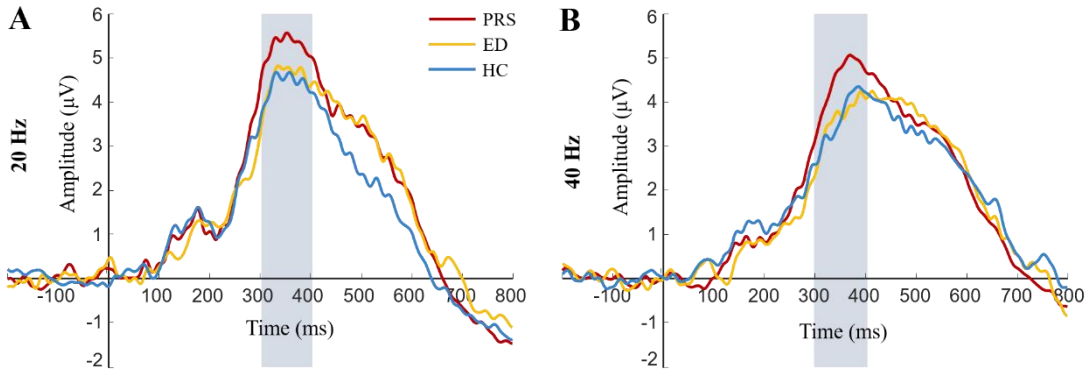

图 2. 随访后各组被试在不同刺激类型下的 P300 波幅

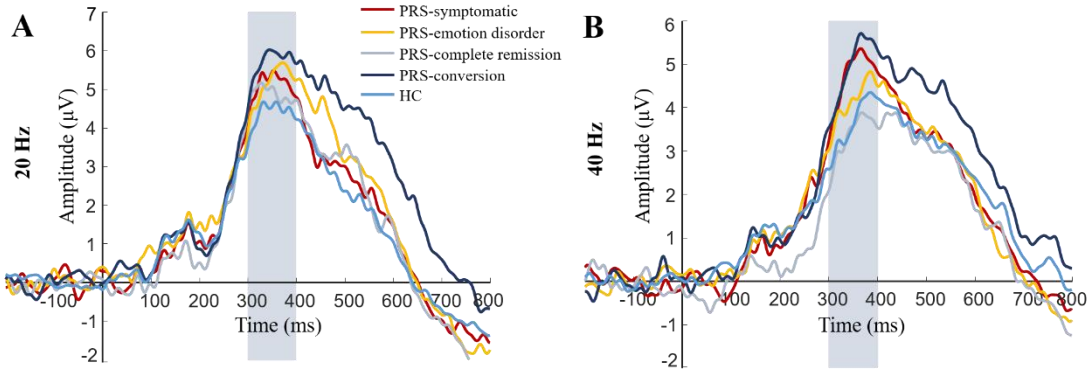

Role of the amygdala in disrupted integration and effective connectivity of cortico-subcortical networks in apathy

Ningning Zeng, André Aleman, Chong Liao, Huihua Fang, Pengfei Xu*, Yuejia Luo*

Magnetic Resonance Imaging Center, Center for Brain Disorders and Cognitive Sciences, Shenzhen University

(luoyj@szu.edu.cn)

Objective

Apathy is a quantitative reduction in motivation and goal-directed behaviors, not only observed in neuropsychiatric disorders, but also present in healthy populations. Although brain abnormalities associated with apathy in clinical disorders have been studied, the organization of brain networks in healthy individuals has yet to be identified.

Methods

We examined properties of intrinsic brain networks in healthy individuals with varied levels of apathy (49 low apathy, 50 high apathy). By using functional magnetic resonance imaging in combination with graph theory analysis and dynamic causal modeling analysis, we tested communications among nodes and modules as well as effective connectivity among brain networks.

Results & Discussion

the average participation coefficient of the subcortical network, especially the amygdala, was lower in individuals with high than low apathy. We further observed weaker effective connectivity from the hippocampus and parahippocampal gyrus to the amygdala, and from the amygdala to the parahippocampal gyrus and medial frontal cortex in individuals with apathy. These findings reveal that individuals with high apathy exhibit aberrant communication within the cortical-to-subcortical network, characterized by differences in amygdala-related effective connectivity.

Conclusions

Our findings shed light on the neural basis of apathy in subclinical populations and may have implications for understanding the development of clinical conditions that feature apathy.

Acknowledgement: This work was supported by the NSFC (31920103009, 31871137, and 32071100).

Figure 1. Intra- and inter-module connections between the cortical and the subcortical networks of (a) high apathy and (b) low apathy groups, as well as (c) the group difference. (d) Average participant coefficient of two groups.

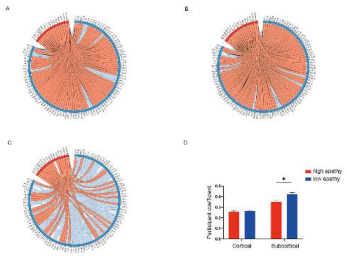

网络游戏成瘾者对游戏相关社会奖赏的加工优势：一项ERP研究

贺金波*　聂余峰

华中师范大学心理学院暨青少年网络心理与行为教育部重点实验室

武汉，430079（hjb@mail.ccnu.edu.cn）

目的

社会功能受损是网络游戏成瘾的核心症状和主要诊断依据之一。但既往研究发现这种功能受损只表现在现实社会认知和功能上，而游戏相关社会认知和功能却显著增强。本研究采用 ERP 技术，从社会奖赏功能失调角度探讨了这种现象背后的认知神经机制。

方法

研究使用网络游戏障碍量表筛选了网络游戏成瘾者和普通游戏者各 22 名，采用社会评价任务，设计了相匹配的游戏社会评价情境和现实社会评价情境，每种评价情境下各有 200 个试次。每个试次主要分为预期和反馈两个阶段，预期阶段被试对评价进行预期，反馈阶段给被试呈现反馈结果。在被试执行任务的过程中记录其脑电。

结果和讨论

行为学结果发现，网络游戏成瘾者对游戏社会评价具有显著更积极的预期倾向。ERP 结果发现：（1）网络游戏成瘾者由游戏面孔诱发的 Cue-P3（与个体对奖赏线索投入的动机性认知神经注意资源有关）成分显著大于现实面孔（图 1A）；（2）网络游戏成瘾者由非预期游戏社会奖赏反馈诱发的 RewP 成分（与奖赏反馈对个体的奖赏效应大小有关）显著大于非预期现实社会奖赏反馈（图 1B）。

结论

本研究结果表明，相比于现实社会奖赏，网络游戏成瘾者对游戏相关社会奖赏具有更高的寻求动机，能在游戏相关社会奖赏反馈中获得更大的奖赏体验。

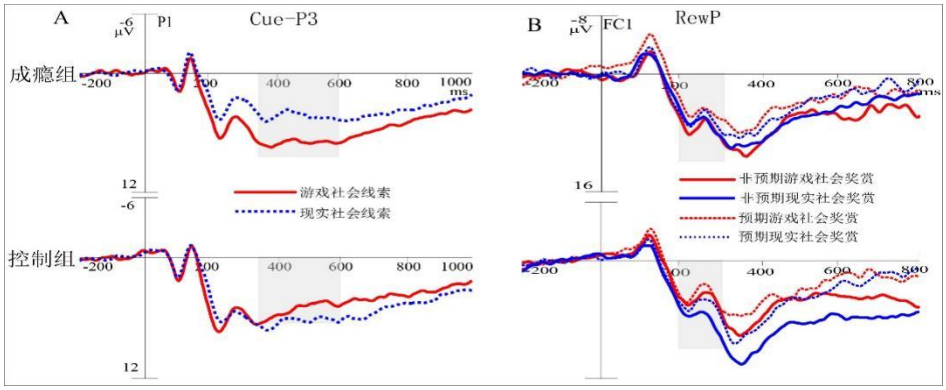

图 1 网络游戏成瘾者在不同奖赏条件下 Cue-P3（A）和 RewP（B）的差异

Altered effective connectivity from the posterior insula to the amygdala mediates the relationship between psychopathic traits and endorsement of the Harm foundation

Shuer Ye , Wei Li , Bing Zhu , Yating Lv ,* Qun Yang *, Frank Krueger

Department of Psychology, School of Education, Hangzhou Normal University, Hangzhou, China (qunyang@hznu.edu.cn)

Objective

Psychopathy has been recognized as a personality disorder which is typically characterized by abnormalities in interpersonal (i.e., manipulation, superficial charm, pathological lying, grandiose sense of self-worth), affective (i.e., shallow affect, callousness, lack of remorse or guilt), lifestyle (i.e., lack of long-term goals, impulsivity, irresponsibility), and antisocial (i.e., poor self-control, hostility, antisocial behavior and disregard of various socio-moral norms) dimensions. This study examined the effective connectivity (EC) of psychopathy-related brain regions and its association with endorsement to moral foundations (Harm, Fairness, Loyalty, Authority, and Purity)—combining questionnaire measures, resting-state fMRI (RS-fMRI), and Granger causality analysis.

Methods

After undergoing task-free fMRI, 78 college students completed two questionnaires (the Levenson Self-Report Psychopathy Scale and Moral Foundation Questionnaire) of which the order was counterbalanced among participants.

Results & Discussion

Our results showed that total and primary psychopathy negatively predicted endorsement of the Harm foundation. The EC from the posterior insula to the amygdala was negatively associated with primary psychopathy but positively associated with endorsement of the Harm foundation. Altered posterior insula amygdala EC partially mediated the relationship between primary psychopathy and endorsement of the Harm foundation.

Conclusions

Our findings demonstrated that individuals with elevated psychopathic traits may have atypical processes in recognizing and integrating bodily state information into emotional responses —leading to less concern for harm-related morality. Our findings deepen the understanding of the neuropsychological mechanism underlying the relationship between psychopathic traits and morality, providing potential

neurobiological explanations for increased moral transgressions, especially those harm-related transgressions, committed by psychopathic individuals.

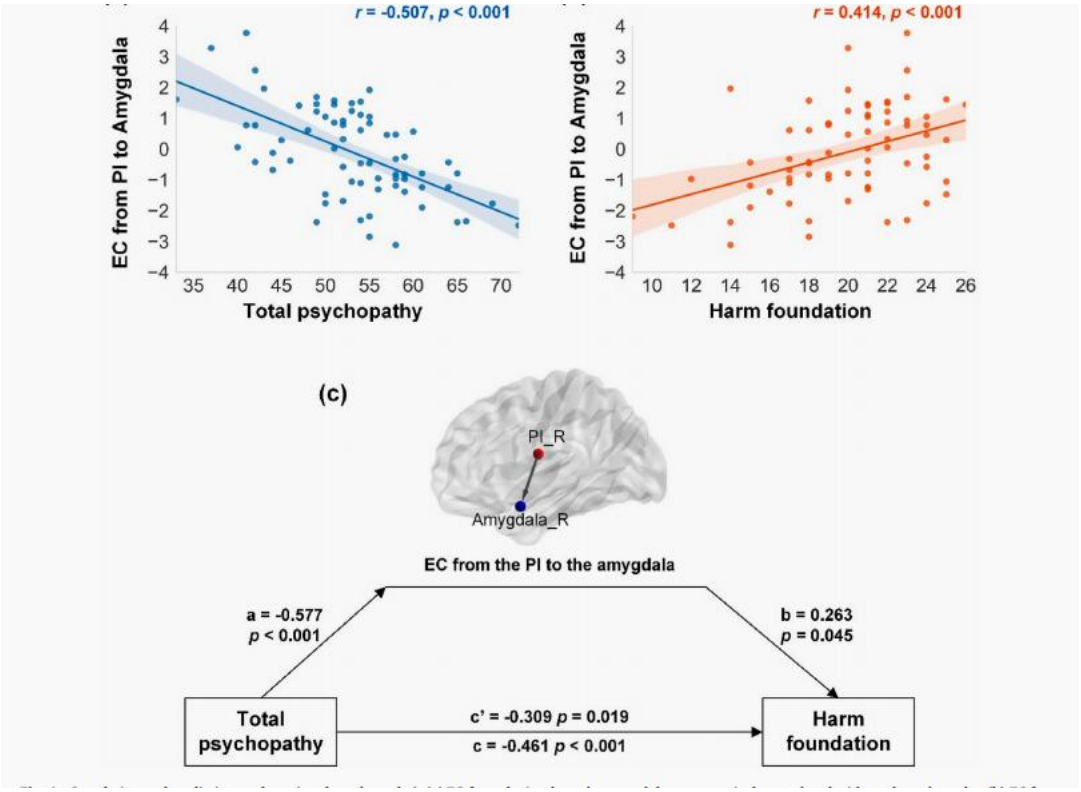

Figure 1. Correlation and mediation analyses (total psychopathy). (a) EC from the insula to the amygdala was negatively correlated with total psychopathy. (b) EC from the posterior insula to the amygdala was positively associated with endorsement of the Harm foundation. (c) EC from the insula to the amygdala partially mediated

脑电网络分析在脑认知与脑疾病中的应用研究

姜林[1,2]，何润阳[1,2]，易婵琳[1,2]，尧德中[1,2]，李发礼[1,2]，徐鹏[1,2*]

1 电子科技大学 神经信息教育部重点 成都脑科学研究院临床医院 成都 611731

2 电子科技大学 信息医学研究中心 生命科学与技术学院 成都 611731

(xupeng@uestc.edu.cn)

目的

作为一个复杂网络，大脑内信息的加工依赖于脑区间的高效交互，其潜在交互模式可以通过脑网络分析进行精准量化。当前工作将基于个体脑电数据，开展相应的脑电网络分析，从功能网络、效应网络、时变网络及时间变异性网络出发，探索情绪加工相关的脑网络机制以及临床神经和精神类疾病潜在的病理性机制。

方法、结果、讨论

首先，针对情绪感知的信息加工机制，本研究在健康群体上开展了格兰杰因果分析并统计其因果耦合交互差异。结果发现：负性情绪相关的双侧额-颞中回因果连接强于正性，而正性情绪表现出左额上回与其他脑区间更强的因果交互，进一步证实了左额上回或为正性有别于中性与负性情绪的关键脑区。随后，在脑瘫与卒中等神经类疾病中，脑网络分析结果发现：运动执行任务中，卒中患者非损伤侧运动区以及额叶与顶枕叶非运动区有效连接显著增强，以实现对损伤脑区的功能代偿；而通过开发适用于脑瘫儿童的运动康复系统，并基于此开展长时程运动康复训练，脑瘫儿童的运动相关功能网络被证实发生了可塑性变化，且网络交互效率显著提升。最后，针对精神分裂症等精神类疾病，研究进一步结合滑动窗相干与模糊熵方法刻画患者静息脑电网络的时间变异性，发现患者静息网络时间变异性显著存在于颞叶、左前额以及左枕叶等局部脑区，而在全连接尺度下的时间变异性则低于正常组；与此同时，患者网络时间变异性指标与 P300 幅值显著负相关，而正常组呈现显著的正相关关系。

结论

开展脑电网络分析不仅有助于加深对大脑认知功能以及相应神经与精神类疾病的认识，还将为量化认知和疾病相关的神经活动提供可靠的脑电网络指标，并有效促进认知神经科学和临床康复诊断治疗的发展进程。

Connectome-Based Predictive Modeling of Individual Anxiety

Zhihao Wang, Katharina S. Goerlich, Hui Ai, André Aleman, Yuejia Luo*, Pengfei Xu*

Beijing Key Laboratory of Applied Experimental Psychology, Faculty of Psychology, Beijing Normal University, Beijing 100875, China

Department of Biomedical Sciences of Cells & Systems, Section Cognitive Neuroscience, University Medical Center Groningen, University of Groningen, Groningen 9713 AW , the Netherlands

Objective

Anxiety-related illnesses are highly prevalent in human society. Being able to identify neurobiological markers signaling high trait anxiety could aid the assessment of individuals with high risk for mental illness. Previous neuroimaging studies collapsed group data to decode anxiety in the brain (Dubois and Adolphs, 2016), but little is known with respect to predicting individual anxiety levels using neural models. It has been shown that resting-state functional connectivity (rsFC), like fingerprinting, can accurately capture neural signatures of individual differences in anxiety (Finn et al., 2015). Here, we aim to predict individual levels of trait anxiety in healthy participants from whole-brain rsFC data.

Methods

We applied connectome-based predictive modeling (CPM) to whole-brain rsFC data to predict the degree of trait anxiety in 76 healthy participants. Using a computational “lesion” approach in CPM, we then examined the weights of the identified main brain areas as well as their connectivity.

Results & Discussion

Results showed that the CPM successfully predicted individual anxiety based on whole-brain rsFC, especially the rsFC between limbic areas and prefrontal cortex. The prediction power of the model significantly decreased from simulated lesions of limbic areas, lesions of the connectivity within limbic areas, and lesions of the connectivity between limbic areas and prefrontal cortex. Importantly, this neural model generalized to an independent large sample (n = 501). These findings highlight important roles of the limbic system and prefrontal cortex in anxiety prediction.

Conclusions

Our work provides evidence for the usefulness of connectome-based modeling in

predicting individual personality differences and indicates its potential for identifying personality factors at risk for psychopathology.

References:

Dubois J, Adolphs R (2016) Building a Science of Individual Differences from fMRI. Trends Cogn Sci 20:425–443 Available at: http://dx.doi.org/10.1016/j.tics.2016.03.014.

Finn ES, Shen X, Scheinost D, Rosenberg MD, Huang J, Chun MM, Papademetris X, Constable RT (2015) Functional connectome fingerprinting: Identifying individuals using patterns of brain connectivity. Nat Neurosci 18:1664–1671 Available at: http://dx.doi.org/10.1038/nn.4135.

Altered representation in somatomotor networks in different aspects of anxiety

Jing Yuana, JianFeng Zhangb,c, Yuejia Luoa,*

[a] State Key Laboratory of Cognitive Neuroscience and Learning, Beijing Normal University, Beijing China

[b] Center for Brain Disorders and Cognitive Sciences, Shenzhen University, Shenzhen China

[c] College of Psychology, Shenzhen University, Shenzhen China

(luoyj@bnu.edu.cn)

Objective

Anxiety can be characterized by two aspects in psychometric, i.e., fear affect and somatic arousal. The shared and distinct neural representations of these two aspects remained unclear. We here introduced a whole-brain approach (i.e., global signal topography) to investigate their underlying neural representations.

Methods

We recruited 795 participants under resting-state fMRI from the Human Connectome Project (HCP). Global signal topography was calculated as the correlation map between the global signal and each local region.

Results & Discussion

We firstly replicated the spatial pattern of global signal topography observed in previous studies, revealing higher level of representation in the sensory regions and lower level in associative regions. We further assessed the subject-based correlation between global signal topography and anxiety. The shared network was observed as somatomotor network. And the distinct networks were observed at executive control network with higher representations in global signal topography associating with higher fear affect, and at dorsal attention network with lower representations in global signal topography associating with somatic arousal.

Conclusions

Together, our results demonstrated shared and distinct neural networks that associated with two dimensions of anxiety, i.e., fear affect and somatic arousal. These findings were helpful in understanding the interaction between cognitive and somatic aspects in anxiety.

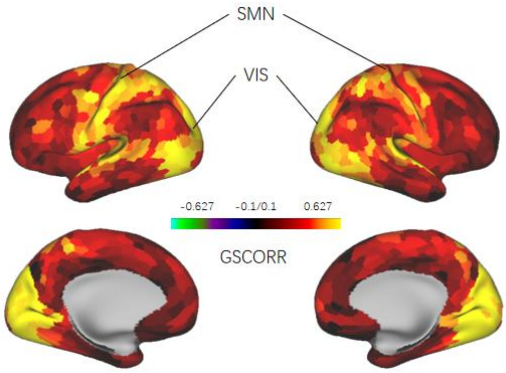

Figure 1. Group-level spatial topography of global signal correlation. GSCORR, global signal correlation; SMN, somatomotor network; VIS, visual network.

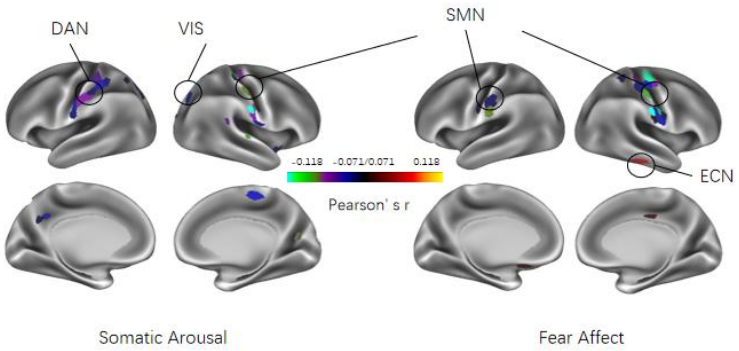

Figure 2. Correlation between ROI-wise global signal topography and different aspects of anxiety ($p<0.01$). DAN: dorsal attention network; VIS: visual network; SMN: somatomotor Network; ECN, executive control network; ROI, region of interest.

Attention Bias Modification Enhances Response Inhibition in Socially Anxious Individuals: Evidence from Event-related Potentials

Ling-yun Li, Yi Wang, Yang Wang, Dong-ni Pan, Delhii Hoid, Xuebing Li*

Key Laboratory of Mental Health, Institute of Psychology, Chinese Academy of Sciences, Beijing 100101, China

（lixb@psych.ac.cn）

Objective

Attention bias modification (ABM) has been widely used as an intervention in anxiety disorders, but its underlying mechanisms remain to be elucidated. We investigated the impact of attention training on response inhibition and the associated neural mechanisms in individuals with social anxiety.

Methods

Seventy-two college students with social anxiety were assigned randomly to ABM (n=26), attention control condition (ACC, n=24), and passive waiting (n=22) groups. At the pre-training assessments, the participants in all groups completed the self-report scales consisting of the Beck Depression Inventory-Ⅱ, the Social Phobia Scale, the Spielberger State-Trait Anxiety Inventory, and the fear subscale of the LSAS-SR questionnaire. Subsequently, all participants performed a spatial cueing task to assess attention bias, and an ERP eGo/No-go task to assess inhibition function and emotional information processing. The whole pre-training assessment lasted approximately 90 minutes, which included 45 minutes of preparation for ERP recording.

One to two days after the pre-training assessment, the participants from the ABM and ACC groups returned to the lab to perform their first training task. Training occurred twice a week and lasted for four weeks. A single training session for both groups lasted approximately 21 minutes. One to two days after completing the whole training schedule, all participants returned to participate in the post-training assessment, which was the same as the pre-training assessment.

Results & Discussion

The present study showed significantly improved scores post-training in two anxiety symptom indicators (BDI and LSAS-fear) in both the ABM and ACC groups. Consistent with previous reports, this result indicated that ABM training was able to ease symptoms among individuals with social anxiety. Although attention bias scores did not change, such a difference can be explained by two factors. First, attention bias assessments are affected by the stability of the testing task and the degree to which it

matches the training task that is being used to attenuate the bias. In addition, the indistinguishable results of attention bias scores in both training groups may imply that changes in anxiety symptoms may be irrelevant to the task of avoiding threat stimuli during attention training. Event-related potentials showed an increased Nogo-N2 and decreased Nogo-P3 post-training in the ABM and ACC groups when confronted with neutral contexts and in the ABM group only when confronted with negative contexts. This result indicates that both the ABM and ACC groups were able to enhance response inhibition, and the ABM group was better able to avoid emotional interference in a negative emotional environment, whereas participants in the ACC group did not deliberately avoid background interference.

Conclusions

ABM and ACC may relieve anxiety symptoms and improve response inhibition in socially anxious individuals. This suggests that attention training can improve the symptoms of social anxiety irrespective of whether a change in attention bias has occurred. ABM may also help avoid emotional interference in negative environments and facilitate acquisition of more favorable cognitive strategies.

Acknowledgement

This work was supported by CAS Engineering Laboratory for Psychological Service [grant number KFJ-PTXM-29].

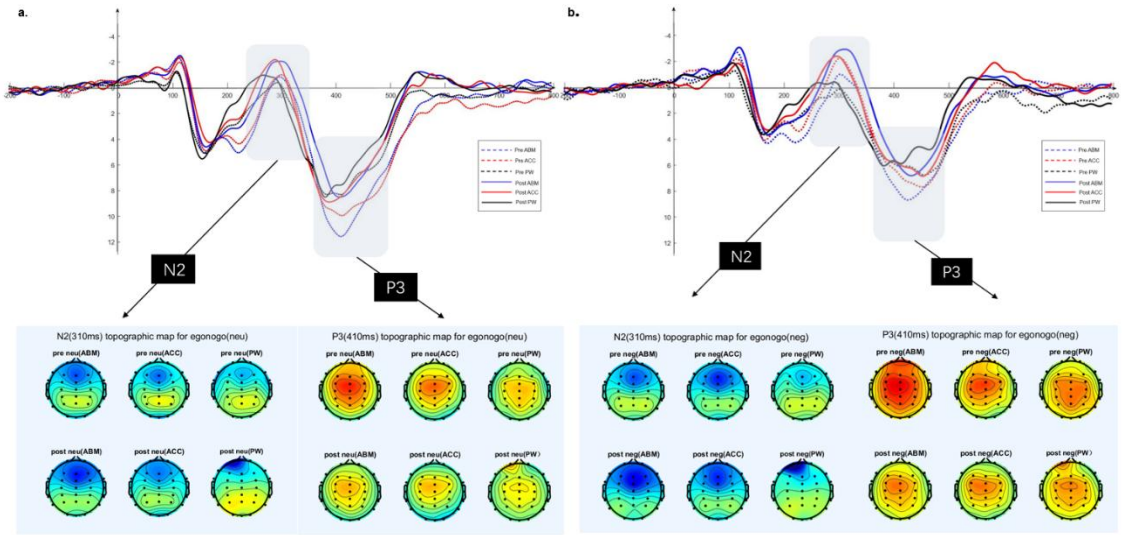

Figure 1. Changes in ERP components(N2 and P3).a)Grand average of components(N2 and P3) and topography changes under neutral condition at FZ/FCZ/CZ for the ABM, ACC, PW in eGo/Nogo task. b)Grand average of components(N2 and P3) and topography changes under negative condition at FZ/FCZ/CZ for the ABM, ACC and PW in eGo/Nogo task.

老年人睡眠质量与认知功能关系存在性别差异的静息态fMRI研究

黄蓉[1] 雷萌萌[1] 朱虹霏[1] 孙晓宇[1] 陶伍海[1*]

1深圳大学心理学院，深圳，518060，E-mail:taowh@szu.edu.cn

目的

探究负性情绪核心脑区——杏仁核与全脑的功能连接不同是否是老年人睡眠质量与认知功能关系中存在性别差异的关键。

方法

招募深圳市社区 55 岁以上的老年人 53 名，其中，男性 21 人，女性 32 人。使用参照 Albert 的诊断标准制定的《老年认知功能测查量表》对其认知功能进行评估；使用匹茨堡睡眠质量指数（the Pittsburgh Sleep Quality Index，PSQI）量表对其睡眠质量进行评估，并根据量表总分将老年人分为睡眠质量好（PSQI≤5 分）与差（PSQI≥6 分）两组：男性老年人中，睡眠质量好的 12 人，睡眠质量差的 9 人；女性老年人中，睡眠质量好的 10 人，睡眠质量差的 22 人。以上数据均使用 SPSS 21.0 进行统计分析。同时邀请被试到深圳大学磁共振成像中心进行静息态功能磁共振成像扫描，并选取杏仁核为感兴趣区，使用 dpabi 进行功能连接分析。

结果和讨论

（1）杏仁核与全脑功能连接的结果发现，女性老年人睡眠质量好与差两组中，杏仁核与全脑功能连接显著差异脑区有双侧小脑、颞叶、双侧海马旁回、枕叶、楔叶和前额叶（进行了 GRF 校正，体素水平 p=0.005，团块水平 p=0.05）。男性老年人睡眠质量好与差两组中，没有发现杏仁核与全脑功能连接有差异的脑区。（2）睡眠质量差的女性老年人中，杏仁核和全脑的连接性与认知功能测验中的画钟测验、数字广度测验和 Stroop C 测验得分呈显著负相关。而睡眠质量好的女性老年人中，没有发现杏仁核和全脑连接性与认知测验的相关性。

结论：

负性情绪核心脑区——杏仁核与全脑的连接性不同或许是老年人睡眠质量与认知功能关系中存在性别差异的神经机制之一。

关键词 睡眠质量，认知功能，性别差异，静息态功能磁共振成像，老年人

轻度认知障碍老人认知控制容量减退的脑电信号特征

杨嘉望[1] 何昊[1,2] 陈毅琦[3] 罗跃嘉[4] 关青[1,2*]

1深圳大学心理学院，深圳，518060

2深港脑科学创新研究院，深圳，518055

3曼海姆大学，心理学系，曼海姆，68159

4北京师范大学心理学部，北京，100875

(guanqing@szu.edu.cn)

目的

轻度认知障碍（mild cognitive impairment，MCI）是阿尔茨海默病的临床前阶段。以往研究表明，除了记忆功能损伤之外，MCI 老人也表现出认知控制功能减退。新近证据显示认知控制容量下降在识别 MCI 甚至遗忘型 MCI 中扮演着关键作用。然而，目前尚不知晓认知控制容量减低所伴随的脑电信号的时-频域特征及其对应的神经振荡机制。因此本研究旨在考察 MCI 老人认知控制容量减退的相关神经振荡能量及跨频耦合特征，以理解其认知神经机制。

方法

招募 20 名 MCI 老人以及在人口学变量上与之匹配的 30 名认知正常老人（healthy control，HC），让其完成一项视知觉多数函数任务，同时采集其脑电信号。采用计算模型对行为数据进行拟合以估计每名被试的认知控制容量。剔除脑电信号中的事件相关电位成分后，分别提取脑电信号中的 delta(1~4Hz)、theta(4~8Hz)、alpha(8~12Hz)、beta(12~30Hz)频段，采用 Hilbert 变换求取时频能量。采用滑窗算法及基于聚类的（cluster-based）统计方法，考察各实验条件中与认知控制容量显著相关的时频特征。依据文献及本实验的头皮脑电信号分布，提取额中线 Fz、FCz、Cz 点的 delta 和 theta 振荡功率、顶枕区 POz、PO3、PO4 点的 alpha 振荡功率、额区 Fz、F1、F2 点的 beta 功率。对于检测出的认知控制容量的相关时频振荡信号，计算其与所属时间窗内其他频段之间的相幅耦合调制指数（modulation index，MI）并采用置换检验检验其显著性。对于认知控制容量的显著相关时频振荡能量以及具有统计显著性的 MI 值，分别采用多元方差分析（MANOVA）考察其中哪些指标体现出了显著的组间差异。最后，纳入显著的 MI 指标以构建多元回归模型，以考察这些跨频耦合特征与认知控制容量之间是否存在显著的相关性。

结果和讨论

MCI 组的认知控制容量显著低于 HC 组（MCI=3.24 bps, HC=3.58 bps, $p < .05$）。相关分析揭示了与认知控制容量显著相关的不同条件下的时频振荡特征，其中 3 项条件（信息比特率分别为 2.46、2.91、3.16 bps）下的 delta、alpha、beta 振荡特征体现出了显著的组别差异。跨频耦合结果显示，与认知控制容量显著相关的额、顶区 beta 振荡嵌套在额区 delta 振荡中，且二者之间的 MI 与认知控制容量之间存在显著相关，但 MI 指标未体现显著的组别差异。

结论

额区的低频（delta、theta）与高频（beta）振荡是视知觉认知控制容量的关键脑电信号特征，也是 MCI 老人认知控制功能损伤的神经振荡基础。

Altered functional coupling between the cerebellum and cerebrum in patients with amnestic mild cognitive impairment

Hehui Li [1,†], Qing Guan[1,†], Rong Huang[1], Mengmeng Lei[1], Yue-Jia Luo[1,2], Zhanjun Zhang[2], Wuhai Tao[1,*]

1 Center for Brain Disorders and Cognitive Sciences, Shenzhen University, 3688 Nanhai Avenue, Nanshan District, Shenzhen 518060, P.R. China,

2 State Key Laboratory of Cognitive Neuroscience and Learning & IDG/McGovern Institute for Brain Research, Beijing Normal University, No. 19, Xinjiekouwai St,Haidian District, Beijing 100875, P.R. China

*Corresponding author: Center for Brain Disorders and Cognitive Sciences, Shenzhen University, 3688 Nanhai Avenue, Nanshan District, Shenzhen 518060, P.R.China. (taowh@szu.edu.cn)

†Hehui Li and Qing Guan contributed equally.

Objective

Cognitive processing relies on the functional coupling between the cerebrum and cerebellum. However, it remains unclear how the 2 collaborate in amnestic mild cognitive impairment (aMCI) patients.

Methods

A total of 44 participants were included in the discovery sample, consisting of 22 participants with aMCI and 22 age- and sex-matched HCs. To further validate the main results, a total of 138 participants from the ADNI project were included as the replication sample, consisting of 69 MCI patients and 69 sex- and age-matched HCs. All participants performed a battery of neuropsychological tests. General cognitive function was measured by the MMSE, and memory was estimated by the Auditory Verbal Learning Test and the Rey-Osterrieth Complex Figure test. The attention tests included the Symbol Digit Modalities Test and part A of the Trail Making Test (TMT) , while part B of the TMT and part C of the Stroop Color and Word Test were used to test executive function. Brain images of participants were acquired via functional magnetic resonance imaging. Regions of interests (ROIs) were defined based on Yeo et al. (2011) and Buckner et al. (2011).

Results & Discussion

ROI-based analyses were first conducted, during which we compared the rsFC between functionally corresponding and noncorresponding areas. For corresponding areas, we observed that rsFC of FP_1 in the cerebrum and cerebellum was reduced in

the aMCI group compared with the HC group. For noncorresponding areas, rsFC seeded by L_FP_1 to R_FP_1e (brain areas external to R_FP_1 in the cerebrum) was significantly less negative in the aMCI group than that in the HC group (Figure 2). These results suggest that network configuration across the cerebellum and cerebrum has changed in individuals with aMCI, especially in frontoparietal areas. Dynamic rsFC analysis showed that rsFC between L_FP_1 and the right MFG was consistently greater in the HC group than in the aMCI group across time. Increased rsFC between L_FP_1 and the calcarine in the aMCI group was also consistently observed from the second to the end of the time bin. In addition, the decreased FC appeared at least 13TR (19.5s) before the increased FC (Figure 3). The above reported results were replicated in the replication sample. Brain-behavioral correlation analyses were further conducted separately in two groups, we observed that rsFC in patients with aMCI was significantly correlated with behavioral performance on the attention test and this effect was absent in the HC group, supporting that there exists a compensatory mechanism in patients.

Conclusions

In general, the results demonstrated decreased rsFC between both functionally corresponding and noncorresponding areas, and increased rsFC only from functionally noncorresponding areas. By investigating the functional coupling between the cerebrum and the cerebellum, this study contributes to illustrating how the cerebellum adjusts its coupling with the cerebrum in individuals with cognitive impairment and extends the closed-loop architecture and functional mapping pattern proposed by previous studies.

Acknowledgment:

This work was supported by grants from the National Natural Science Foundation of China (NSFC: 32000793 and 32100846), Shenzhen-Hong Kong institute of Brain Science-Shenzhen Fundamental Research Institutions (2021SHIBS0003), and Shenzhen Science and Technology Planning Project of Guangdong Province, China Program (JCYJ20210324093208021). It was also supported by Project funded by China Postdoctoral Science Foundation (Grant No. 2020 M682846) and by Open Research Fund of the State Key Laboratory of Cognitive Neuroscience and Learning (Grant No. CNLYB2005).

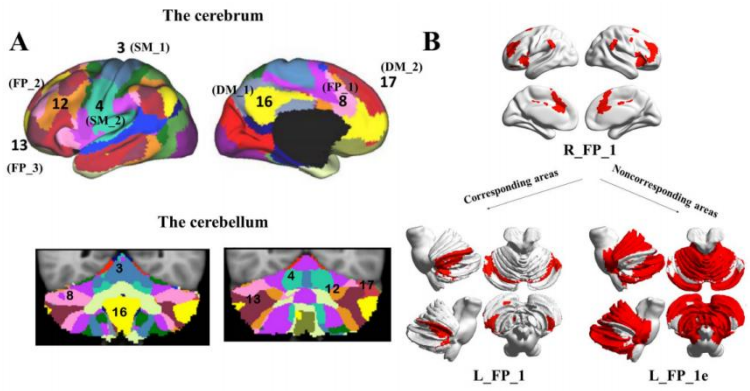

Figure 1: ROIs in the cerebrum and cerebellum. (A) Functional parcellations were from Thomas Yeo et al. (2011) and Buckner et al. (2011). In the current study, 7 functional areas were selected, 2 from the sensorimotor networks (networks 3 and 4), 3 (including networks 8, 12, and 13) belonging to the frontoparietal network, and 2 from the DMN (networks 16 and 17). These ROIs in the cerebrum were named R_SM_1, R_SM_2, R_FP_1, R_FP_2, R_FP_3, R_DM_1, and R_DM_2 and those in the cerebellum were labeled L_SM_1, L_SM_2, L_FP_1, L_FP_2, L_FP_3, L_DM_1, and L_DM_2, respectively. (B) An example of functionally corresponding and noncorresponding areas. ROIs with the same functional specificity (e.g. R_FP_1 and L_FP_1) were characterized as functionally corresponding ROIs, whereas those with different functional specificities were characterized as functionally noncorresponding ROIs (e.g. R_FP_1 and L_FP_1e, where L_FP_1e indicates cerebellar areas external to L_FP_1).

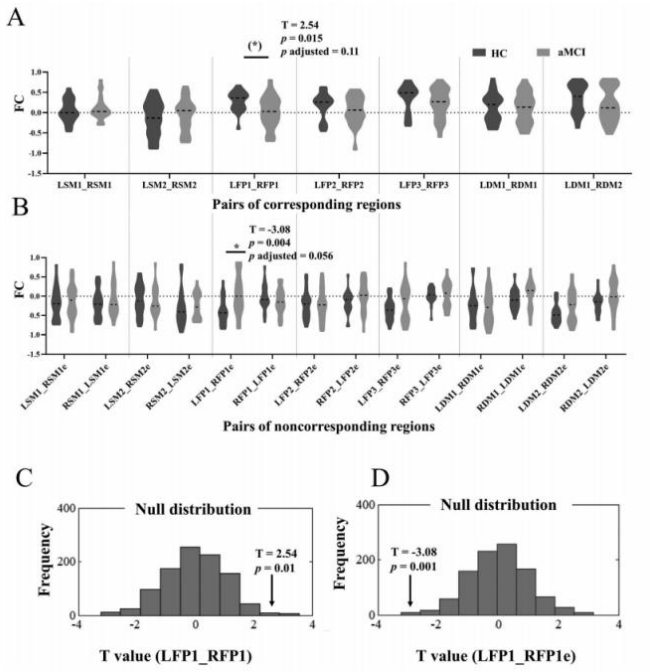

Figure 2: RsFC contrast patterns via ROI-based analysis. (A) rsFC between pairs of corresponding areas. (*) =

significant at the individual *p* level but did not survive after multiple comparisons; (B) the rsFC between pairs of functionally noncorresponding areas. For example, LFP1_RFP1e means rsFC seeded by L_FP_1 in the cerebellum to the cerebral areas external to R_FP_1. RFP1_LFP1e indicates rsFC seeded by R_FP_1 in the cerebrum to the cerebellar areas external to L_FP_1.* *p* adjusted = 0.056. (C and D) Demonstrate the null distribution of T values estimated by comparing rsFC between the HC and aMCI group 1,000 times with permutation tests. (C) The null distribution of T value indicating group difference in rsFC between L_FP_1 and R_FP_1, where L_FP_1 and R_FP_1 denote subregions (FP_1) from the frontoparietal network in the cerebellum and cerebrum, respectively. (D) The null distribution of the T value representing group difference in rsFC seeded by L_FP_1 to R_FP_1e, in which R_FP_1e indicates areas external to R_FP_1 in the cerebrum. Arrows indicate the real observation. The P values were calculated by the ratio of the times that the T value from random assignment was larger (C) or smaller (D) than the real observation.

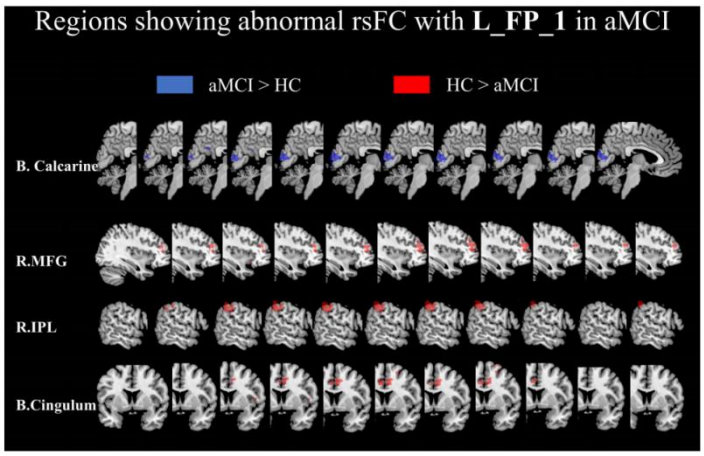

Figure 3: Dynamic rsFC seeded by L_FP_1 to the cerebral areas across groups. Red indicates areas showing greater rsFC in the HC group than the aMCI group across time bins, and blue indicates greater rsFC in the aMCI group than the HC group across time bins. The dynamic rsFC estimated by other seeds is presented in the supplementary file.

Adults with insomnia are associated with altered brain activity related to inhibitory control

Xiaobin Ding, Liang He*, Xiangzi Zhang

School of Psychology, Northwest Normal University, Lanzhou, China, 730070 (18450052500@163.com)

Objective

Insomnia disorder (ID) often have cognitive impairment and its influencing factors, which seriously affect their quality of life. Recent studies have shown that Insomnia affects an individual's ability to cognitive function. Inhibitory control can enable individuals to suppress attention, behavior, or thoughts unrelated to the task, to flexibly adapt to the current goal. Most psychiatric disorders are associated with impaired inhibitory control. Because inhibitory control is important to human good sleep, so we used event-related potentials (ERPs) to assess whether ID has an influence upon control inhibition.

Methods

15 good sleepers (GSs) and 15 adults with insomnia disorder (IDs) had participated in this experiment. All subjects were recruited from a university. All subjects underwent a complete physical and neurological examination, standard laboratory tests, and the following psychological evaluations: Pittsburgh Sleep Quality Index (PSQI), Beck Anxiety Inventory (BAI), Insomnia Severity Index (ISI), and Multidimensional Fatigue Inventory (MFI-20) were completed to assess sleep quality and emotion state. E-prime 3.0 program was designed to understand the inhibition control ability of insomniacs. In two choices oddball task (TCOT), the experimental materials were divided into two categories: standard stimulus and deviant stimulus (75% vs. 25%). The experimental stimuli were circles, including “red” and “green”, where the “red circle” was the standard stimulus and the “green circle” was the deviant stimulus, presented on a gray background. all subjects performed an TCOT task in the laboratory setting with high density EEG recordings.

Results & Discussion

The behavioral results revealed that compared to GSs, under standard stimulus and deviant stimulus, IDs presented significantly longer reaction times, suggesting the impairment of Inhibitory control among IDs. Considering the electrophysiological correlate underlying the longer reaction times, we found reduced N2 amplitude in patients with insomnia in the standard stimulus trials, which might reflect their poor

efficiency of inhibition control. Finally, when we performed exploratory analyses in the standard stimulus trials, IDs presented increased P3 amplitude.

Conclusions

The results suggested that adults with insomnia demonstrated altered brain activity during inhibitory control, and IDs have more worse behavioral performance. Given that impaired inhibitory control is often implicated in psychopathology, future studies with a longitudinal design are could to further explore the long-term impacts and trajectory of altered inhibitory control in adults with insomnia.

疼痛焦虑对疼痛强度心理和生理反应的预测作用

赵源，杨苏勇*

上海体育学院心理学院（*ysy77@163.com）

目的

疼痛焦虑是与疼痛相关的焦虑或恐惧反应倾向，包括疼痛体验和预期的认知、恐惧情绪、回避行为与生理反应。疼痛焦虑及其次级成分是否能预测疼痛强度评价的心理和生理反应目前还不清楚。为此，本研究考察了个体的疼痛焦虑水平与热痛刺激诱发疼痛的心理和生理反应之间的相关性。

方法

本研究选取了 50 名健康大学生(年龄 19-25 岁，女性 26 人)作为被试。被试先完成中文版简化版疼痛焦虑症状量表(ChPASS-20)和状态-特质焦虑问卷的分特质焦虑分量表(STAI-T)，分别评估他们的疼痛焦虑水平和特质焦虑水平。然后，要求被试对 49℃热刺激诱发的疼痛强度进行评估(0-10 分)，同时记录接触性热痛诱发电位(Contact Heat Evoked Potentials，CHEPs)。共呈现 10 次热痛刺激，刺激间隔为 10s。

结果和讨论

热痛刺激在 Cz 点诱发出明显的 CHEPs 波形。本研究以 N1 峰值潜伏期和 N2-P2 峰峰值(P2 峰值减去 N2 峰值)为 CHEPs 的潜伏期和波幅。相关分析结果显示，热痛强度评分与 CHEPs 潜伏期呈显著正相关($r = 0.29$，$p = 0.04$)，但与 CHEPs 波幅无显著相关($r = 0.05$，$p = 0.74$)，提示疼痛信号加工的越慢的个体，疼痛强度的主观感受越强烈。CHEPs 波幅与 ChPASS-20 的疼痛焦虑总分($r = -0.36$)及回避($r = -0.35$)、恐惧($r = -0.32$)、生理焦虑($r = -0.34$)等三个分量得分均与呈显著负相关($ps < 0.023$)。以特质焦虑为协变量进行协相关分析，上述相关系数依然达显著水平($ps < 0.026$)。未发现 ChPASS-20 总分及各分量表得分与 CHEPs 潜伏期或热痛强度评分有显著的相关($ps > 0.139$)。

结论

疼痛焦虑作为一种人格特质，可预测热痛诱发的疼痛生理反应，但不能预测强度心理评价。

The impacts of preprocessed EEG quality on the homogeneity of spectral profiles and the fidelity of brain network

Jie Ruan[1], Zhihao Zhang, Pedro A. Valdes-Sosa[2], Shiang Hu[1*]

1. Anhui Provincial Key Laboratory of Multimodal Cognitive Computation, Key Laboratory of Intelligent Computing & Signal Processing of Ministry of Education, School of Computer Science and Technology, Anhui University, Hefei 230601, China (shiang.hu@hotmail.com)

2. The Clinical Hospital of Chengdu Brain Science Institute, MOE Key Lab for Neuroinformation, School of Life Science and Technology, University of Electronic Science and Technology of China, Chengdu, China

Objective

The quality control after large scale EEG data preprocessing has recently been an issue of great concern. Although there exist many pipelines such as EEGLAB Makoto's preprocessing pipeline, Automagic, HAPPE, APICE, etc., it is still lacking good indicators to measure the EEG quality after pipeline batch processing. The impacts of either insufficient or excessive preprocessing on the further EEG spectral and network profiles have not been clearly understood. Here, we simulate the case of insufficient preprocessing by adding noise with different signal-to-noise ratios to the clean EEG and simulate the case of excessive preprocessing by losing some brain signals from the clean EEG.

Methods

In general, three types of EEG data were synthesized, which were 1) the clean EEG as the benchmark (CE), 2) the preprocessed EEG by insufficient preprocessing (IPE), 3) the preprocessed EEG by excessive preprocessing (EPE).

Firstly, the CE was generated using the forward model and the multivariate autoregressive (MVAR) model. The forward model is the New York Head available on the ICBM-NY platform, which includes 231 sensors on the scalp and 75,000 nodes on the cortical surface. The MVAR model was set with the order 10 and the uncorrelated, zero mean innovation noise through a normally distributed pseudorandom generator. The covariance of the innovation process was set equal to an identity matrix. The noise with different signal-to-noise ratios were produced and mixed with the clean EEG to mimic the IPE. Some brain signals were discarded from the CE to mimic the EPE with brain signals lost.

Subsequently, the PaLOS indices (https://github.com/ShiangHu/PaLOS-index) of EEG spectra were calculated from the three types of EEG data. PaLOS that we

proposed indicate the proportion of the variance explained by the first common principal component[1]. The larger PaLOS means the cross spectra are more likely to be homogenous across frequencies, vice versa.

Additionally, based on the three types of EEG data, the scalp EEG network was constructed using the connectivity measures that are the imaginary part coherence (iCoh), directional transfer function (DTF), partial directional coherence (PDC), phase-lock value (PLV), and phase slope index (PSI). And we calculated the EEG network metrics such as the clustering coefficient, the global/local efficiency, and the characteristic path length, etc. Based on the SimiNet[2], the brain network deviation index (DEVI) represents the degree of deviation between the two networks, in other words, it can also indicate the accuracy of the network. The DEVI of the other two states was also compared relative to the CE.

Results & Discussion

Compared either the IPE or the EPE with the CE, the PaLOS index decreased, and the DEVI index increased; in terms of network features, the characteristic path length decreased while the clustering coefficient and global/local efficiency increased.

On the one hand, the PaLOS results suggest that the cross spectra be more likely to be heterogeneous across frequencies when it was the IPE and the EPE. On the other hand, from the results of DEVI and network features, taking the CE as the benchmark, when it was more insufficient preprocessing (MIP), the greater DEVI, clustering coefficient and global/local efficiency, while the characteristic path length went the opposite; when it was more excessive preprocessing (MEP), the DEVI, clustering coefficient and global/local efficiency was larger, while the characteristic path length were smaller.

Conclusions

This study demonstrated that the preprocessed data quality is crucial for the typical subsequent analysis such as spectral profiles and brain network analysis where the EEG biomarkers deduct from PaLOS indices we proposed may be one of the metrics that could help for quality assurance.

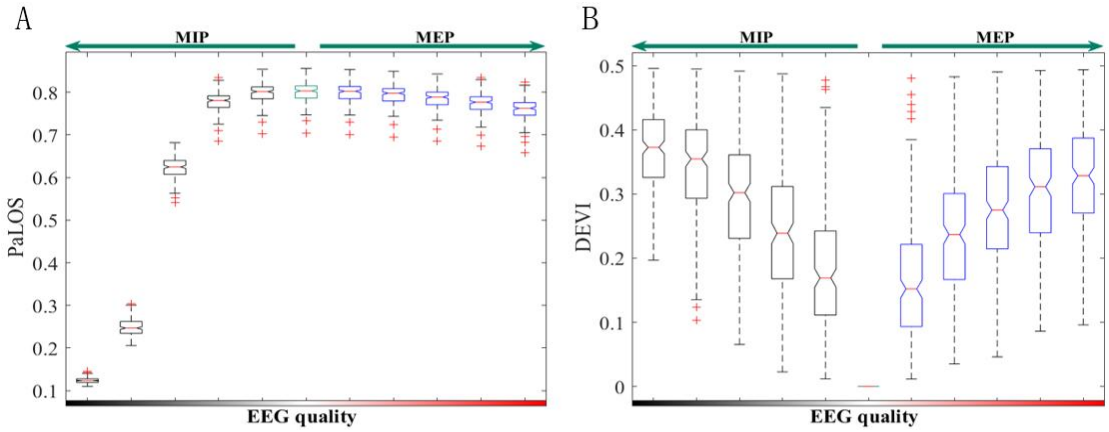

Figure 1. PaLOS and DEVI results of different EEG quality (black: IPE; red: EPE). Compared either the IPE or the EPE with the CE, the PaLOS index decreased, the DEVI increased and the lower accuracy of the network.

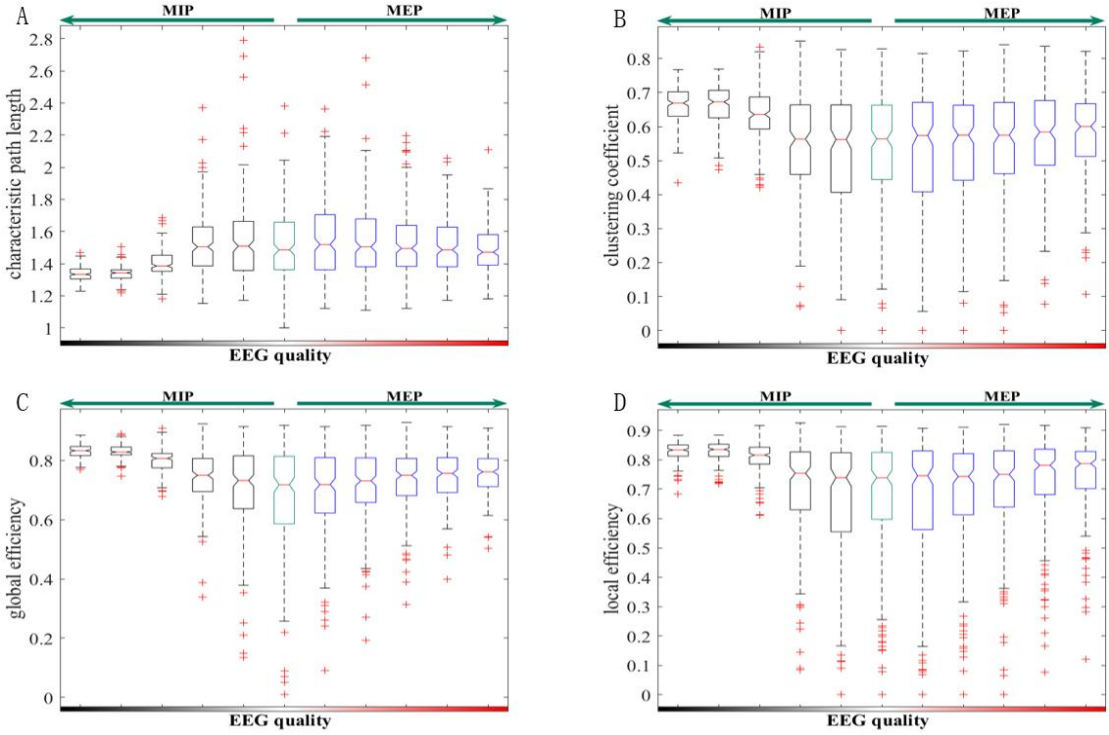

Figure 2. network features results of different EEG quality (black: IPE; red: EPE). (A) characteristic path length. (B) clustering coefficient. (C) global efficiency. (D) local efficiency.

XiPi vs FOOOF: A comparative study of the oscillatory parameters extraction toolboxes for neural rhythmic analysis

Zhihao Zhang[1], Jie Ruan[1], Pedro A. Valdes-Sosa[2], Shiang Hu[1*]

1.Anhui Province Key Laboratory of Multimodal Cognitive Computation, School of Computer Science and Technology, Anhui University, Hefei China, 230000 (shiang.hu@hotmail.com)

2.The Clinical Hospital of Chengdu Brain Science Institute, MOE Key Lab for Neuroinformation, School of Life Science and Technology, University of Electronic Science and Technology of China, China Chengdu

Objective

Recent quantitative EEG studies have raised the imperative needs to decompose the power spectrum into the aperiodic and periodic components. However, since the shape of EEG/MEG power spectrum is irregular, the parametric fitting method like FOOOF(Donoghue et al. 2020) is not precise. Here, we proposed a method using nonparametric fitting to decompose the neural spectrum to aperiodic and periodic components, named XiPi (i.e., ξ-π) where each letter stands for the aperiodic and periodic oscillations, respectively (https://github.com/ShiangHu/XiPeaks).

Methods

The modules of XiPi toolbox consists of spectrum estimation, spectrum decomposing and parameter estimation. The spectrum estimate module is to transform the EEG time series data to frequency domain. As the core of the toolbox, the spectrum decomposing module is based on the Expectation Maximization algorithm, where the E step behaves filtering the multiple components and the M step is to fit components by minimizing the smoothness penalized Whittle likelihood. The parameter estimation module supports outputting the parameters of aperiodic and periodic components.

The data to validate the XiPi toolbox was the simulated data and the real data. The simulation: the artificial time series that was synthesized by mixing the standard aperiodic time series and some sinusoidal oscillations. The real data includes a) the human iEEG from 106 patients' normal cortical areas; b) Monkey ECoG, from wakefulness to sleep. c) CCSHS from 515 teenagers in a sleep study which contains the Wake, NREM and REM stages visually marked by neurophysiologists.

We first calculate the spectrum using spectrum estimation module and then using the spectrum decomposing module to decompose spectrum. In addition to visual inspection, the evaluation methods of the model performance were the metrics for the

goodness of fitting, which consists of error analysis, R square and likelihood (S Hu et al. 2018), and the distance of the oscillatory parameters, and classification accuracy using the linear discriminant analysis. Lastly, we extracted the periodic parameters of human iEEG to build full brain spectra mapping.

Results & Discussion

In simulation, XiPi was more accurate and better in explaining the aperiodic component than FOOOF (Figure 1). In human iEEG, XiPi has less error than FOOOF (96 versus 682). And XiPi has lager R square than FOOOF (0.99826 versus 0.98797). The 98.6% of 500 samples show that XiPi has smaller negative log-likelihood than FOOOF (Figure 2), which means XiPi has larger likelihood than FOOOF.

In Monkey sleep data, XiPi can also work well, which suggests the algorithm is suitable for different species. In CCSHS sleep data, we build a better classifier using XiPi to classify the Wake-NREM, Wake-REM and NREM-REM. Exponents extracted by XiPi rise with sleep stages. And the classification accuracy based on the oscillatory features extracted by using XiPi and FOOOF are 83.47%(±17.22%)-79.73%(±18.28%), 98.43(2.67%)-96.33(±6.08%) and 84.46(±18.11%)-81.68(±21.48%) for the three groups of comparisons of sleep stages, which may indicate that the XiPi can extract the more distinct features to discriminate sleep states (Figure 3).

Besides, the full brain spectra mapping showed that the alpha rhythms(8-12Hz) localize to the occipital regions; the delta rhythms localize to the frontal and occipital regions(<4Hz); the beta rhythms(13-31Hz) are located at the frontal and central partial regions.; gamma rhythms(>31Hz) are located mostly at the left super frontal gyus and the right lateral super temporal lobe gyus. However, it is necessary to accumulate more neurophysiological evidences to conclude the superiority of one over another.

Conclusions

The developed XiPi toolbox can decompose the neural spectrum into the aperiodic and periodic components. XiPi is proved to be effective and superior to FOOOF in some ways.

Acknowledgement: This work was supported by the NSFC Project Number 62101003.

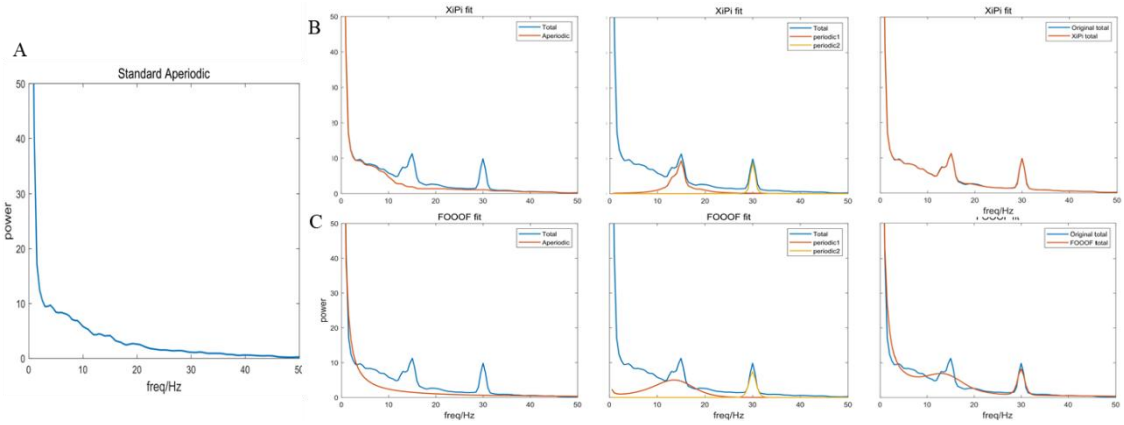

Figure 1. Given the mixture of standard and independence peak/overlapping peak, the comparison of XiPi and FOOOF to decompose the spectra. **A.** The standard aperiodic extract from no peak set. **B, C.** The performance of XiPi and FOOOF to decompose. Left is aperiodic component fitting, middle is perid components fitting, right is the overall fitting.

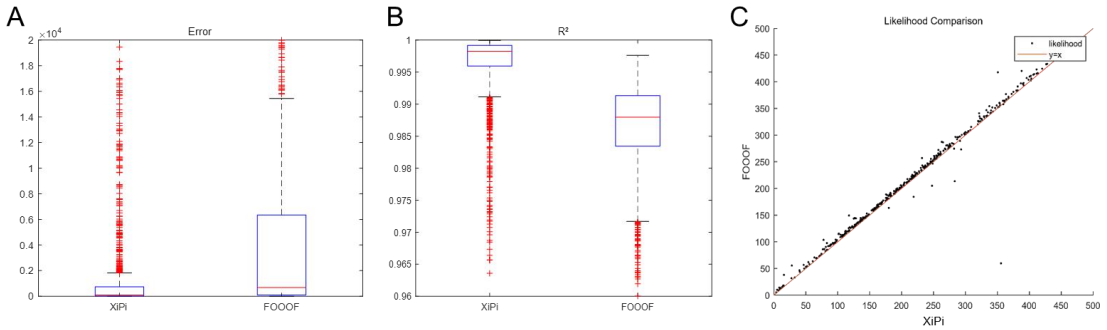

Figure 2. The metrics for goodness of fitting. **A.** Error analysis. **B.** R square analysis. **C.** Likelihood analysis.

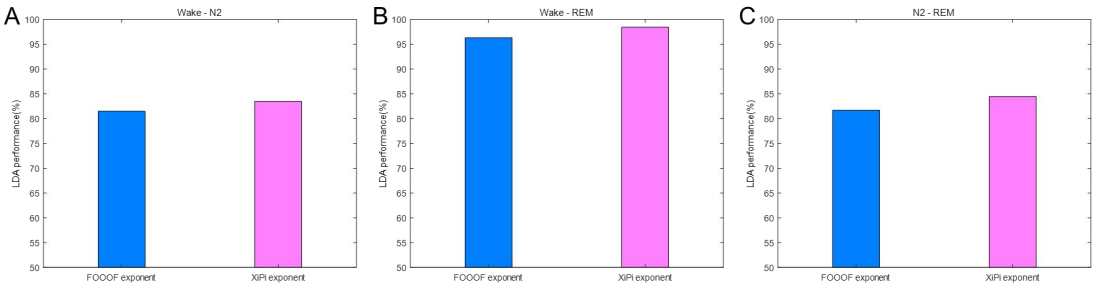

Figure 3. The LDA performance to classify the sleep stage. **A.** the Wake-N2 stage. **B.** Wake-REM stage. **C.** N2-REM stage. Three situations shows that the features extracted by XiPi are better than FOOOF.

Transcranial direct current stimulation and transcranial random noise stimulation facilitate conditioned pain modulation

Xinxin Lin [a], Zhouan Liu [a], Richu Jin [b], Xiaoyun Li [a], Weiwei Peng [a*]

a School of Psychology, Shenzhen University, Shenzhen, China; b Department of Computer Science and Engineering, Southern University of Science and Technology, Shenzhen, China

Objectives

The analgesic effects of anodal stimulation of transcranial direct current stimulation (a-tDCS) and high-frequency transcranial random noise stimulation (tRNS) with direct current (DC)-offset over the primary motor cortex (M1) have different temporal courses, in which the latter induces more sustained analgesia. A potential mechanism for these analgesic effects is the activation of endogenous pain inhibitory pathways, which can be indexed by the psychophysical measure of conditioned pain modulation (CPM). Thus, the present study tested the hypothesis that both a-tDCS and high-frequency tRNS+DC-offset over M1 can improve CPM efficiency, with the latter having more sustained effects.

Methods

A double-blinded sham-controlled design was adopted. A total of 150 healthy participants were recruited to receive a single-session of a-tDCS, high-frequency tRNS+DC-offset, or sham stimulations over M1. We determined their CPM efficiency before, immediately after, and 30 min after the stimulation, and compared the measures across groups.

Results & Discussion

CPM effects were successfully induced for all stimulation groups. Compared with sham stimulation, CPM efficiency increased immediately after a single-session a-tDCS or tRNS+DC-offset over the M1. These effects sustained significantly at least 30 min after stimulation. However, no significant difference in effect was observed between a-tDCS and tRNS+DC-offset. The reason why CPM efficiency was not affected differently by a-tDCS and tRNS+DC-offset in the current study could be that the time window was not long enough. Both types of stimulation appear to lead to sustained enhancement of CPM efficiency, but the short measurement window did not allow us to determine whether tRNS + DC-offset can evoke more prolonged CPM

enhancement.

Conclusion

These findings demonstrate that motor cortex stimulation using tDCS/tRNS activates endogenous pain inhibitory pathways in humans, and supports its application for chronic pain management and prevention. Future studies should use longer testing windows to characterize the temporal courses of these effects in more detail.

Acknowledgement

This study was supported by National Natural Science Foundation of China (31871127 and 62101236), Features Innovative Projects of Guangdong Province Ordinary University (2019KTSCX149), and Shenzhen Basic Research Project (20200812113251002).

Connectivity-directed transcranial magnetic stimulation improves reward learning ability of major depressive patients with suicide ideation

Xinyu Huang, Ya Fang, Fengqiong Yu*

Research Center for Translational Medicine, The Second Hospital of Anhui Medical University, Hefei, China, 230000

(yufengqin1@163.com)

Objective

There are controversial results for transcranial magnetic stimulation (rTMS) efficacy on reward learning ability of major depression disorder (MDD) patients with anhedonia, seldom of them discuss the influence of suicide ideation (SI). The current study investigated the reward learning deficits in MDD patients with SI firstly, and then explored their treatment responses to the individualized rTMS targeted at the specific neural circuit of left dorsolateral prefrontal cortex- neuron accumbens (lDLPFC-NAcc).

Methods

Totally 40 healthy participants (16 females and 24 males, mean age: 20.4 years), 38 MDD patients with anhedonia and accompanied with (n=26, 11 females and 15 males, mean age: 20.23 years) and without SI(n=12, 6 females and 6males, mean age: 22.33 years) patients were enrolled in the data processing procedure of the current study. In the Experiment 1, the demographic information, clinical symptoms (depression, anxiety, anhedonia, and suicide ideation were assessed by Hamilton depression rating scale-17 items (HAMD-17), Hamilton anxiety rating scale(HAMA-14), Temporal Experience Pleasure Scale(TEPS), Self-Report Apathy Evaluation Scale(AES) and Chinese version of the Beck Scale for Suicide Ideation (BSS-CV) separately) and reward-related electrophysiological data (P1, N170, FRN, P3, theta, and alpha) during the modified version of Iowa game task (IGT) were collected in all participants (no anhedonia data collected in health controls). In the Experiment 2, 38 MDD patients were randomly assigned to real or sham group for both SIs and NSIs (SI: 12 real, 14 sham; NSI: 6 real, 6 sham). All of them received 15 once daily sessions of individualized 10 Hz rTMS targeted to the site of strongest left dlPFC-NAcc connectivity, which according to personal fMRI data. All the scale and paradigm mentioned before were administered again.

Results & Discussion

In the Experiment 1, SIs showed bad IGT performance (lower remain money and total net score) and abnormal neurophysiological responses (smaller N170, FRN, and P3; lower alpha power in loss trails) whereas NSIs showed no significant differences compared with HCs. In the Experiment 2, improved anxiety/anhedonia symptom (better HAMA, ASE, TEPS_all, TEPS_ant, and TEPS_con score) and ERP/ERSP alterations (larger P1, N170, FRN amplitudes, and greater alpha power in the loss& low-risk trails) were only found in the real group of SIs, they also revealed alleviated depression/suicide ideation (better HAMD/BBS-CV score) and better IGT performance (greater remain money/total net score) for both of real and sham group posttreatment. Besides, no treatment effect was found in the NSI group.

Conclusions

These findings suggest MDD patients with SI show impaired reward learning ability while NSIs remain functionality. We also found individualized rTMS treatment can significantly alleviate anhedonia symptom and enhance reward learning ability for MDD patients with SI. These findings may provide further understanding to the heterogeneity in reward learning ability in MDD patients with anhedonia. Moreover, the lDLPFC-NAcc circuit plays vital role in reward learning process for MDD patients with SI.

Figure sets:

Experiment 1

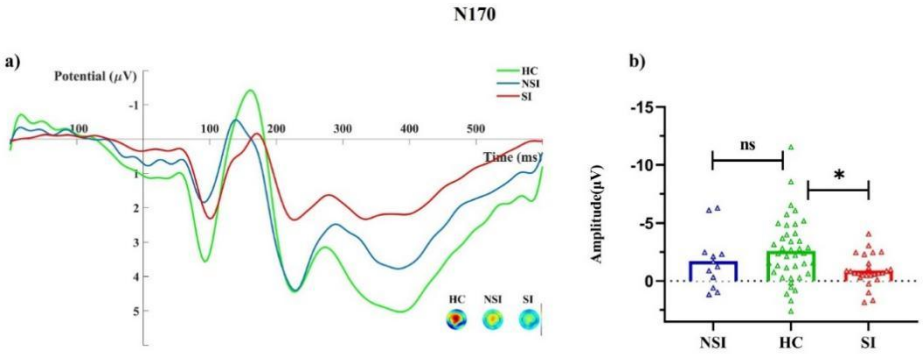

Figure 2. Grand average waves of N170at ROI area (PO7, PO8) in the HC (green line), NSI (blue line), and SI group (red line) correspondingly, and the topography of the FRN component in these three groups. b) Bar graph of N170 peak amplitudes in the HC, NSI, and SI group. HC: healthy control; NSI: no suicide ideation; SI: suicide ideation. ***: p < .001; **: p < .01; *: p < .05; ns: no significant difference

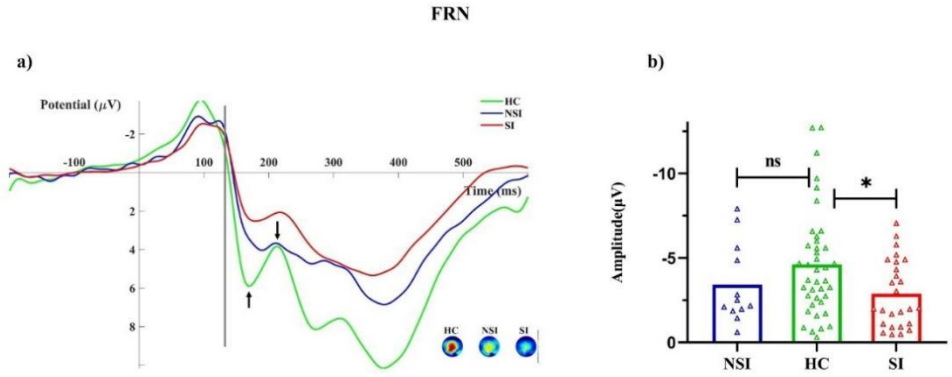

Figure 3. a) Grand average waves of FRN at ROI area (FZ, FC1, FC2, CZ) in the HC (green line), NSI (blue line), and SI group (red line) correspondingly, and the topography of the FRN component in these three groups. The gray line before the FRN time window at 130 ms marks the starting point for the search for the positive peak preceding the FRN, and the black arrow indicates the most positive and negative peak, respectively. b) Bar graph of FRN amplitudes in the HC, NSI, and SI group. HC: healthy control; NSI: no suicide ideation; SI: suicide ideation.

***: p < .001; **: p < .01; *: p < .05; ns: no significant difference.

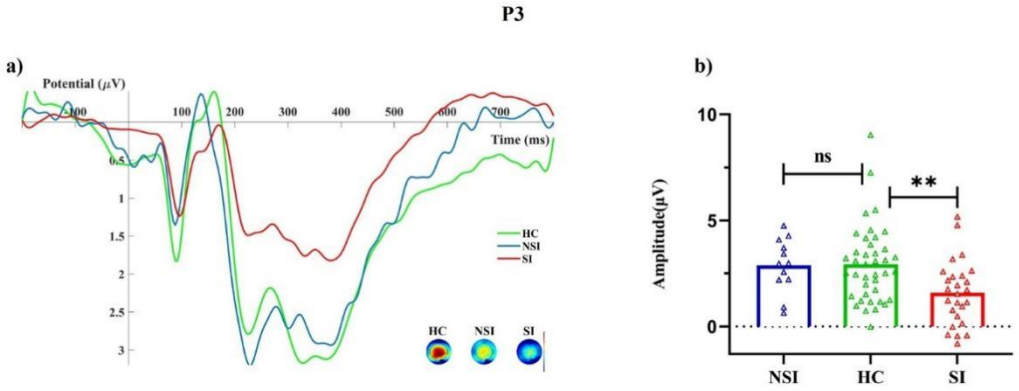

Figure 4. a) Grand average waves of P3 in 350-450 ms at ROI area (O1, O2, OZ) in the HC (green line), NSI (blue line), and SI group (red line) correspondingly, and the topography of the P3 component in these three groups. b) Bar graph of P3 amplitudes in the HC, NSI, and SI group. HC: healthy control; NSI: no suicide ideation; SI: suicide ideation.

***: p < .001; **: p < .01; *: p < .05; ns: no significant difference.

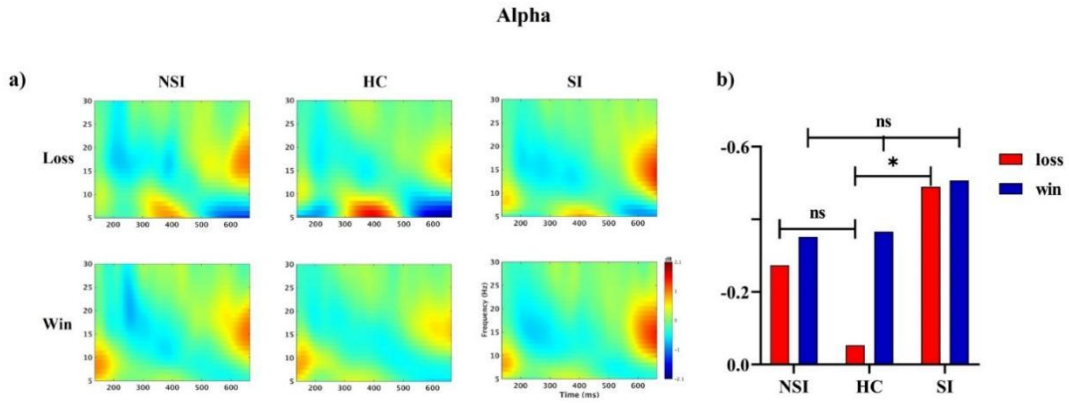

Figure 5. Alpha band power was recorded at Fz among NSI, HC, and SI group during the IGT task. a) A significant difference in alpha power was suggested between HC and SI group in loss trails, but not in win trails. b) Bar graphs of alpha power of three groups, respectively. HC: healthy control; NSI: no suicide ideation; SI: suicide ideation.

***: p < .001; **: p < .01; *: p < .05; ns: no significant difference

Experiment 2

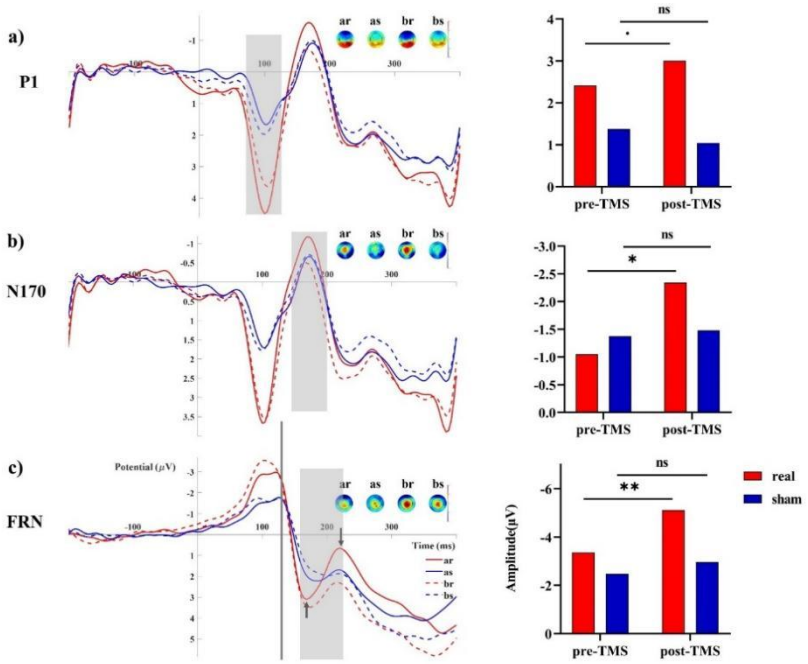

Figure 3 rTMS modulated ERPs components of SI patients during the IGT task. Left panel: Waveforms and topography of the a) P1 component at the electrode PO8, b) N170 at the PO7, PO8, c) FRN at the ROIs (Fz, FC1, FC2, Cz) before (dashed lines) and after (solid lines) the treatment in the real group (red lines) and the sham group(blue lines). Gray squares indicated significant time x group interation; The the gray line in c) at 130 ms marks the starting point for

the search for the positive peak preceding the FRN, and the black arrow indicates the most positive and negative peak, respectively. Right panel: Bar graphs of ERP components amplitudes for real and sham group before and after treatment. ar: real group after rTMS ; as: sham group after rTMS; br: real group before rTMS; bs: sham group before rTMS; ***: p < .001; **: p < .01; *: p < .05; "·" : .05 <p < .1; ns: no significant difference.

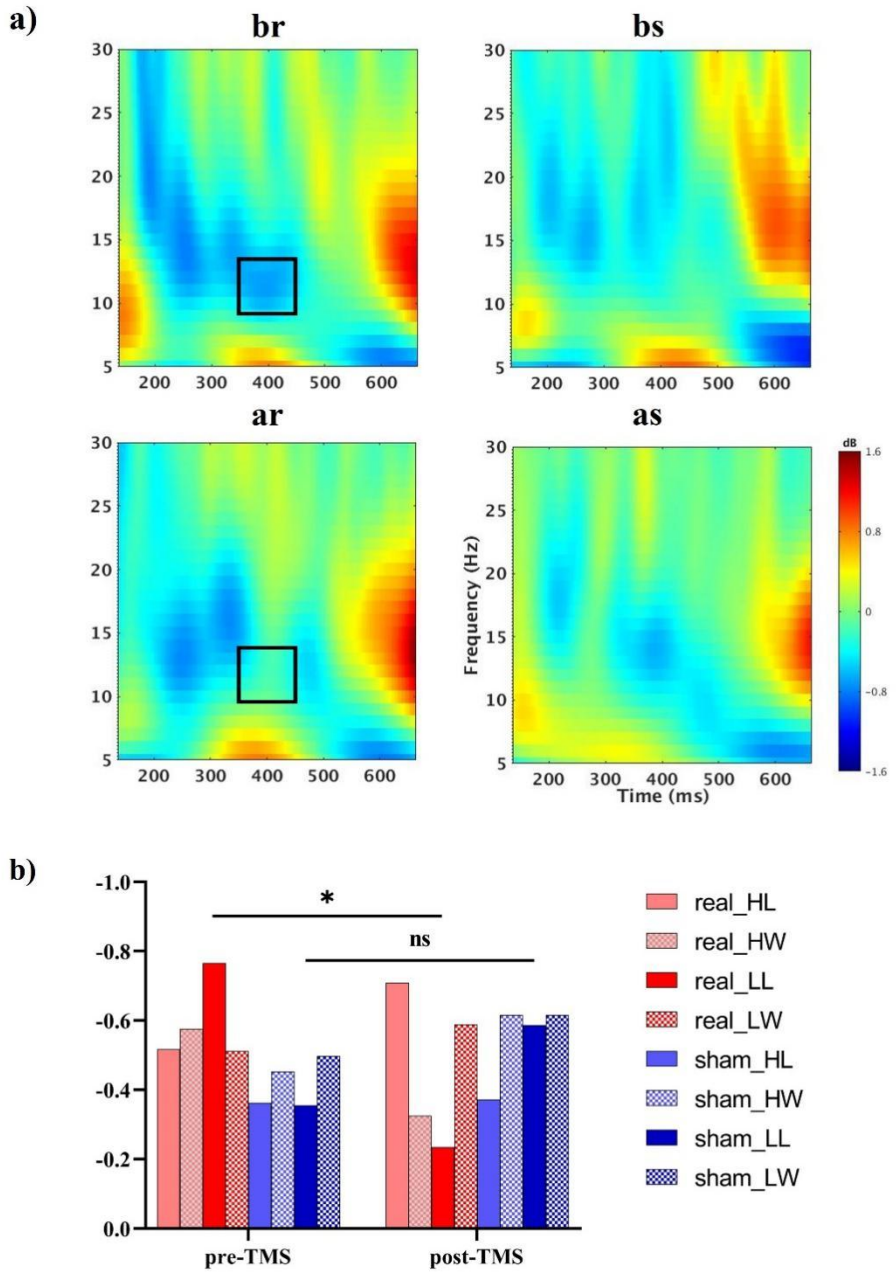

Figure 4. rTMS modulated alpha power of SI patients p during the IGT task. a) Significant increased alpha power at Fz was only found in the real group but not in the sham group under low-risk & win trails. The black boxes define the time-frequency region of interest where the power

increases significantly. b) Bar graphs of alpha power of two groups under risk and feedback factor, respectively. ar: real group after rTMS ; as: sham group after rTMS; br: real group before rTMS; bs: sham group before rTMS; HL: high-risk &loss trails; HW: high-risk &win trails; LL:low-risk &loss trails; LW: low-risk &win trails; ***: $p < .001$; **: $p < .01$; *: $p < .05$; ns: no significant difference.

Oxytocin modulates the perception and aversion of advantageous- and disadvantageous-inequity: Converging evidence from behavior and fMRI

Jiayuan Wang, Yanan Qing, Haochen Zou, Yuanyuan Zhang, Wenjie Chen, Menghan Zhou, Benjamin Becker, Keith M. Kendrick, Shuxia Yao*

The Clinical Hospital of Chengdu Brain Science Institute, School of Life Science and Technology, Chengdu China, 610054

(yaoshuxia@uestc.edu.cn)

Objective

Inequity aversion, or the preference for fairness, is a widely observed behavioral preference in humans and is of great importance in maintaining social cooperation and fairness. Inequity aversion can be triggered by either when individuals receive more (i.e., advantageous inequity, AI) or when they receive less (i.e., disadvantageous inequity, DI) than others. However, it is not clear yet that whether oxytocin (OT), a neuropeptide having widely modulatory effects on human behaviors and emotions, can modulate processing of these two types of inequities and the underlying neural mechanisms. The present study thus combined computational modeling with pharmaco-functional magnetic resonance imaging to investigate the modulatory effect of OT on perception of inequity and its underlying neural mechanisms.

Methods

80 healthy male participants from the University of Electronic Science and Technology of China were recruited and randomly assigned to the oxytocin group (n = 40) or the placebo (PLC) group (n = 40). Participants were asked to complete a modified inequity decision-making task starting with shape matching coopering with a partner and were financially rewarded or punished for successful or unsuccessful matches. Reward or punishment was allocated by a third-party decider and participants were asked to rate the fairness and preference levels in response to the money allocation. In the end of each trial, participants were given a virtual scenario in which they were instructed to choose between the actual allocation and the other fair allocation.

Results & Discussion

Results of rating scores showed that OT increased participants' perception of fairness and preference ratings to allocations of advantageous inequity(Figure 1).

These findings suggest that OT may bias participants' perception of fairness depending on whether those allocations are beneficial to themselves. On the neural level, parametric modulator analyses based on fairness ratings found stronger activity in the dorsolateral prefrontal cortex (DLPFC) and dorsal anterior cingulate cortex (dACC) in response to allocations of advantageous inequity compared to disadvantageous inequity in the OT than the PLC group (Figure 2), indicating that OT increased fairness associated neural responses in brain regions typically associated with cognitive control and conflict detection. Furthermore, allocations of disadvantageous inequity were found to induce stronger activity in the posterior insula in the OT relative to the group.

Conclusions

In contrast to the well-documented prosocial effects of OT in human behavior, our results suggest that OT improves individuals' concern about their own interests. These OT's effects on inequity processing may be underpinned by brain regions including the DLPFC and dACC involved in cognitive control and conflict detection. OT may promote cognitive control and conflict detection to approach more self-beneficial outcomes when individuals were confronted with the advantageous inequity compared to the disadvantageous inequity. Our study provides the first evidence that OT modulates the fairness perception and inequity aversion of advantageous- vs. disadvantageous-inequity.

Acknowledgement: This work was supported by the NSFC (31700998).

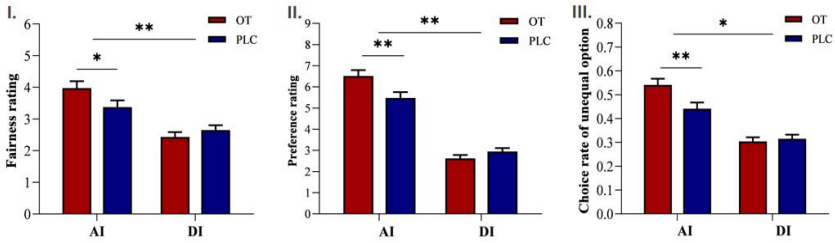

Figure 1. Oxytocin's effects on the rating of fairness, preference and choice rates of unequal option.

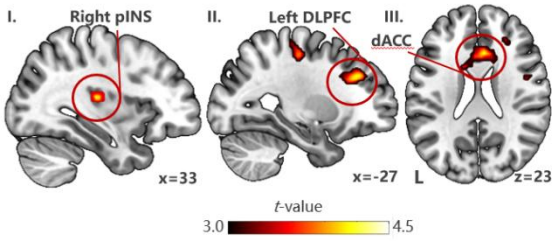

Figure 2. Neural modulation of advantageous- and disadvantageous-inequity processing by oxytocin.

Common neural but distinct computational mechanisms underlie a facilitatory effect of intranasal oxytocin on reinforced learning in stable and volatile contexts

Menghan Zhou[1], Siyu Zhu[1], Ting Xu[1], Jiayuan Wang[1], Qian Zhuang[2], Yuan Zhang[1], Benjamin Becker[1], Keith M. Kendrick[1], Shuxia Yao[1,*]

[1] The Clinical Hospital of Chengdu Brain Science Institute, MOE Key Laboratory for Neuroinformation, University of Electronic Science and Technology of China, Chengdu, China

[2] Center for Cognition and Brain Disorders, The Affiliated Hospital of Hangzhou Normal University, Hangzhou, Zhejiang Province, China

(yaoshuxia@uestc.edu.cn)

Objective

Outcomes of past decisions can profoundly shape our behavior, with rewarding outcomes being reinforced and aversive ones being avoided. However, choice-outcome associations are never stable and can switch to become volatile in a rapidly changing world and learning to adapt to such changes can be problematic in high-anxious individuals. We combined pharmaco-electroencephalography with computational modeling in a modified associative learning task to examine whether intranasally administered oxytocin (24 IU) can modulate reinforcement learning under a volatile relative to a stable association and the underlying neural and computational mechanisms.

Methods

Eighty healthy male subjects (mean age = 20.65 years, SD = 1.77) were recruited from the University of Electronic Science and Technology of China. Subjects were randomly assigned into two groups and self-administered either oxytocin or placebo nasal spray. After 45 min post-treatment, subjects were asked to a modified associative learning task consisting of two blocks. In the stable block, choice-outcome contingencies were stable (shape A was associated with a high reward probability of 75% and shape B was associated with a low reward probability of 25%). In the volatile block, choice-outcome contingencies were volatile by switching contingencies every 20 trials (shape A was associated with a high reward probability of 80% and shape B was associated with a low reward probability of 20% for 20 trials and vice versa in another 20 trials). Subjects were instructed to choose one of the two hiragana syllables that they considered being more likely associated with a reward.

Results & Discussion

On the behavioral level oxytocin increased the choice accuracy of optimal shape independent of learning contexts. On the neural level oxytocin decreased amplitudes of the P300 component but increased amplitudes of the N2pc component across contexts (Figure 1). These findings suggest that the general enhancement effect of oxytocin on learning may be derived from improved early attentional selection and increased neural processing efficiency. Importantly, computational modeling analyses further revealed that while oxytocin promoted learning by accelerating the value update of outcomes in the volatile context, as reflected by higher learning rates, in the stable context it did so by improving choice consistency, as indicated by increased inverse temperature (Figure 2).

Conclusions

The present study showed similar facilitatory effects of oxytocin on reinforcement learning under volatile and stable environments using multi-methodological approaches. However, while oxytocin's facilitatory effects on learning share similar neural mechanisms under volatile and stable associations, they are distinct in terms of computational mechanisms. Our findings provide proof of concept evidence for the therapeutic potential of oxytocin in mental disorders with adaptive learning dysfunction.

Acknowledgement: This work was supported by the Humanity and Social Science Foundation of Ministry of Education of China (grant number: 22XJC190003).

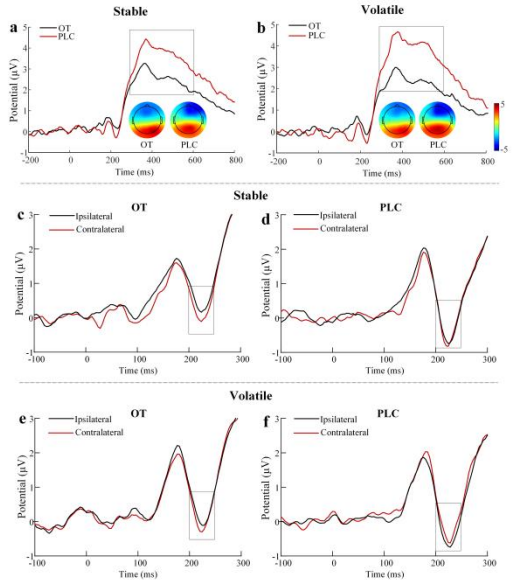

Figure 1. Oxytocin's effects on P300 (a and b) and N2pc (c-f) components.

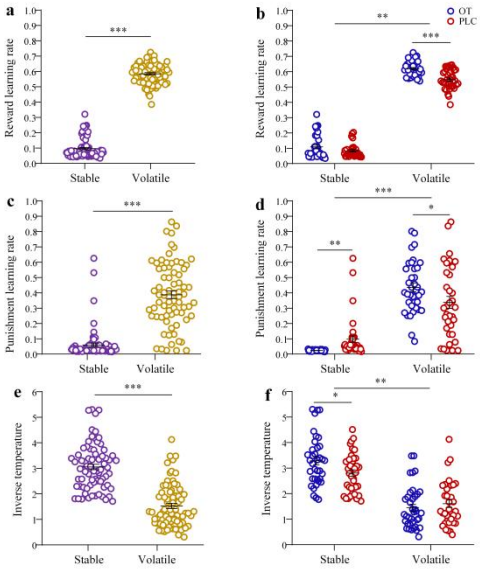

Figure 2. Oxytocin's effects on learning rates (a-d) and inverse temperature (e and f).

Real-time fMRI Neurofeedback Training on the Anterior Insula via an interoceptive strategy and Its Behavioral Effects

Yuan Zhang, Qiong Zhang, Jiayuan Wang, Menghan Zhou, Yanan Qing, Haochen Zou, Jianfu Li, Benjamin Becker, Keith M. Kendrick, Shuxia Yao*

The Clinical Hospital of Chengdu Brain Science Institute, School of Life Science and Technology, Chengdu China, 610054

(yaoshuxia@uestc.edu.cn)

Objective

Real-time functional magnetic resonance imaging neurofeedback (rt-fMRI NF) training is a novel non-invasive technique that can aid individuals to volitionally self-modulate neural activity of brain regions or pathways. The insula, a core hub of the emotion and salience networks, has become one of the most investigated target regions in rt-fMRI studies. Accumulating evidence has shown that self-regulation of the insula activity can be acquired via rt-fMRI NF training in both healthy and clinical populations and most of those studies have utilized the negative mental imagery (e.g., imagining or recalling negative emotion or memory) as their regulation strategy. This regulation strategy may not be appropriate for individuals with emotional disorders characterized by sustained or hyper-negative moods or emotions. Therefore, based on the functional relevance of the insula involved in interoceptive processing, the present study aimed to examine the feasibility of interoceptive strategy in regulating the anterior insula activity using a randomized double-blind, sham feedback-controlled between-subject design.

Methods

63 healthy participants from the University of Electronic Science and Technology of China (UESTC) were recruited and randomly assigned to the neurofeedback group (NF, n = 33) receiving feedback from the left anterior insula (LAI) or the sham control group (CTR, n = 30) receiving feedback from the middle temporal gyrus. After defining the LAI for each participant using a functional localizer task of pain empathy, all participants underwent the NF training task comprising four training sessions with real-time feedback or sham feedback and one transfer session without feedback. Each session included 5 regulation blocks (i.e., to increase the activity of the LAI/control region by feeling their heartbeat) alternated with 5 baseline blocks (i.e., to return the activity to the baseline by relaxing themselves). Neurofeedback was presented by a thermometer of which the more bars

were filled the stronger the activity was. Behavioral effects were examined by comparing differences in interoceptive accuracy and empathic responses between pre- and post-training tests of the heartbeat counting task and empathy task.

Results & Discussion

The whole-brain analyses showed that the LAI was significantly activated only in the NF group during NF training ($p < 0.01$, FWE-corrected) and the ROI analysis further revealed that the LAI activity in the NF group was significantly stronger than in the CTR group across the four training sessions and in the transfer session (Figure 1). Correlation analyses showed a significant positive correlation between the LAI activity and the interoceptive accuracy in the post-training test only in the NF group (Figure 1c), suggesting that the stronger the LAI activity induced by NF training the higher the interoceptive accuracy after NF training. However, we did not find any significant behavioral effects on empathy associated with NF training effects.

Conclusions

The present study provided evidence that interoception can be used as a novel regulation strategy in regulating the LAI activity. Successful regulation of the LAI activity was positively associated with interoceptive accuracy after NF training. Given the important role of the AI in human emotional and salience processing, our findings may suggest great potential of the interoceptive strategy for translational therapeutic application in individuals with dysfunctional insula and emotional disorders particularly characterized by sustained or hyper-negative moods or emotions.

Acknowledgement: This work was supported by the National Key Research and Development Program of China (grant number: 2018YFA0701400) and the National Natural Science Foundation of China (NSFC) grants (grant number: 31700998).

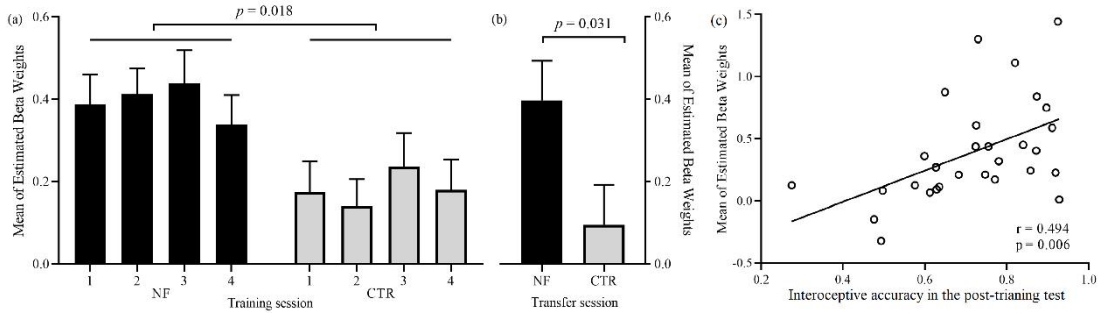

Figure 1. (a) LAI activity during regulation relative to baseline conditions across the four training sessions and (b) in the transfer session; (c) A significant positive correlation between the LAI activity and the interoceptive accuracy in the post-training test only in the NF group.

A voxel and surface morphology-based study of brain structure in male endurance runners

Wen Xiao[1]，Jinlong Wu[1]，Long Cao[2], Yuanchao Zhang[2], Ruiwang Huang[3], Lunxiong Li[4], Fengguang Xia[4], Yudan Ma[5], Zhanbing Ren[1*]

1. Shenzhen University, Shenzhen, 518060, China; 2. Key Laboratory for NeuroInformation of Ministry of Education, School of Life Science and Technology, University of Electronic Science and Technology of China, Chengdu 610054, China; 3. School of Psychology, South China Normal University, Guangzhou 510631, China; 4. Key Laboratory of Brain, Cognition and Education Sciences, Ministry of Education, China; Institute for Brain Research and Rehabilitation, South China Normal University, Guangzhou 510631, China; 5. Jilin Institute of Sport Science, Changchun 130022, China(rzb@szu.edu.cn)

Objective

Studies have shown that long-term complex fine exercise can change the brain's structure, such as the volume and morphology of gray matter white matter. Although endurance running is a simple repetitive exercise, it still relies on good human physiology (maximal oxygen uptake, maximal oxygen uptake utilization, running economy, muscular strength and muscular endurance, etc.) during the exercise. Moreover, it requires the participation of multiple cognitive functions. So, can endurance running change the structure of the brain? This study will explore the structural characteristics of the brain in male endurance runners based on multimodal magnetic resonance technology and provide a neuroscientific basis for endurance running.

Methods

Twenty-two male endurance runners (26.27 ± 6.07) years old and 20 general subjects (24.60 ± 4.13) were recruited openly from the community utilizing online media or posters. Based on a Siemens 3.0 T magnetic resonance imaging system, structural brain images of the subjects were acquired. SPM8 software was used to compare the two groups of gray matter volumes in voxels; specifically, a general linear model was used to compare the differences in voxels between the two groups of subjects, and subsequently, the statistics were thresholded at voxel $P<0.001$ and corrected for multiple comparisons at the cluster level using Gaussian random field theory. After numerous comparison corrections, the significance level was set at $P<0.05$. The SurfStat software package was used to compare the cortical thickness and surface area maps in the two groups. Specifically, the cortical thickness and surface area of the two groups of subjects were compared separately using a general

linear model, with a group as a covariate. Subsequently, the statistics were thresholded at P<0.005 and corrected for multiple comparisons at the cluster level using random field theory. After numerous comparison corrections, the significance level was set at P<0.05.

Results & Discussion

The results of the structural brain imaging study revealed a significant increase in gray matter volume in the left precentral gyrus of male endurance runners (cluster size = 1016 voxels; MNI peak coordinates: x = -43.5, y = -18, z = 49.5; peak t = 5.413), with no significant difference in cortical thickness between the two groups; compared to the regular control group, the left precentral gyrus of the male endurance runners group had a significantly higher cortical The surface area was significantly increased in the male endurance runner group compared to the regular control group (cluster size = 2319 vertices; Talairach peak coordinates: x = -51.7, y = 6.3, z = 24.2; peak t = 4.16, FDR corrected P = 0.00067).

Conclusions

Male endurance runners had significantly increased gray matter volume in the left precentral gyrus and surface area of the left precentral gyrus cortex compared to non-endurance runners.

Acknowledge: The article was supported by National Natural Science Foundation of China (NSFC) [grant number 11002036] ; Research Foundation for Young Teacher of Shenzhen University [grant number QNJS0274]; High-level Scientific Research Foundation for the Introduction of Talent of Shenzhen University [grant number RC00228]; Natural Science Featured Innovation Projects in Ordinary Universities in Guangdong Province [grant number 2021KTSCX297];Scientific Research Platform and Project of Colleges and Universities of Education Department of Guangdong Province (2022ZDZX2087).

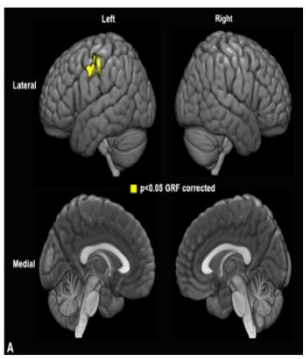

Figure1 Results of cortical morphological differences in the group of male endurance runners compared to the general c

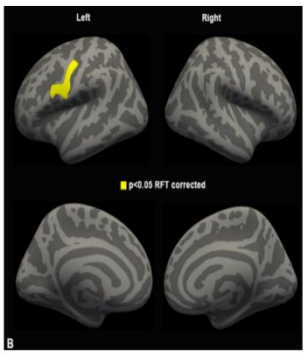

Figure 2 Results of the difference in cortical surface area between the endurance runner group compared to the standard control group

Characterization of brain white matter microstructure in male endurance runners: a whole-brain diffusion tensor imaging study

Jinlong Wu[1], Wen Xiao[1], Long Cao[2], Yuanchao Zhang[2], Yudan Ma[3],

Ruiwang Huang[4], Lunxiong Li[5], Fengguang Xia[5], Zhanbing Ren[1*]

1. College of Physical Education, Shenzhen University, Shenzhen, 518060, China; 2. Key Laboratory for NeuroInformation of Ministry of Education, School of Life Science and Technology, University of Electronic Science and Technology of China, Chengdu 610054, China; 3. Jilin Institute of Sport Science, Changchun 130022, China

4. School of Psychology, South China Normal University, Guangzhou 510631, China; 5. Key Laboratory of Brain, Cognition and Education Sciences, Ministry of Education, China; Institute for Brain Research and Rehabilitation, South China Normal University, Guangzhou 510631, China;

(rzb@szu.edu.cn)

Objective

Previous studies have identified certain differences in brain structure and function between endurance and non-endurance runners, and these differences may be the neural basis for the superior endurance performance of endurance runners. However, the brain white matter microstructure in endurance runners has not yet been explored. Therefore, we used diffusion whole-brain tensor imaging (DTI) data to investigate the difference in the brain white matter microstructure of endurance runners and non-endurance runners.

Methods

22 male endurance runners and 20 non-endurance runners were recruited through online media and posters. The 22 male endurance runners had been training for (6.23±2.41) years. For comparison, 20 age- and sex-matched non-endurance runners were included who had no regular exercise habits. A 3.0-T system (Siemens Magnetom Trio Tim, Erlangen, Germany) with a 12-channel head array coil was used to acquire DTI data from two groups. FSL and SPM8 were used for preprocessing and statistical analyses, respectively. Specific statistical analyses included a general linear regression model for the pre-processed DTI data to test for differences in fractional anisotropy values between the two groups. Statistics were thresholded at voxel $P < 0.01$ and corrected for multiple comparisons at the clustering level using Gaussian Random Field Theory. After correction for multiple comparisons, the significance level was set at $P < 0.05$.

Results & Discussion

We found three clusters had significantly higher FA in male endurance runners compared with non-endurance runners. These clusters involved the left posterior lobe of the cerebellum, the bilateral precuneus and the genu of the corpus callosum, left anterior limb of the internal capsule, left anterior

corona radiata, and left external capsule.

Conclusions

We found significant differences in brain white matter microstructure in male endurance runners and non-endurance runners, and these differences in brain white matter microstructure may be the neural mechanism by which endurance runners have superior endurance performance.

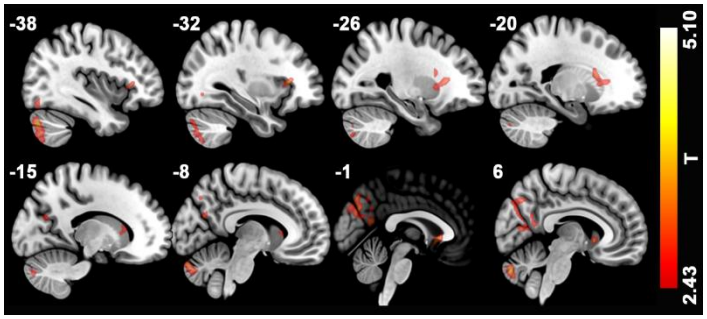

Fig 1. Brain regions show higher FA in male endurance runners compared with non-endurance runners. The results were corrected for multiple comparisons using random field theory. The color bar denotes the t values.

Acknowledge: the article was supported by National Natural Science Foundation of China (NSFC) [grant number 11002036] ; Research Foundation for Young Teacher of Shenzhen University [grant number QNJS0274]; High-level Scientific Research Foundation for the Introduction of Talent of Shenzhen University [grant number RC00228]; Natural Science Featured Innovation Projects in Ordinary Universities in Guangdong Province [grant number 2021KTSCX297];Scientific Research Platform and Project of Colleges and Universities of Education Department of Guangdong Province (2022ZDZX2087).

Working memory Performance during moderate-intensity exercise in individuals of different aerobic capacities: a fNIRS study

Jingxuan Yu, Bowen Liu, Jinlong Wu, Zhanbing Ren[1]*

Shenzhen University, Institute of Physical Education, Shenzhen China, 518060 (rzb@szu.edu.cn)

Objective

The benefits of exercise on cognitive function have been well established in many studies, however the potential changes in cognitive activity and the brain during exercise remain unclear. At present, the differences in cognitive performance of participants with different aerobic fitness levels have not been clearly defined. Therefore, the main purpose of this paper is to explore the working memory performance and cortical activity characteristics of young people with different aerobic fitness levels during exercise.

Methods

Twenty-eight healthy participants participated in the study. Aerobic capacity was assessed by the cost of oxygen during an 8km/h run. A high aerobic capacity fitting group (29.16±2.25 ml/kg/min) and a low aerobic capacity fitting group (34.17±2.84 ml/kg/min) were created according to the median oxygen consumption. Lower oxygen consumption at a given load represents better aerobic capacity. In the second experiment, participants performed the 0, 2-back task to evaluate their working memory while running quietly and at a moderate intensity (64-76%HRmax). The 19-channel fNIRS tracked changes in oxyhemoglobin levels in the left prefrontal (LPFC), middle prefrontal (MPFC), and right prefrontal (RPFC) lobes during this period.

Results & Discussion

Our results showed that both the high-fit and low-fit groups exhibited higher error rates ($F=19.486$, $P<0.001$) and response times ($F=42.618$, $P<0.001$) in 2-back compared to 0-back, both in the quiet and motion states. The high-fit group showed faster reaction times when performing the 2-back task in motion than in the quiet state (MD=-85.746ms, $P=0.043$). fNIRS results showed that the high-fit group exhibited lower oxygenation of the left prefrontal lobe during the 0, 2-back task during exercise compared to the quiet group ($\Delta\beta=-0.055$, $P=0.002$; $\Delta\beta=-0.048$, $P=0.018$). However, the low fitting group only showed lower prefrontal oxygenation ($\Delta\beta=-0.037$, $P=0.023$) in the 0-back task.

Conclusions

Moderate-intensity aerobic exercise improved the reaction time of working memory in individuals with high aerobic capacity, and the reduction in task-related prefrontal oxygenation did not hinder the performance of cognitive control and was more efficient in cognitive tasks.

Acknowledge: The article was supported by National Natural Science Foundation of China (NSFC) [grant number 11002036] ; Research Foundation for Young Teacher of Shenzhen University [grant number QNJS0274]; High-level Scientific Research Foundation for the Introduction of Talent of Shenzhen University [grant number RC00228]; Natural Science Featured Innovation Projects in Ordinary Universities in Guangdong Province [grant number 2021KTSCX297];Scientific Research Platform and Project of Colleges and Universities of Education Department of Guangdong Province (2022ZDZX2087).

Inhibitory control performance during exercise is associated with aerobic capacity: a fNIRS study

Bowen Liu, Jingxuan Yu, Jinlong Wu, Wen Xiao，Zhanbing Ren*

College of Physical Education, Shenzhen University, Shenzhen China, 816050 (rzb@szu.edu.cn)

Objective

Acute exercise at moderate intensities has been found in many studies to improve inhibitory control. It is unclear whether individuals at any level of fitness can benefit from exercise. The purpose of the present study was to examine performance and prefrontal oxygen content during exercise in individuals of varying aerobic capacity performing inhibitory control tasks.

Methods

Twenty-eight healthy adult participants took part in this study. In the first session, the energy cost of running(Cr) at 10 km/h speed was measured and used to assess their aerobic capacity. A high aerobic capacity fitting group (n=14, Cr =33.34±2.84 ml/kg/min) and a low aerobic capacity fitting group (n=14, Cr =39.90±2.80 ml/kg/min) were created based on the median oxygen cost. In the second session, participants completed the Stroop task during quiet and moderate intensity (64-76% HRmax) running exercise to evaluate inhibitory control. Changes in oxygenated hemoglobin (O2Hb) levels in the left prefrontal cortex (LPFC), middle prefrontal cortex (MPFC) and right prefrontal cortex (RPFC) were observed using 19 channels of fNIRS.

Results & Discussion

For reaction time, the interaction between state and fitness level was significant (F=9.676, P=0.004). Compared to the quiet state, only the high-fit group improved reaction time during exercise (MD=-81.45ms, P<0.001). During exercise, the high-fit group showed faster reaction times than the low-fit group (MD=-82.90ms, P=0.026). For the fNIRS results, O2Hb was significantly lower in RPFC during exercise in both groups. The high fit group had significantly lower O2Hb in LPFC during exercise and lower than the low fit group (Figure 1).

Conclusions

Moderate intensity aerobic exercise only improved inhibitory control performance in participants with high aerobic fitness levels and was accompanied lower LPFC oxyhemoglobin levels. This has implications for guiding daily life practice, which offers the potential to improve cognitive performance through improved fitness levels.

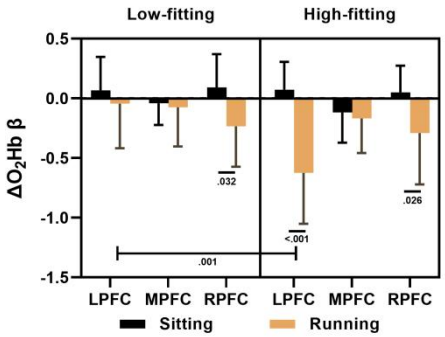

Fig. 1 Changes in prefrontal oxyhemoglobin concentrations in the high and low fitting groups during quiet and exercise.

Acknowledge: The article was supported by National Natural Science Foundation of China (NSFC) [grant number 11002036] ; Research Foundation for Young Teacher of Shenzhen University [grant number QNJS0274]; High-level Scientific Research Foundation for the Introduction of Talent of Shenzhen University [grant number RC00228]; Natural Science Featured Innovation Projects in Ordinary Universities in Guangdong Province [grant number 2021KTSCX297];Scientific Research Platform and Project of Colleges and Universities of Education Department of Guangdong Province (2022ZDZX2087).

主办单位

中国心理学会脑电相关技术专委会

广东省认知科学学会

承办单位

深圳市神经科学研究院

广东医科大学人文与管理学院

协办单位

深圳大学心理学院

暨南大学管理学院

中国认知科学学会社会认知分会

赞助单位

深圳市瀚翔生物医疗电子股份有限公司

博睿康科技(常州)股份有限公司

上海心仪电子科技有限公司

赢富仪器科技(上海)有限公司

武汉格林泰克科技有限公司

北京誉商科技有限公司

丹阳慧创医疗设备有限公司